การเกิดสารประกอบเชิงซ้อนของแอนไอออนกับทริปพอดัลแอมโมเนียมแคปคาลิก[4]ซารีน

นางสาวศิริลักษณ์ พุ่มประดับ

วิทยานิพนธ์นี้เป็นส่วนหนึ่งของการศึกษาตามหลักสูตรปริญญาวิทยาศาสตรมหาบัณฑิต
สาขาวิชาเคมี ภาควิชาเคมี
คณะวิทยาศาสตร์ จุฬาลงกรณ์มหาวิทยาลัย
ปีการศึกษา 2543

ISBN 974-347-137-5

COMPLEXATION OF ANIONS WITH TRIPODAL AMMONIUM CAPPED CALIX[4]ARENES

MISS SIRILUX POOMPRADUB

A Thesis Submitted in Partial Fulfillment of the Requirements
for the Degree of Master of Science in Chemistry
Department of Chemistry
Faculty of Science
Chulalongkorn University
Academic Year 2000

ISBN 974-347-137-5

Thesis Title	Complexation of Anions with Tripodal Ammonium Capped Calix[4]arenes
By	Miss Sirilux Poompradub
Field of Study	Chemistry
Thesis Advisor	Assistant Professor Thawatchai Tuntulani, Ph.D.

Accepted by the Faculty of Science, Chulalongkorn University in Partial Fulfillment of the Requirements for the Master's Degree

……Dean of Faculty of Science
(Associate Professor Wanchai Phothiphichitr, Ph.D.)

Thesis Committee

……Chairman
(Associate Professor Udom Kokpol, Ph.D.)

……Thesis Advisor
(Assistant Professor Thawatchai Tuntulani, Ph.D.)

……Member
(Assistant Professor Warinthorn Chavasiri, Ph.D.)

…… Member
(Nongnuj Jaiboon, Ph.D.)

ศิริลักษณ์ พุ่มประดับ : การเกิดสารประกอบเชิงซ้อนของแอนไอออนกับทริปพอดัลแอมโมเนียมแคปคาลิก[4]ซารีน (COMPLEXATION OF ANIONS WITH TRIPODAL AMMONIUM CAPPED CALIX[4]ARENES) อ.ที่ปรึกษา : ผศ.ดร.ธวัชชัย ตันฑุลานิ; 116 หน้า. ISBN 974-347-137-5.

ทำการสังเคราะห์ลิแกนด์ **6a** คือ 25,26,27-*N,N′,N″*-tri((2-ethoxy)benzyl)ethylenetetra amine-*p*-*tert*-butylcalix[4]arene·4HCl สาร **6a** ตกผลึกแบบโมโนคลินิกโดยมีสเปสกรุ๊ปเป็น C_2/c การศึกษาการเกิดสารประกอบเชิงซ้อนของลิแกนด์ **6a** และ **6b** (25,26,27-*N,N′,N″*-tri((4-ethoxy)benzyl) ethylenetetraamine-*p*-*tert*-butylcalix[4]arene·4HCl) กับแอนไอออนชนิดต่าง ๆ อาทิเช่น ฟลูโอไรด์, โบรไมด์, ไอโอไดด์, ไนเตรต, คาร์บอเนต, ซัลเฟต, ฟอสเฟต, ไฮโดรเจนฟอสเฟต และ ไดไฮโดรเจนฟอสเฟต โดยมีเค้าเตอร์แคทไอออนเป็น โซเดียมไอออน กระทำโดยการไทเทรตด้วยเทคนิคโปรตอนนิวเคลียร์แมกเนติกเรโซแนนซ์ (เอ็นเอ็มอาร์) ในไดเมทิลซัลฟ็อกไซด์-d_6 สำหรับ **6a** สารละลายผสมระหว่างเมธานอล-d_4 และคลอโรฟอร์ม-*d* สำหรับ **6b** ตามลำดับ ลิแกนด์ **6a** และ **6b** สามารถเกิดสารประกอบเชิงซ้อนในอัตราส่วน 1:1 กับโบรไมด์ (log K = 2.23, 2.28), ไอโอไดด์ (log K = 2.62, 2.44) และไนเตรต (log K = 2.47, 2.34) โดยความสามารถในการเกิดสารประกอบเชิงซ้อนเป็นดังนี้ ไอโอไดด์ > ไนเตรต > โบรไมด์ นอกจากนี้ยังได้ทำการศึกษาผลกระทบของเค้าเตอร์แคทไอออนต่อการเกิดสารประกอบเชิงซ้อนกับแอนไอออน สำหรับเค้าเตอร์แคทไอออนที่ไม่ใช่โลหะเช่น เตตระบิวทิลแอมโมเนียม จะให้ค่าคงที่ของการเกิดสารประกอบเชิงซ้อน (log K's) ของลิแกนด์ **6a** และ **6b** ที่มีต่อโบรไมด์และไอโอไดด์คือ 2.13, 2.38 และ 1.78, 2.40 ตามลำดับ อย่างไรก็ตาม ค่าคงที่ของการเกิดสารประกอบเชิงซ้อนของลิแกนด์ **6a** และ **6b** ที่มีต่อโบรไมด์และไอโอไดด์เมื่อใช้โพแทสเซียมไอออนเป็นเค้าเตอร์แคทไอออนคือ 2.14, 2.22 และ 2.19, 2.35 ตามลำดับ จากผลการทดลองแสดงให้เห็นว่าการใช้แคทไอออนที่แตกต่างกันทำให้ค่าคงที่ของการเกิดสารประกอบเชิงซ้อนของ ลิแกนด์ **6a** ที่มีต่อโบรไมด์และไอโอไดด์ มีค่าแตกต่างกันออกไปดังนี้คือ โซเดียม > โพแทสเซียม > เตตระบิวทิลแอมโมเนียม ในทางตรงกันข้ามค่าคงที่ของการเกิดสารประกอบเชิงซ้อนของลิแกนด์ **6b** ที่มีต่อแอนไอออนจะมีค่าใกล้เคียงกัน ไม่ว่าเค้าเตอร์แคทไอออนจะเป็นอะไรก็ตาม ความสามารถในการเกิดสารประกอบเชิงซ้อนของ ลิแกนด์ **6a** กับแอนไอออนที่เพิ่มขึ้น อาจจะมีผลมาจากการจัดรูปใหม่ของหน่วยทริปพอดัลแอมโมเนียมเมื่อมีอัลคาไลแคทไอออนปรากฏอยู่

ภาควิชา เคมี ลายมือชื่อนิสิต.....

สาขาวิชา เคมี ลายมือชื่ออาจารย์ที่ปรึกษา.....

ปีการศึกษา 2543 ลายมือชื่ออาจารย์ที่ปรึกษาร่วม.....

4172461723 : MAJOR CHEMISTRY.

KEY WORDS: ANION RECEPTOR, CALIX[4]ARENE, COMPLEXATION, PROTON NMR TITRATION

SIRILUX POOMPRADUB : COMPLEXATION OF ANIONS WITH TRIPODAL AMMONIUM CAPPED CALIX[4]ARENES. THESIS ADVISOR: ASSIST. PROF. THAWATCHAI TINTULANI, Ph.D. 116 pp. ISBN 974-347-137-5.

25,26,27-*N,N′,N″*-tri((2-ethoxy)benzyl)ethylenetetraamine-*p-tert*-butylcalix[4]arene·4HCl, **6a**, has been synthesized. The compound **6a** was crystallized in a monoclinic C_2/c space group. Complexation studies of **6a** and 25,26,27-*N,N′,N″*-tri((4-ethoxy)benzyl)ethylenetetraamine-*p-tert*-butylcalix[4]arene·4HCl, **6b**, towards anions such as F^-, Br^-, I^-, NO_3^-, CO_3^{2-}, SO_4^{2-}, PO_4^{3-}, AsO_2^-, HPO_4^{2-} and $H_2PO_4^-$ using Na^+ as countercation were carried out by ^{1}H-NMR titration in dimethylsulfoxide-d_6 and the mixture of chloroform-*d* and methanol-d_4, respectively. Ligands **6a** and **6b** were able to form 1:1 complexes with Br^- (log K = 2.23, 2.28), I^- (log K = 2.62, 2.44) and NO_3^- (log K = 2.47, 2.34) and the complexation ability varied as follows: $I^- > NO_3^- > Br^-$. The effect of countercations towards anion complexation was also investigated. For a non-metal countercation, $^nBu_4N^+$, the association constants (log K's) of **6a** and **6b** towards Br^- and I^- were 2.13, 2.38 and 1.78, 2.40, respectively. However, the association constants (**6a** and **6b**) when K^+ was employed as countercation were 2.14, 2.22 and 2.19, 2.35 towards Br^- and I^-, respectively. The results showed that the association constants of **6a** towards Br^- and I^- in the presence of various cations varied as $Na^+ > K^+ > {}^nBu_4N^+$. On the other hand, the association constants of **6b** towards anions were comparable no matter what countercation was used. The enhancement in anion complexation ability of **6a** may result from the rearrangement of the tripodal ammonium unit in the presence of alkali cations.

Department……Chemistry…….. Student's signature…….
Field of study……Chemistry…….. Advisor's signature ……...
Academic year……2000…… Co-advisor's signature ……..

Acknowledgement

I am grateful to my thesis advisor, Assist. Prof. Dr. Thawatchai Tuntulani for his suggestions, assistance, encouragement and personal friendship throughout my master degree career. I would like to thank Assoc. Prof. Dr.Udom Kokpol, Assist. Prof. Dr. Warinthorn Chavasiri and Dr. Nongnuj Jaiboon for their valuable suggestions and comments as committee members and thesis examiners.

This thesis can not be completed without kindness of many people. Firstly, I would like to thank Dr. Nongnuj Jaiboon for X-ray Crystallography. Then, I would like to express my appreciation to Mr.Sanchai Akethawatchai at the National Center for Genetic Engineering and Biology for 400 MHz ^{1}H-NMR and ESI-TOF results. In addition, the Thailand Research Fund and the Department of chemistry, Faculty of Science, Chulalongkorn University is gratefully acknowledged for financial supports.

Finally, I would like to express my deepest gratitude to my family for their kindness, encouragement and supports throughout the course of my education. Moreover, I thank my friends and staffs in Supramolecular Chemistry Laboratory for their friendship and helps during my graduate study.

CONTENTS

Page

List of Abbreviations and signs

Å	Angtrom
ATP	Adenosine triphosphate
^{0}C	Celcius
equiv.	Equivalence
δ	Chemical shift
DNA	Deoxyribonucleic acid
g	Gram
2D-NMR	Two-dimension nuclear magnetic resonance
^{1}H-NMR	Proton nuclear magnetic resonance
Hz	Hertz
J	Coupling constant
K, K_a	Association contant
MLCT	Metal to ligand charge transfer
mmol	Millimole
MQA^{4+}	Macrotricyclic quaternary ammonium ions
pm	Picometer
ppm	Part per million

List of Schemes

List of Figures

List of Tables

CHAPTER I

INTRODUCTION

1.1 Role of anions

Anion coordination[1] and molecular recognition[2] of anionic substrates by synthetic receptor molecules have been much less studies than cation complexation despite the important role of anions in chemistry and in biology. Specific receptors which are capable of binding anionic guests are dependent on the characteristic features of anions such as negative charge, size, shape (Table 1.1) and pH dependence[3] (Table 1.2). Anions are of key importance across many fields as the following illustrative examples indicate:

1.1.1 Biologically, adenosine triphosphate (ATP)[4], the free energy of life process, is itself an anion bound by enzymes in order to perform its many metabolic functions. Deoxyribonucleic acid (DNA)[5] is also a polyanion. Its protein binding property is of great importance in transcription and translation processes.

1.1.2 Chemically, anions have various roles as nucleophiles, bases, redox mediators and phase-transfer catalysts.[6] Use of receptors to coordinate anions can alter their chemical reactivity[7] and may also be helpful for separating hazardous anions or stabilization of unstable anionic species.

1.1.3 Environmentally, anions are a pollution problem. In particular, the nitrate anion that used in fertilizers on agricultural land often pollutes river water to unacceptable levels.[8]

1.1.4 Medically, anions are of great importance in many disease pathways. Cystic fibrosis is caused by misregulation of chloride channels.[9] There is a real need for selective halide detection as established methods of chloride analysis are unsuitable for biological applications.[10] Cancer is caused by the uncontrolled replication of polyanionic DNA. Anion-binding proteins have also been implicated in the mechanism of Alzheimer's disease.[11]

Table 1.1 The size and geometry of various anions.[12]

Anions	Radius (pm)	Geometry
F^-	133	spherical
Cl^-	181	spherical
Br^-	196	spherical
I^-	220	spherical
NO_3^-	179	trigonal planar
CO_3^{2-}	178	trigonal planar
SO_3^{2-}	200	trigonal planar
$H_2PO_4^-$	200	tetrahedral
ClO_4^-	250	tetrahedral
SO_4^{2-}	230	tetrahedral
PO_4^{3-}	238	tetrahedral
$PdCl_6^{2-}$	319	octahedral

Table 1.2 The pK_A of inorganic acids.[13]

Inorganic acids		pK_A
HF		3.14
HCl		-3
HBr		-6
HI		-8
HNO_3		-1.32
HCN		9.40
HSCN		4
H_3AsO_3		9.22
H_3AsO_4	St 1	2.32
	St 2	7
	St 3	13
H_2CO_3	St 1[a]	6.52
	St 2	10.40
H_3PO_4	St 1	1.96
	St 2	7.12
	St 3	12.32
H_2SO_4	St 1	-3
	St 2	1.92

[a] Dehydration

1.2 Host-guest compounds[14]

In the beginning to describe modern host-guest chemistry,[15] it is useful to divide host compounds into two major classes according to the relative topological relationship between hosts and guests. *Cavitands* can be described as hosts possessing intramolecular cavities. This means that the cavity available for guest binding is an intrinsic molecular property of the host and exists both in solution and in the solid state. Conversely, *clathrands* are hosts with extramolecular cavities (the cavity essentially represents a gap between two or more host molecules) and is relevant only in the crystalline or solid state. The host-guest aggregate formed by a cavitand is termed *cavitate*, while clathrands form *clathrates*. The distinction between the two host classes is illustrated schematically in Figure 1.1.

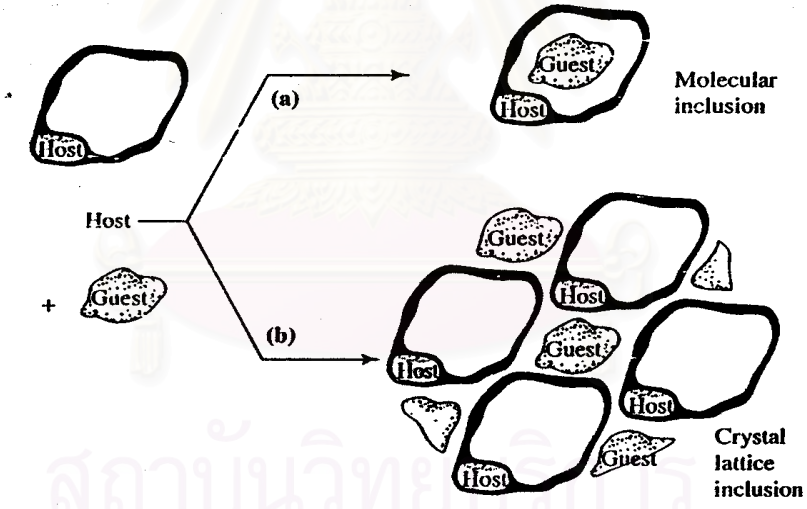

Figure 1.1 The difference between a cavitate (**a**) and a clathrate (**b**).

A further fundamental subdivision may be made on the basis of the forces between hosts and guests. If the host-guest aggregate is welded by primarily electrostatic force (including ion-dipole, dipole-dipole, hydrogen bonding etc.) the term ‘complex’ is used. On the other hand, species held together by less specific, nondirectional interactions, such as hydrophobic, van der Waals or crystal close-packing effects, then the terms ‘cavitate’ and ‘clathrate’ are more appropriate.

1.3 Design of anion receptors[16.17]

Anion receptors are divided into two classes:[18]

1.3.1 The positively charged receptors and/or organometallic receptors

The first synthetic anion receptor was based on a protonated nitrogen system. The source of interaction with anions in such a system is therefore two-fold: electrostatic attraction and hydrogen bonding.

1.3.1.1 Polyammonium receptors[19,20]

Kazuhiko Ichikawa and his coworker[21] designed four-macrotricyclic cage hosts (Figure 1.2) which had the characteristic feature of four positive binding sites converged to the center for the encapsulation and selectivity of halide ions.

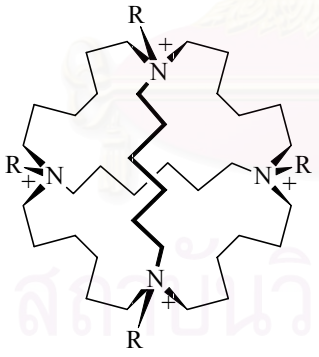

MQA^{4+} 666

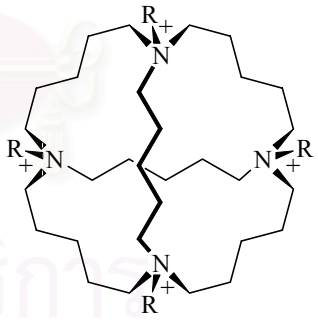

MQA^{4+} 555

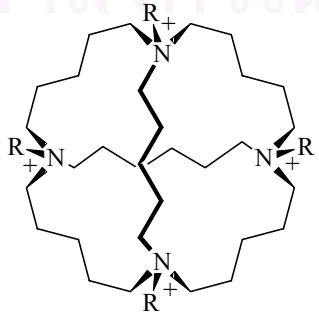

MQA^{4+} 556

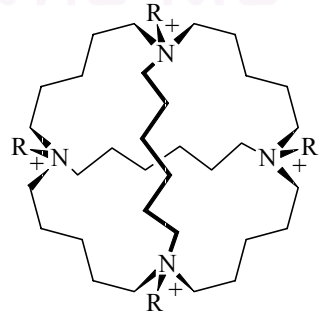

MQA^{4+} 566

Figure 1.2 Macrotricyclic ammonium cage hosts.

The selectivity of halide ions could be inferred from the intracavity diameters of the macrotricyclic quaternary ammonium ions (MQA^{4+}). The sizes of the intracavity can be calculated from CPK models: MQA^{4+} 555 (3.0 Å), MQA^{4+} 556 (3.5 Å), MQA^{4+} 566 (4.0 Å) and MQA^{4+} 666 (4.5Å). The MQA^{4+} 666 showed selectivity and complexibility toward iodide ion.[22-24] In case of a fluoride selective host MQA^{4+} 555 was inaccessible to other halide ions.[25] Crystal structures of $[(PhCH_2)N_4(C_5H_{10})_3(C_6H_{12})_3]^{4+}$, **b**, into which Cl^- was included, as well as the corresponding macrocyclic amine $N_4(C_5H_{10})_3(C_6H_{12})_3$, **a**, are shown in Figure 1.3. ^1H and ^{35}Cl-NMR data showed that the host **b** discriminated the two guest species and that chloride displace bromide from the cavity of the host: when $[Br^-] \leq [Cl^-]$ no encapsulated bromide ions occurred. The encapsulated chloride ion was held by the electrostatic potential of four positive units located at the corners of the distorted tetrahedral structure.

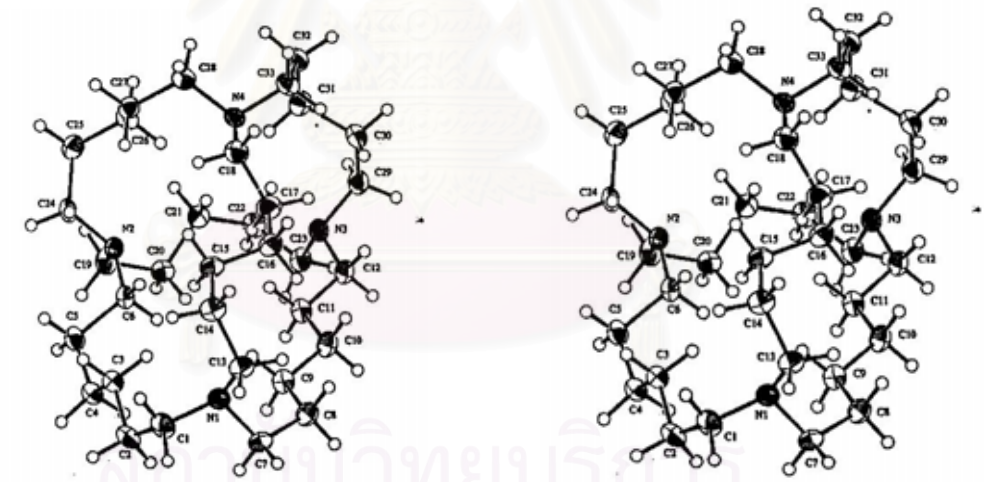

1) 2)

Figure 1.3 1) ORTEP representation of the structure of **a**.

2) ORTEP representation of the structure of **b**·Cl^-·$3H_2O$.

1.3.1.2 Guanidinium based receptors[26]

Unfortunately, the pH range over which they are protonated limits polyammonium hosts. This pH range is the same as that at which anions such as phosphate and carboxylate also begin to protonate. Consequently, the utility of this class of receptor was limited, thus causing the development of guanidinium based hosts.

Bicyclic guanidinium derivatives[27] had also been incorporated into *bis* (guanidinium) receptors capable of recognizing tetrahedral oxoanions, particularly polyphosphate residues of important biological molecules. The flexibility of receptor in Figure 1.4 allowed the two guanidinium arms to swing into a mutually perpendicular arrangement in order to effectively complex polyphosphates even in water. NMR data showed that this compound indeed formed 1:1 complexes.

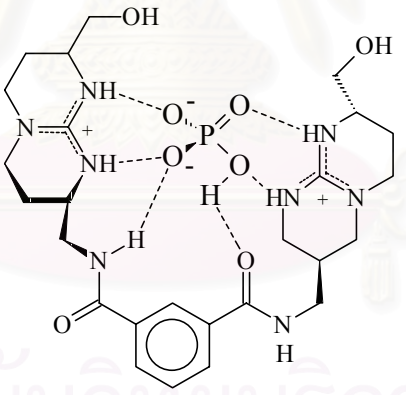

Figure 1.4 A bicyclic guanidinium derivative formed complex with polyphosphate anion.

However, the strength of anion binding was less than for analogous polyammonium systems, probably due to the greater charge delocalization across guanidinium.

1.3.1.3 Porphyrins[15,28]

Another method enabling protonation of a nitrogenous host molecule at accessible pH values has been developed based on the ease of protonation of expanded porphyrins. Sessler et al.[29,30] studied anion complexation ability of sapphyrin (Figure 1.5). A crystal structure of the diprotonated host with a bound anion, fluoride, is shown and fluoride was found to be in the plane of the macrocyclic ring. These readily protonated expanded porphyrin systems are now well established as receptors for fluoride anion.

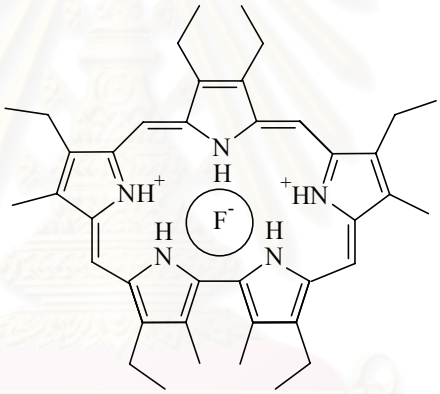

Figure 1.5 The complexation of sapphyrin with F^-.

1.3.1.4 Organometallic receptors[31,32]

Paul D. Beer and coworkers[6,33,34] have recently incorporated the Lewis-acidic redox and photo-active ruthenium(II) bipyridyl moiety, in combination with amide group, into lower-rim calix[4]arene structural frameworks to produce a new class of anion receptors with the dual capability of sensing anionic guest species via electrochemical and optical methods.

Calix[4]arene ruthenium(II) bipyridyl receptor (Figure 1.6) formed a complex with $H_2PO_4^-$ showing an important role of hydrogen bonding by X-ray crystallography. Determination of stability constant in DMSO demonstrated that this receptor formed a strong and highly selective complex with $H_2PO_4^-$. Substantial anion-induced cathodic perturbations of this ligand were detected in electrochemical anion recognition experiment. The results were in agreement with stability-constant values. The ligand was able to sense $H_2PO_4^-$ in the presence of ten-fold excess amounts of $H_2PO_4^-$ and Cl^-. Fluorescence emission spectroscopic measurements were also undertaken to probe anion bonding. This receptor exhibited significant blue shifts in the respective MLCT λ_{max} emission bands on addition of Cl^- and $H_2PO_4^-$. In case of upper-rim substitution calix[4]arenes functionalised with two ruthenium(II) bipyridylamide groups selectively sense $H_2PO_4^-$ by fluorescence emission and electrochemical responses.

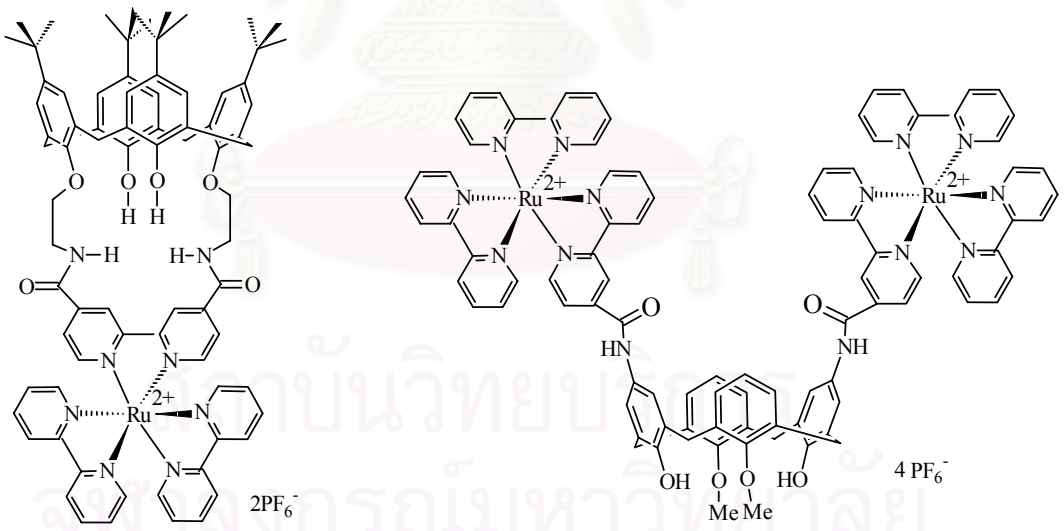

1) 2)

Figure 1.6 1) The structure of calix[4]arene ruthenium(II)bipyridyl.
2) The structure of bis-ruthenium(II)bipyridyl calix[4]arene.

1.3.2 The neutral anion receptors[35,36]

Another way of avoiding the problems of pH range and counterion competition is to use a neutral hydrogen-bonding receptor. David N. Reinhoudt and coworkers[37] described the synthesis of the macrocyclic and acyclic cleft-like anion receptors (Figure 1.7) in which four hydrogen bond donating urea moieties were present in a preorganized fashion. NMR spectroscopy showed the complex formation with $H_2PO_4^-$ and Cl^-. A cleft-like receptor (**A**) bound $H_2PO_4^-$ in a 2:1 guest-host stoichiometry by Job plot method ($K_a = 10^7\ M^{-2}$) in DMSO, whereas Cl^- was bound in a 1:1 stoichiometry ($K_a = 10^3\ M^{-1}$). The macrocyclic receptor (**B**) formed a 1:1 complex with $H_2PO_4^-$ ($K_a = 10^3\ M^{-1}$) in DMSO with a 100-fold selectivity for $H_2PO_4^-$ over Cl^-.

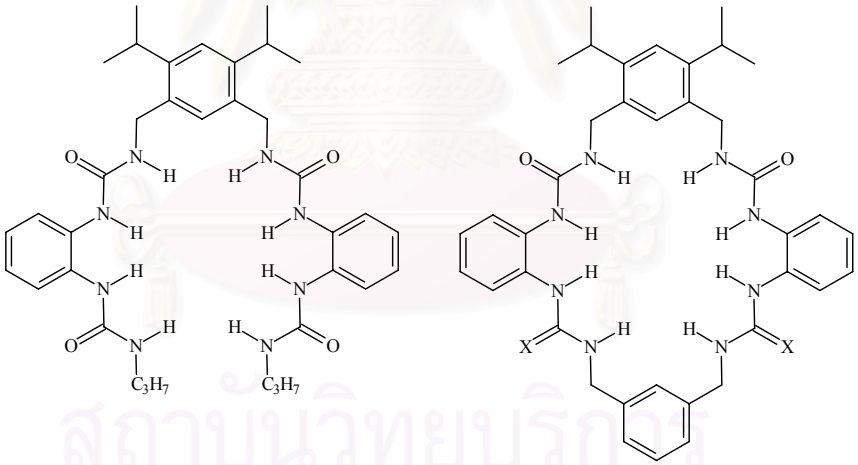

A **B**

Figure 1.7 Structure of an acyclic cleft-like (**A**) and a macrocyclic (**B**) neutral anion receptors.

1.4 Bifunctional cation-anion receptors [38]

Receptors containing two individual recognition units, one for a cation and one for an anion (Figure 1.8), have also been synthesized. A question of crucial importance with such ditopic ion pair receptors is whether the binding of the cation enhances the binding of the anion, or vice versa (cooperative recognition through favorable electrostatics). There are many applications that could stem from selectivity ion pair recognition, for example, enhanced extraction of toxic species from aqueous industrial waste, enabling environmental clean-up.

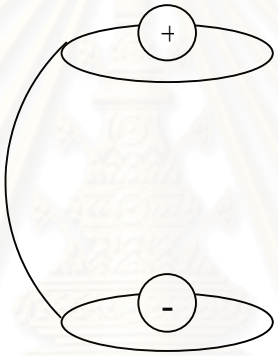

Figure 1.8 A receptor with individual cation and anion recognition sites.

Receptor **C**, synthesized by Reinhoudt and coworkers,[39] displays very elegant cation-anion cooperativity. The receptor consists of a calix[4]arene with cation binding ester groups at the lower rim and anion binding urea groups at the upper rim. In chloroform solution the two urea groups are hydrogen bonded together, and so are not available for hydrogen bonding to any putative anionic guest species. However when sodium cations are added, they bind the ester groups of the calixarene, causing the lower rim to contract. This force apart the urea groups at the upper rim apart which are then available for binding anionic species such as chloride (Scheme 1.1).

Scheme 1.1 Anion and cation cooperative binding in receptor **C**.

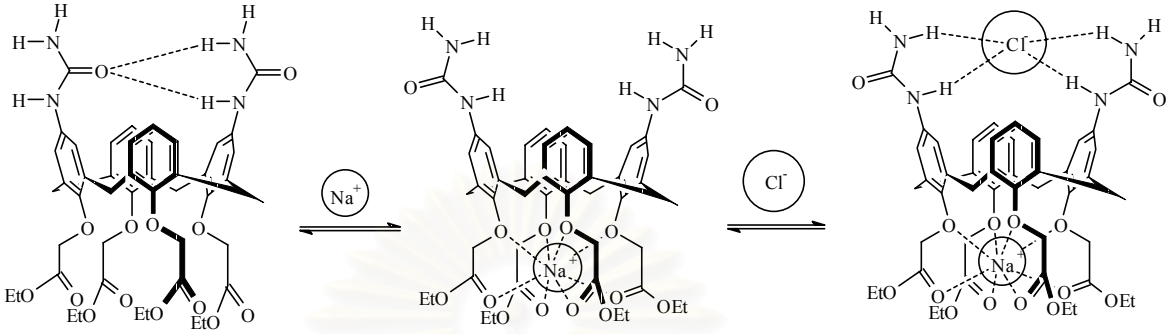

C **C-Na$^+$** **C-Na$^+$-Cl$^-$**

1.5 Nuclear magnetic resonance titration[40,41]

If the exchange of a complex and an uncomplexed guest is slow on the nuclear magnetic resonance (NMR) time scale, then the binding constant may be evaluated under the prevailing conditions of concentrate, temperature, solvent, etc. by simple integration of the NMR signals for bound hosts or guests. Most host-guest equilibria are fast in the NMR time scale, however the chemical shift observed for a particular resonance is a weighed average between the chemical shift of the free and bound species.

In a typical NMR titration experiment, a small aliquot of a guest may be added to a solution of host of known concentration in a deuterated solvent and the NMR spectrum of the sample monitored as a function of the guest concentration or a host : guest ratio. Commonly, changes in chemical shift ($\Delta\delta$) are noted for various atomic nuclei present as a function of the influence the guest binding has on their magnetic environment. As a result, two kinds of information are gained. Firstly, the location of nuclei most affected may give qualitative information about the regioselectivity of guest binding. More importantly, however, the shape of the titration curve plot of $\Delta\delta$ against added guest concentration in Figure 1.9 gives quantitative information about the binding constant. Such titration curves are often analyzed by computer least-squares curve fitting (e.g. by program such as EQNMR).[42]

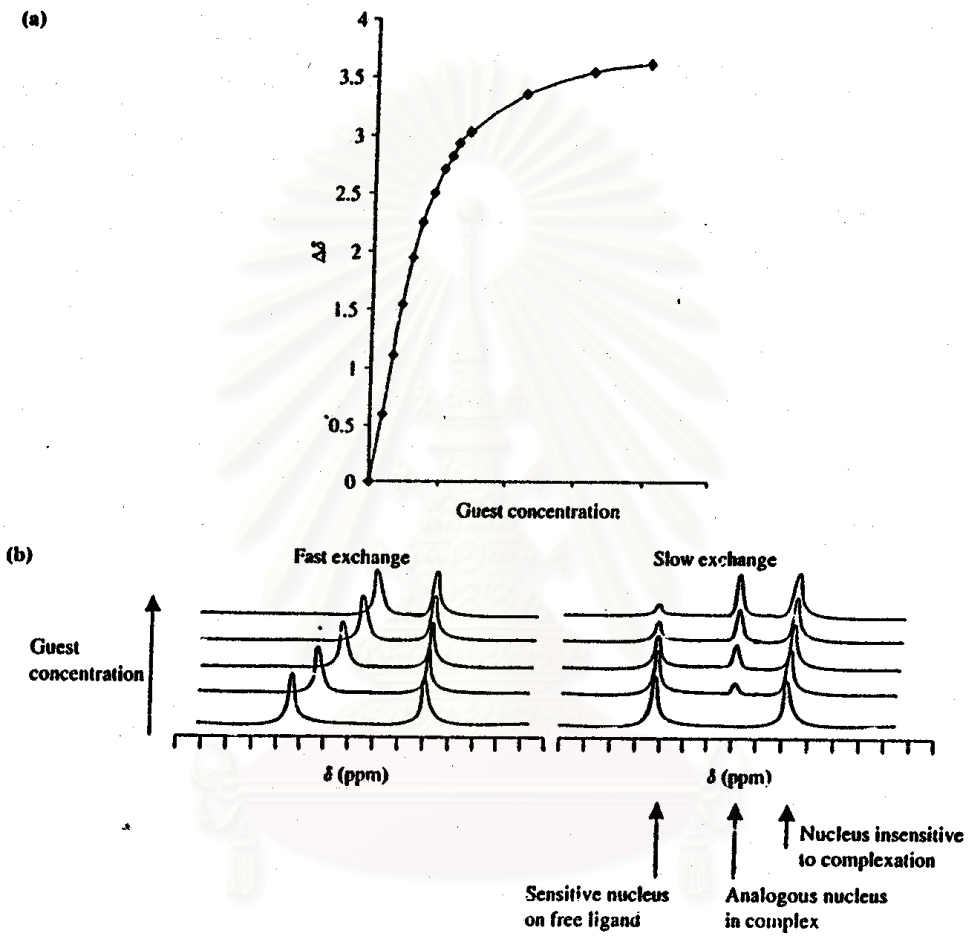

Figure 1.9 (a) NMR titration plot.
(b) Schematic NMR spectra.

1.6 Objective and scope of the research

The target of this thesis is to synthesize the cone conformation tetraaza calix[4] arene derivatives, **6a** and **6b** (Figure 1.10). These ligands consist of both cation and anion binding units in the same molecules. However, they have different cavity sizes for binding guests. The association constants towards various anions such as F^-, Br^-, I^-, NO_3^-, AsO_2^-, SO_4^{2-}, CO_3^{2-}, PO_4^{3-}, HPO_4^{2-} and $H_2PO_4^-$ will be determined. The relationship between cavity size of the ligands and anion binding ability can then be deduced. The effect of cations towards anion binding ability will also be investigated.

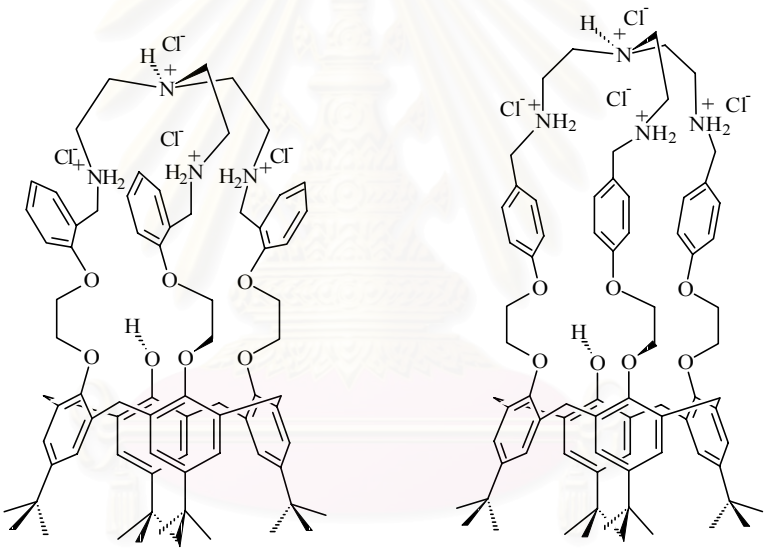

ortho substituted **6a** para substituted **6b**

Figure 1.10 The cone conformation tetraaza calix[4]arene derivatives, **6a** and **6b**.

CHAPTER II

EXPERIMENTAL SECTION

2.1 General procedure

2.1.1 Analytical instruments

The ^{1}H-NMR spectra were recorded on a Bruker ACF 200 MHz nuclear magnetic resonance spectrometer and 400 MHz on a Bruker DRX 400 spectrometer. In all cases, samples were dissolved in deuterated chloroform or methyl sulfoxide, and chemical shifts were recorded using a residual proton signal as internal reference.

Elemental analyses were analyzed on a Perkin Elmer CHON/S analyzer (PE2400 series II). Mass spectra were determined using VG-Analytical ZAB HF Mass Spectrometer. The ESI-TOF mass spectra were obtained from a Micromass LCT Mass Spectrometer and the electrospray ion trap mass spectra were recorded on a Bruker Mass Spectrometer. Melting points were taken on an Electrothermal 9100 apparatus. The FT-IR spectra were recorded on a Nicolet Impact 410 FT-IR spectrophotometer.

2.1.2 Materials for synthesis

All materials and reagents were standard analytical grade, purchased from BDH, Fluka, J.T. Baker or Merck, and used without further purification. Commercial grade solvents such as acetone, dichloromethane, ethyl acetate, hexane and methanol were distilled and stored over 4 Å molecular sieves. DMF was dried according to the published procedure and distilled before used.[43] Chromatographic separations were performed on silica gel column (kieselgel 60, 0.063-0.200 mm, Merck). Thin layer chromatography (TLC) was carried out using silica gel plates (kieselgel 60 F_{254}, 1 mm, Merck). *p-tert*-Butylcalix[4]arene (Figure A.1), **2**,[44] was prepared according to the literature.[45,46] The synthetic procedures of 4-(2′-bromoethoxy)benzaldehyde **1b**, 25,26,27-tri((4-ethoxy)benzaldehyde-*p-tert*-butylcalix[4]arene **4b**, 25,26,27-*N,N′,N″*-tri((4-ethoxy)benzyl)ethylenetriimine-*p-tert*-butylcalix[4]arene **5b**, 25,26,27-*N,N′,N″*-tri((4-ethoxy)benzyl)ethylenetetraamine-*p-tert*-butylcalix[4]arene·4HCl **6b** and 25,26,27-*N,N′,N″*-tri((4-ethoxy)benzyl)ethylenetetraamine-*p-tert*-butylcalix[4]arene **7b** have been reported by our research group.[47] All compounds were characterized by ^{1}H-NMR spectroscopy, mass spectrometry and elemental analysis.

2.2 Synthesis of calix[4]arene derivatives

2.2.1 Preparation of 2-(2′-bromoethoxy)benzaldehyde, 1a

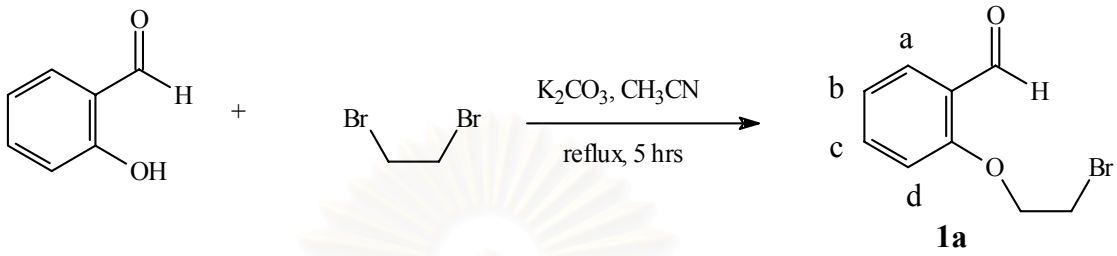

1a

Into a 1-L two-necked round bottom flask equipped with a magnetic bar and a reflux condenser, salicylaldehyde (14.80 g, 121.20 mmol), potassium carbonate (23.00 g, 167.40 mmol) and acetonitrile (200 mL) were mixed and stirred. Into the mixture, 1,2-dibromoethane (224.00 g, 1.1 mol) in acetonitrile (50 mL) was then added dropwise through an addition funnel over 30 minutes. The mixture was refluxed under nitrogen atmosphere for 5 hours and then allowed to cool to room temperature. The mixture was filtered, and the solid residue was washed with dichloromethane. The combined filtrate was evaporated to give a yellowish oily residue. It was then dissolved in 5% w/v aqueous solution of sodium hydroxide for eradicating all traces of salicyaldehyde, and the organic phase was dried over sodium sulfate anhydrous, filtered and evaporated to give a yellowish oil which was redissloved in dichloromethane. Hexane was then added into the yellowish solution to precipitate a yellowish solid. The yellowish solid was redissolved in a minimum amount of dichloromethane and the yellowish solution was eluted through a silica gel column with dichloromethane as eluent. The desired product, 2-(2′-bromoethoxy) benzaldehyde, **1a**, crystallized as white crystals by adding dichloromethane and hexane (16.29 g, 59 %).

Characterization data for 1a:

^{1}H-NMR spectrum ($CDCl_3$): δ (ppm) = 10.52 (s, 1H, -Ar(C=O)*H*); 7.83 (d, 1H, $J_{H\text{-}H}$ = 7.66 Hz, H_a); 7.53 (t, 1H, $J_{H\text{-}H}$ = 8.00 Hz, H_b); 7.04 (t, 1H, $J_{H\text{-}H}$ = 7.46 Hz, H_c); 6.94 (d, 1H, $J_{H\text{-}H}$ = 8.40 Hz, H_d); 4.39 (t, 2H, $J_{H\text{-}H}$ = 5.90 Hz, OCH_2CH_2Br); 3.69 (t, 2H, $J_{H\text{-}H}$ = 6.14 Hz, OCH_2CH_2Br) (Figure A.2).

2.2.2 Preparation of 25,26,27-tri((2-ethoxy)benzaldehyde-*p-tert*-butylcalix [4]arene, 4a

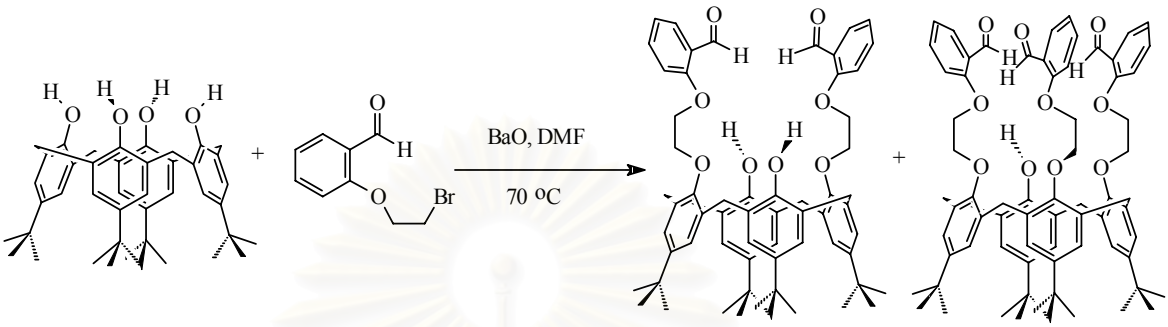

2 **3a** **4a**

Into a 250-mL two-necked round bottom flask equipped with a magnetic bar and a reflux condenser, a mixture of *p-tert*-butylcalix[4]arene , **2**, (6.05 g, 9.34 mmol), barium oxide (5.20 g, 33.90 mmol) and dry DMF (150 mL) was stirred for 1 hour. Into this mixture, 2-(2′-bromoethoxy)benzaldehyde, **1a**, (6.56 g, 28.64 mmol) in DMF (50 mL) was then added dropwise through an addition funnel. The mixture was stirred and heated at 70^0C under nitrogen atmosphere for 7 days. The reaction was allowed to cool to room temperature, and the solvent was evaporated under reduced pressure to give an orange-brown residue. The residue was dissolved in dichloromethane and it was then added 3M hydrochloric acid until the pH of the solution reached 1. The organic phase was separated, and the aqueous layer was extracted again with dichloromethane. The combined organic layer was dried over sodium sulfate anhydrous. After filtration of sodium sulfate, the solvent was removed to give an oily orange-brown residue. The residue was redissolved in a minimum amount of dichloromethane. The orange-brown solution was eluted through a silica gel column with dichloromethane as eluent. The 25,26,27-tri((2-ethoxy)benzaldehyde-*p-tert*-butylcalix[4]arene, **4a**, eluted out of the column after 25,27-di((2-ethoxy) benzaldehyde-*p-tert*-butylcalix[4]arene, **3a**.[48] White needle crystals of **4a** can be obtained by adding CH_3OH into its (CH_2Cl_2) solution (2.17 g, 21%).

Characterization data for 3a:

^{1}H-NMR spectrum ($CDCl_3$): δ (ppm) = 10.48 (s, 2H, -Ar(C=O)*H*)); 7.81 (d (J = 7.64 Hz), 2H, H_a); 7.53 and 7.49 (m, 2H, H_b); 7.45 (s, 2H, ArO*H*); 7.04-6.94 (m, 4H, H_c, H_d); 7.00 (s, 4H, HOAr*H*); 6.85 (s, 4H, ROAr*H*); 4.41-4.38 (m, 8H, OCH_2CH_2O); 4.29, 3.30 (d each, 8H, $J_{H\text{-}H}$ = 13 Hz, ArC$H_A H_B$Ar); 1.25 (s, 18H, HOAr-*t*-C_4H_9); 1.02 (s, 18H, ROAr-*t*-C_4H_9) (Figure A.3).

Characterization data for 4a:

^{1}H-NMR spectrum ($CDCl_3$): δ (ppm) = 10.41 and 9.74 (s each, 2H and 1H, -Ar(C=O)*H*); 7.63-6.32 (m, 20H, aromatic protons); 5.22 (s, 1H, ArO*H*); 4.90, 4.42 and 4.16 (m, 12H, -OCH_2CH_2O-); 4.24 and 3.29 (m, 4H each, ArC$H_A H_B$Ar); 1.36-0.82 (m, 36H, -Ar-*t*-C_4H_9) (Figure A.4).

FAB MS (m/z): 1092.5

Elemental analysis:

Anal. Cald. for **4a** ($C_{77}H_{80}O_{10}$): C,77.99; H, 7.37.

Found: C, 78.11; H, 7.17.

2.2.3 Preparation of 25,26,27-*N,N′,N″*-tri-((2-ethoxy)benzyl) ethylenetriimine-*p-tert*-butylcalix[4]arene, 5a

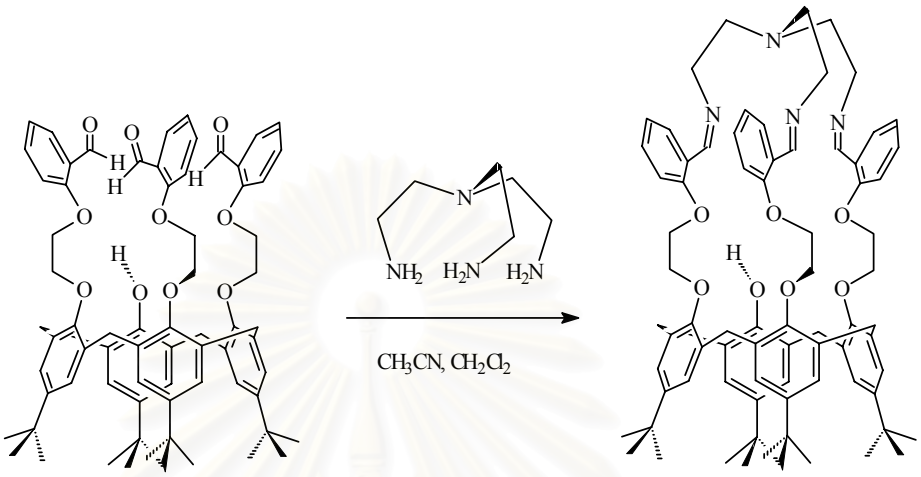

4a **5a**

Into a 500-mL two-necked round bottom flask equipped with a magnetic bar and a reflux condenser, a mixture of 25,26,27-tri((2-ethoxy)benzaldehyde-*p-tert*-butylcalix[4]arene, **4a**, (1.00 g, 0.92 mmol) and acetonitrile (250 mL) was stirred. Into this mixture, tris(2-amino)ethylamine (0.16 g, 1.10 mmol) in dichloromethane (10 mL) and acetronitrile (50 mL) was then added dropwise through an addition funnel over 30 minutes. The mixture was refluxed under nitrogen atmosphere for 8 hours. White solid precipitated from the solution. The mixture was allowed to cool to room temperature and filtered. The white solid residual of **5a** was washed with acetronitrile and dried *in vacuo* (1.03 g, 95 %).

Characterization data for 5a:

^{1}H-NMR spectrum ($CDCl_3$): δ (ppm) = 8.93 and 8.83 (s each, 1H and 2H, -C*H*=N-); 7.91-6.45 (m, 20H, aromatic protons); 5.30 (s, 1H, -ArO*H*); 5.16, 4.53 and 4.04 (m, 12H, -OCH_2CH_2O); 2.89 (m, 12H, -NCH_2CH_2N-); 4.39 and 4.33, 3.39 and 3.32 (d each, 2H each, $J_{H\text{-}H}$ = 13 Hz, ArC$H_A H_B$Ar); 1.36, 1.27 and 0.79 (s each, 9H, 9H and 18H, ROAr-*t*-C$_4H_9$ and HOAr-*t*-C$_4H_9$ (Figure A.5).

FAB MS (m/z): 1185.7

Elemental analysis:

Anal. Cald. for **5a**·H_2O ($C_{77}H_{94}N_4O_8$): C, 76.84; H, 7.87; N, 4.65.

Found: C, 76.70; H, 7.61; N, 4.24.

2.2.4 Preparation of 25,26,27-*N,N′,N″*-tri((2-ethoxy)benzyl) ethylenetetraamine-*p-tert*-butylcalix[4]arene·4HCl, 6a

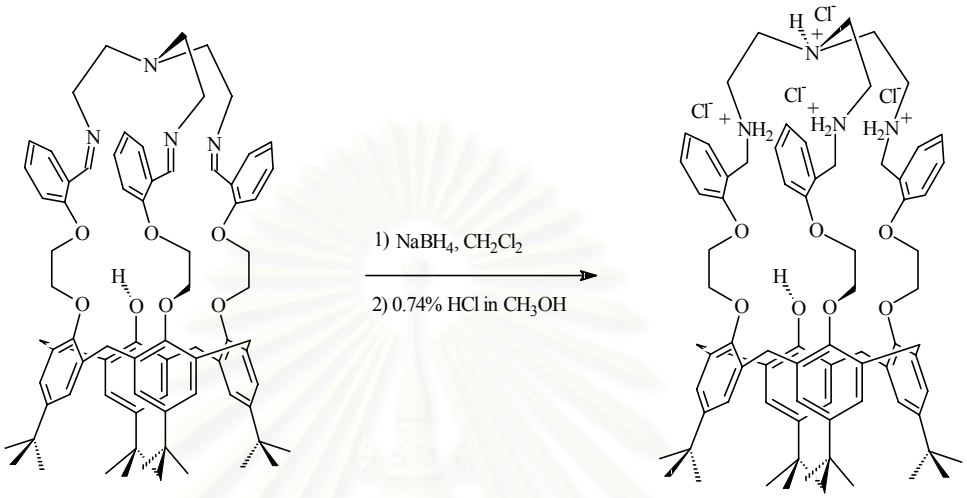

5a **6a**

Into a 500-mL one-necked round bottom flask equipped with a magnetic bar and a reflux condenser, 25,26,27-*N,N′,N″*-tri-((2-ethoxy)benzyl)ethylenetriimine-*p-tert*-butylcalix[4]arene, **5a**, (1.00 g, 0.84 mmol) was dissolved in dry dichloromethane (50 mL). The solution was added excess sodium borohydride (0.63 g, 0.02 mmol) and stirred overnight under nitrogen atmosphere. A copious amount of deionized water was then added to destroy excess sodium borohydride. The organic phase was separated and washed again with deionized water until the pH of the aqueous layer became neutral. The combined organic layer was dried over sodium sulfate anhydrous. After filtration of sodium sulfate, the solvent was removed to dryness. The solid residue was dissolved in a minimum amount of methanol and acidified with 0.74% V/V hydrochloric acid in methanol until the pH of the solution reach 1. Upon slow evaporation of the solvent, the white crystals of **6a** were precipitated (0.92 g, 81 %).

Characterization data for 6a:

^{1}H-NMR spectrum (DMSO-d_6) δ (ppm) = 9.78 and 9.38 (s each, broad, 4H and 2H, $ArCH_2NH_2^+Cl^-$); 7.86, 7.66, 7.57, 7.34 and 7.03 (m, 12H, H_a, H_b, H_c and H_d); 7.17 and 7.11 (s each, 2H each, ROAr*H* and HOAr*H*); 6.54 and 6.46 (s each, 2H each, ROAr*H*); 5.80 (s, 1H, ArO*H*); 5.13 (m, broad, 2H, OCH_2CH_2O); 4.62-4.39 (m, 6H, $H_2N^+CH_2$-Ar and 4H, $ArCH_2Ar$); 4.18 (m, broad, 10 H, OCH_2CH_2O and 4H, $ArCH_2Ar$); 2.82-2.75 (m, 12H, $^+NHCH_2CH_2N^+H_2$); 1.30, 1.20 and 0.73 (s each, 9H, 9H and 18H, HOAr-*t*-C_4H_9 and ROAr-*t*-C_4H_9) (Figure A.6)

TOF MS (m/z): 1192.1(Figure A.7)

Elemental analysis:

Anal. Cald. for **6a**·$4H_2O$ ($C_{77}H_{110}N_4Cl_4O_{11}$): C, 65.69; H, 8.44; N, 3.78.
Found: C, 65.61; H, 7.87; N, 3.97.

2.2.5 Preparation of 25,26,27-*N,N′,N″*-tri((2-ethoxy)benzyl) ethylenetetraamine-*p-tert*-butylcalix[4]arene, 7a

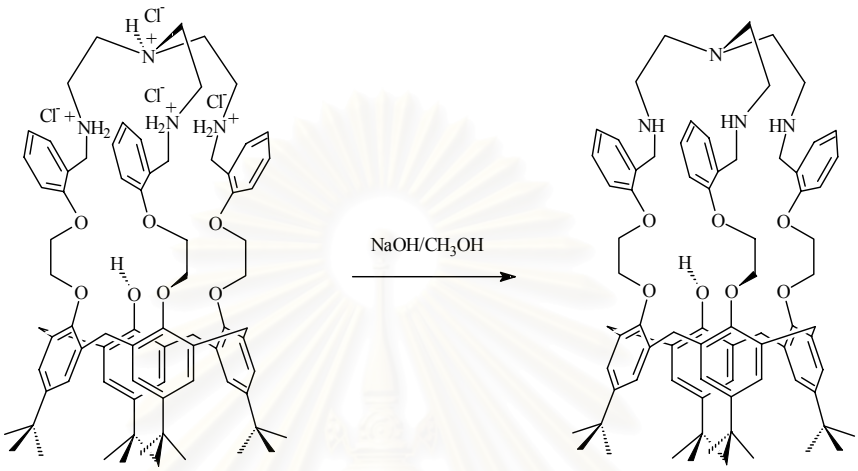

6a **7a**

Into a 50-mL round bottom flask equipped with a magnetic bar, 25,26,27-*N,N′,N″*-tri-((2-ethoxy)benzyl)ethylenetetraamine-*p-tert*-butylcalix[4]arene·4HCl, **6a**, (0.10 g, 0.07 mmol) was dissolved in dry methanol (30 mL). NaOH solution (CH_3OH) was then slowly added until the pH of the solution reached 10. The reaction was stirred under nitrogen atmosphere for 1 hour. The solvent was subsequently removed under reduced pressure. The residue was redissolved in dichloromethane and extracted with deionized water until the aqueous phase contained no Cl^-. The organic layer was then dried over sodium sulfate anhydrous and concentrated on a rotary evaporator. Upon slow evaporation of the solvent, the white solid of **7a** (Figure A.8 in DMSO-d_6) precipitated (0.06 g, 72 %).

Characterization data for 7a

^{1}H-NMR spectrum (4OO MHz, $CDCl_3$) δ(ppm) = 7.20 and 6.56 (s each, 4H, *t*-C(CH_3)$_3$Ar*H*CH_2-); 7.47, 7.15, 6.93 and 6.25 (m, 12 H, -Ar*H*OCH_2-); 5.19 (s, 1H, -ArO*H*); 4.98,4.32, 4.03 and 3.86 (m, 12H, -O*C*H_2C*H*$_2$O-); 4.18 and 3.75 (d, 2H and 4H, J_{H-H} = 14 Hz, ArC*H*$_2$NR); 7.34 (t, 3H, H_c aromatic); 4.85, 4.45, 3.37 and 3.23 (d, 2H each, J_{H-H} = 13 Hz, ArCH_ACH_BAr); 2.66-1.99 (m, broad, 12H, RNCH_2CH_2NR); 1.41, 1.39 and 0.86 (s each, 9H, 9H and 18H, HOAr-*t*-C_4H_9 and ROAr-t-C_4H_9) (Figure A.9)

FAB MS (m/z): 1191.7

Elemental analysis:

Anal. Cald. for **7a** ($C_{77}H_{98}N_4O_7$): C, 77.61; H, 8.29; N, 4.70.

Found: C, 77.57; H, 7.85; N, 4.32.

2.3 X-ray crystallography

The crystal of **6a** was mounted on the end of a hollow glass fiber approximately parallel to the long dimension of the crystal using cyanoacrylate glue. Preliminary examination and data collection were performed using MoK_α X-radiation (λ = 0.71073 Å) on Bruker AXS SMART area detector diffractrometer. The program used to solve the structures was SHELX86. Data were corrected for Lorentz and polarization effects. The structures were solved by full-matrix least squares on F^2 refinement method. All hydrogen atoms were in calculated positions and their parameter fixed during the refinement. Crystallographic parameters for [**6a**-$2Cl^-$]$(Cl^-)_2(OH^-)_2\cdot(CH_3OH)\cdot(H_2O)_2$ are described in Table 2.1.

Table 2.1. Crystal data and structure refinement details for compound [**6a**-$2Cl^-$]$(OH^-)_2$ $\cdot(CH_3OH)\cdot(H_2O)_2$.

empirical formula	$C_{78}H_{112}Cl_2N_4O_{12}$
fw	1368.69
T, K	293(2)
λ, Å	0.71073
crystal system	Monoclinic
space group	C_2/c
a (Å)	43.6552(14)
B (Å)	15.9085(5)
C (Å)	25.1856(7)
α (deg)	90
β (deg)	109.4630(10)
γ (deg)	90
V ($Å^3$)	16491.6(9)
Z	8
ρ (cald) (Mg/m^3)	1.119
abs coffe (μ, mm^{-1})	0.136

Table 2.1. (continued) Crystal data and structure refinement details for compound [**6a**-2Cl^-]$(OH^-)_2$·(CH_3OH)·$(H_2O)_2$.

F(000)	5976
Crystal size (mm)	0.20 x 0.20 x 0.10
θ range for data collection (deg)	0.99 - 30.46
Limiting indices	-56<=h<=60
	-22<=k<=12
	-34<=l<=31
Reflections collected / unique	58283 / 23606
	[R(int) = 0.0954]
Data	23606
Restraints	45
Parameters	884
Goodness-of-fit on F^2	1.058
final R indices [I>2σ(I)]	R1 = 0.1325
	wR2 = 0.3401
R indices (all data)	R1 = 0.3067
	wR2 = 0.4376
Largest diff. peak and hole (e.A^{-3})	1.059 and -0.570

2.4 Inclusion studies

2.4.1 Apparatus

One-dimensional proton NMR spectra were taken on a Bruker ACF 200 MHz and 400 MHz on a Bruker DRX 400 nuclear magnetic resonance spectrometer. For anion complexation studies in case of **6a**, with arsenite, bromide, carbonate, fluoride, hydrogen phosphate, hydrogen phosphate, iodide, nitrate, sulfate and phosphate anion, spectra were recorded in methyl sulfoxide-d_6 (DMSO-d_6) and using a residual proton signal as internal standard. Another ligand, **6b**, was studied with various of anions such as arsenite, bromide, carbonate, fluoride, hydrogen phosphate, hydrogen phosphate, iodide, nitrate, sulfate and phosphate anion. Spectra were recorded in the mixture of chloroform-*d* and methanol-d_4 (1:1) with chemical shifts referred to a residual proton signal.

2.4.2 Experimental procedures of inclusion studies with ligand 6a

2.4.2.1 Anion complexation of ligand 6a with sodium bromide, sodium iodide and sodium nitrate

Typically, a 0.0250 M solution of ligand **6a** (0.0836 g, 0.0625 mmol) in DMSO-d_6 (2.50 mL) was prepared. To 0.20 mL of this solution in NMR tubes were added 0.0-4.0 equivalents of 0.1000 M sodium salts (0.1500 mmol) in DMSO-d_6 (1.50 mL), which showed in Table 2.2. In each NMR tube, the amount of DMSO-d_6 was then adjusted to the same quantity. The spectra were recorded every 24 hours until the complexation reached the equilibrium.

Table 2.2 Volume of sodium salt solution and the ligand **6a** used to prepare various sodium salt:ligand **6a** ratios.

Mole ratio of sodium salt:ligand **6a**	Volume of (mL)		
	0.1000 M Na salt in DMSO-d_6	0.0250 M ligand **6a** in DMSO-d_6	DMSO-d_6
0.0 : 1.0	0.00	0.20	0.20
0.2 : 1.0	0.01	0.20	0.19
0.4 : 1.0	0.02	0.20	0.18
0.6 : 1.0	0.03	0.20	0.17
0.8 : 1.0	0.04	0.20	0.16
1.0 : 1.0	0.05	0.20	0.15
1.2 : 1.0	0.06	0.20	0.14
1.4 : 1.0	0.07	0.20	0.13
2.0 : 1.0	0.10	0.20	0.10
2.4 : 1.0	0.12	0.20	0.08
3.0 : 1.0	0.15	0.20	0.05
4.0 : 1.0	0.20	0.20	0.00

2.4.2.2 Anion complexation of ligand 6a with sodium fluoride, sodium arsenite, sodium carbonate, sodium sulfate, sodium phosphate, sodium dihydrogen phosphate and sodium hydrogen phosphate

Typically, excess sodium salts were brought into NMR tubes. A 0.0250 M solution of ligand **6a** (0.1003 g, 0.0750 mmol) in DMSO-d_6 (3.00 mL) was prepared and 0.40 mL of this solution was added in each NMR tube (Table 2.3). ^{1}H-NMR spectra were then recorded every 24 hours until the complexation reached the equilibrium.

Table 2.3 Amount of various salts and the ligand **6a** used to prepare various salts:ligand **6a** ratios.

Type of sodium salt	Mole ratio of salt:ligand **6a**	Weight of sodium salts (g)	Ligand **6a** in DMSO-d_6 (mL)
NaF	15.0 : 1.0	0.0063	0.40
$NaAsO_2$	15.0 : 1.0	0.0195	0.40
Na_2CO_3	15.0 : 1.0	0.0159	0.40
Na_2SO_4	15.0 : 1.0	0.0213	0.40
$Na_3PO_4 \cdot 12H_2O$	15.0 : 1.0	0.0570	0.40
$NaH_2PO_4 \cdot H_2O$	15.0 : 1.0	0.0207	0.40
Na_2HPO_4	15.0 : 1.0	0.0213	0.40

2.4.2.3 Anion complexation of ligand 6a with tetrabutylammonium bromide and tetrabutylammonium iodide

Typically, a 0.0250 M solution of ligand **6a** (0.0836 g, 0.0625 mmol) in DMSO-d_6 (2.50 mL) was prepared. To 0.20 mL of this solution in NMR tubes were added 0.0-4.0 equivalents of 0.1000 M tetrabutylammonium salts (0.1500 mmol) in DMSO-d_6 (1.50 mL), which showed in Table 2.4. In each NMR tube, the amount of DMSO-d_6 was adjusted to the same quantity. The spectra were then recorded every 24 hours until the complexation reached the equilibrium.

Table 2.4 Volume of the sodium salt and the ligand **6a** used to prepare various tetrabutylammonium salt:ligand **6a** ratios.

Mole ratio of Salt:ligand **6a**	Volume of (mL)		
	0.1000 M salt in DMSO-d_6	0.0250 M ligand **6a** in DMSO-d_6	DMSO-d_6
0.0 : 1.0	0.00	0.20	0.20
0.2 : 1.0	0.01	0.20	0.19
0.4 : 1.0	0.02	0.20	0.18
0.6 : 1.0	0.03	0.20	0.17
0.8 : 1.0	0.04	0.20	0.16
1.0 : 1.0	0.05	0.20	0.15
1.2 : 1.0	0.06	0.20	0.14
1.4 : 1.0	0.07	0.20	0.13
2.0 : 1.0	0.10	0.20	0.10
2.4 : 1.0	0.12	0.20	0.08
3.0 : 1.0	0.15	0.20	0.05
4.0 : 1.0	0.20	0.20	0.00

2.4.2.4 Anion complexation of ligand 6a with potassium bromide and potassium iodide

Typically, a 0.0250 M solution of ligand **6a** (0.0836 g, 0.0625 mmol) in DMSO-d_6 (2.50 mL) was prepared. To 0.20 mL of this solution in NMR tubes were added 0.0-4.0 equivalents of 0.1000 M potassium salts (0.1500 mmol) in DMSO-d_6 (1.50 mL) as showed in Table 2.5. In each NMR tube, the amount of DMSO-d_6 was adjusted to the same quantity. The spectra were then recorded every 24 hours until the complexation reached the equilibrium.

Table 2.5 Volume of the potassium salt solution and the ligand **6a** used to prepare various potassium salt:ligand **6a** ratios.

Mole ratio of potassium salt:ligand **6a**	Volume of (mL)		
	0.1000 M Na salt in DMSO-d_6	0.0250 M ligand **6a** in DMSO-d_6	DMSO-d_6
0.0 : 1.0	0.00	0.20	0.20
0.2 : 1.0	0.01	0.20	0.19
0.4 : 1.0	0.02	0.20	0.18
0.6 : 1.0	0.03	0.20	0.17
0.8 : 1.0	0.04	0.20	0.16
1.0 : 1.0	0.05	0.20	0.15
1.2 : 1.0	0.06	0.20	0.14
1.4 : 1.0	0.07	0.20	0.13
2.0 : 1.0	0.10	0.20	0.10
2.4 : 1.0	0.12	0.20	0.08
3.0 : 1.0	0.15	0.20	0.05
4.0 : 1.0	0.20	0.20	0.00

2.4.3 Experimental procedures of inclusion studies with ligand 6b

2.4.3.1 Anion complexation of ligand 6b with sodium bromide, sodium iodide and sodium nitrate

Typically, a 0.1000 M solution of a sodium salt (0.1500 mmol) in CD_3OD (1.50 mL) was prepared. Ligand **6b** was brought into the NMR tubes and 0.0-4.0 equivalents of 0.1000 M sodium salt were added. In each NMR tube, the amount of the solvents was adjusted to the same quantity as shown in Table 2.6. The spectra were then recorded every 24 hours until the complexation reached the equilibrium.

Table 2.6 Amount of the sodium salt and the ligand **6b** used to prepare various sodium salt:ligand **6b** ratios.

Mole ratio of sodium salt:ligand **6b**	0.1000 M Na salt in CD_3OD (mL)	Ligand **6b** (mmol)	$CDCl_3$ (mL)	CD_3OD (mL)
0.0 : 1.0	0.00	0.0050	0.30	0.30
0.2 : 1.0	0.01	0.0050	0.30	0.29
0.4 : 1.0	0.02	0.0050	0.30	0.28
0.6 : 1.0	0.03	0.0050	0.30	0.27
0.8 : 1.0	0.04	0.0050	0.30	0.26
1.0 : 1.0	0.05	0.0050	0.30	0.25
1.2 : 1.0	0.06	0.0050	0.30	0.24
1.4 : 1.0	0.07	0.0050	0.30	0.23
2.0 : 1.0	0.10	0.0050	0.30	0.20
2.4 : 1.0	0.12	0.0050	0.30	0.18
3.0 : 1.0	0.15	0.0050	0.30	0.15
4.0 : 1.0	0.20	0.0050	0.30	0.10

2.4.3.2 Anion complexation of ligand 6b with sodium carbonate, sodium phosphate and sodium arsenite

Typically, a 0.0083 M solution of a ligand (0.3344 g, 0.2500 mmol) in dry $CHCl_3$ (30 mL) was prepared. A sodium salt (0.0-10.0 equivalents) was added into 1.8 mL of ligand solution at various ratios (Table 2.7). The mixture was stirred at room temperature for 48 hours. Non-soluble material was separated by filtration, and the supernatant was evaporated under reduced pressure. The residual was dissolved in $CDCl_3$ and ^{1}H-NMR spectra were recorded.

Table 2.7 Amount of the sodium salt and the ligand **6b** used to prepare various sodium salt:ligand **6b** ratios.

Mole ratio of sodium salt:ligand **6b**	Sodium salt (mmol)	0.0083 M ligand **6b** in $CDCl_3$ (mL)
0.0 : 1.0	0.00	1.80
0.2 : 1.0	3.0×10^{-6}	1.80
0.4 : 1.0	6.0×10^{-6}	1.80
0.6 : 1.0	9.0×10^{-6}	1.80
0.8 : 1.0	1.2×10^{-5}	1.80
1.0 : 1.0	1.5×10^{-5}	1.80
1.2 : 1.0	1.8×10^{-5}	1.80
1.4 : 1.0	2.1×10^{-5}	1.80
2.0 : 1.0	3.0×10^{-5}	1.80
2.4 : 1.0	3.6×10^{-5}	1.80
3.0 : 1.0	4.5×10^{-5}	1.80
4.0 : 1.0	6.0×10^{-5}	1.80
6.0 : 1.0	9.0×10^{-5}	1.80
8.0 : 1.0	1.2×10^{-4}	1.80
10.0 : 1.0	1.5×10^{-4}	1.80

2.4.3.3 Anion complexation of ligand 6b with sodium dihydrogen phosphate

Ligand **6b** (0.0067 g, 0.0050 mmol) and 0.0-4.0 equivalents of sodium dihydrogen phosphate were brought into the NMR tubes. In each NMR tube, the amount of solvents was adjusted to the same quantity as shown in Table 2.8. ^{1}H-NMR spectra were then recorded every 24 hours until the complexation reached the equilibrium.

Table 2.8 Amount of sodium dihydrogen phosphate and the ligand **6b** used to prepare various sodium dihydrogen phosphate:ligand **6b** ratios.

Mole ratio of $Na_2HPO_4 \cdot H_2O$:ligand **6b**	Na_2HPO_4 (mmol)	Ligand **6b** (mmol)	$CDCl_3$ (mL)	CD_3OD (mL)
0.0 : 1.0	0.00	0.0050	0.30	0.30
0.2 : 1.0	1.0×10^{-6}	0.0050	0.30	0.30
0.4 : 1.0	2.0×10^{-6}	0.0050	0.30	0.30
0.6 : 1.0	3.0×10^{-6}	0.0050	0.30	0.30
0.8 : 1.0	4.0×10^{-6}	0.0050	0.30	0.30
1.0 : 1.0	5.0×10^{-6}	0.0050	0.30	0.30
1.2 : 1.0	6.0×10^{-6}	0.0050	0.30	0.30
1.4 : 1.0	7.0×10^{-6}	0.0050	0.30	0.30
2.0 : 1.0	1.0×10^{-5}	0.0050	0.30	0.30
2.4 : 1.0	1.2×10^{-5}	0.0050	0.30	0.30
3.0 : 1.0	1.5×10^{-5}	0.0050	0.30	0.30
4.0 : 1.0	2.0×10^{-5}	0.0050	0.30	0.30

2.4.3.4 Anion complexation of ligand 6b with sodium fluoride, sodium hydrogen phosphate and sodium sulfate

Typically, ligand **6b** (0.0100 g, 0.0075 mmol) and the excess of various sodium salts were brought into the NMR tubes. In each NMR tube, the amount of solvents was adjusted to the same quantity as showed in Table 2.9. The ^{1}H-NMR spectra were then recorded every 24 hours until the complexation reached the equilibrium.

Table 2.9 Amount of various salts and the ligand **6b** used to prepare various salts:ligand **6b** ratios.

Type of sodium salt	Mole ratio of salt:ligand **6b**	Weight of Na salts (g)	Weight of ligand (g)	$CDCl_3$ (mL)	CD_3OD (mL)
NaF	15.0 : 1.0	0.0047	0.0100	0.30	0.30
$Na_2HPO_4 \cdot H_2O$	15.0 : 1.0	0.0155	0.0100	0.30	0.30
Na_2SO_4	15.0 : 1.0	0.0160	0.0100	0.30	0.30

2.4.3.5 Anion complexation of ligand 6b with tetrabutylammonium bromide and tetrabutylammonium iodide

A 0.1000 M solution of the tetrabutylammonium salt (0.1500 mmol) in CD_3OD (1.50 mL) was prepared. Ligand **6b** was brought into the NMR tubes and 0.0-4.0 equivalents of 0.1000 M tetrabutylammonium salt were added. In each NMR tube, the amount of $CDCl_3$ and CD_3OD were adjusted to the same quantity as shown in Table 2.10. The ^{1}H-NMR spectra were then recorded every 24 hours until the complexation reached the equilibrium.

Table 2.10 Amount of solution of a sodium salt and a ligand **6b** used to prepare various tetrabutylammonium salt:ligand **6b** ratios.

Mole ratio of $C_{16}H_{36}IN$:ligand **6b**	0.1000 M $C_{16}H_{36}IN$ in CD_3OD (mL)	Ligand **6b** (mmol)	$CDCl_3$ (mL)	CD_3OD (mL)
0.0 : 1.0	0.00	0.0050	0.30	0.30
0.2 : 1.0	0.01	0.0050	0.30	0.29
0.4 : 1.0	0.02	0.0050	0.30	0.28
0.6 : 1.0	0.03	0.0050	0.30	0.27
0.8 : 1.0	0.04	0.0050	0.30	0.26
1.0 : 1.0	0.05	0.0050	0.30	0.25
1.2 : 1.0	0.06	0.0050	0.30	0.24
1.4 : 1.0	0.07	0.0050	0.30	0.23
2.0 : 1.0	0.10	0.0050	0.30	0.20
2.4 : 1.0	0.12	0.0050	0.30	0.18
3.0 : 1.0	0.15	0.0050	0.30	0.15
4.0 : 1.0	0.20	0.0050	0.30	0.10

2.4.3.6 Anion complexation of ligand 6b with potassium bromide and potassium iodide

Typically, a 0.1000 M solution of a sodium salt (0.1500 mmol) in CD_3OD (1.50 mL) was prepared. Ligand **6b** was brought into the NMR tubes and 0.0-4.0 equivalents of 0.1000 M potassium salts were added. In each NMR tube, the amount of solvents was adjusted to the same quantity as shown in Table 2.11. The ^{1}H-NMR spectra were then recorded every 24 hours until the complexation reached the equilibrium.

Table 2.11 Amount of solution of a potassium salt and a ligand **6b** used to prepare various potassium salt:ligand **6b** ratios.

Mole ratio of potassium salt:ligand **6b**	0.1000 M Na salt in CD_3OD (mL)	Ligand **6b** (mmol)	$CDCl_3$ (mL)	CD_3OD (mL)
0.0 : 1.0	0.00	0.0050	0.30	0.30
0.2 : 1.0	0.01	0.0050	0.30	0.29
0.4 : 1.0	0.02	0.0050	0.30	0.28
0.6 : 1.0	0.03	0.0050	0.30	0.27
0.8 : 1.0	0.04	0.0050	0.30	0.26
1.0 : 1.0	0.05	0.0050	0.30	0.25
1.2 : 1.0	0.06	0.0050	0.30	0.24
1.4 : 1.0	0.07	0.0050	0.30	0.23
2.0 : 1.0	0.10	0.0050	0.30	0.20
2.4 : 1.0	0.12	0.0050	0.30	0.18
3.0 : 1.0	0.15	0.0050	0.30	0.15
4.0 : 1.0	0.20	0.0050	0.30	0.10

CHAPTER III

RESULTS AND DISCUSSION

3.1 Synthesis and characterization of *p-tert*-butylcalix[4]arene derivatives

It is our interest to combine a *p-tert*-butylcalix[4]arene framework with a cage constructing unit to form a compound that can simultaneously bind metal ions and anions. Ligands **6a** and **6b** are ditopic ion receptors containing both 4 nitrogen donors and 6 oxygen donors. The molecules have positive charges on ammonium moieties that are well-known to bind anions.[15,20,49] In addition, they can possibly accommodate metal ions in the cavity of phenolic oxygen donors similar to a cryptand.[50] Thus both **6a** and **6b** can possibly exhibit appealing host-guest chemistry with both metal ions and anions.

In the past, the synthesis of the trialdehyde derivative of *p-tert*-butylcalix[4] arene, **4a**[51] was prepared from a nucleophilic substitution reaction of **2** with 2.7 equivalents of **1a** in the presence of K_2CO_3 in acetronitrile. However, a low yield of **4a** was obtained. Therefore, the new pathway is developed and described in this thesis.

The synthesis of compound **6a** was carried out as shown in Scheme 3.1. In the first step, **4a,** was prepared by a nucleophilic substitution reaction of **2** with **1a** in the presence of BaO as base and DMF as solvent for 7 days. Both dialdehyde calix[4] arene, **3a**, and trialdehyde calix[4]arene, **4a**, were obtained and purified by silica gel chromatography using CH_2Cl_2 as eluent. The yields of **3a** and **4a** are 25% and 21%, respectively. The compound **4a** was characterized by spectroscopy and elemental analysis. The ^{1}H-NMR spectrum of **3a** showed (C=O)*H* at 10.48 ppm and **4a** showed (C=O)*H* at 9.74 and 10.41 ppm in 1:2 integral ratio. FAB MS of **4a** showed an intense peak at 1092.5 m/z and the elemental analysis was agreeable with the proposed structure.

The condensation reaction of **4a** with 1.1 equivalents of *tris*(2-amino) ethylamine in a mixture of CH_3CN and CH_2Cl_2 (high dilution) precipitated an imine or Schiff base product, **5a** (95%). The signals due to (C=O)*H* proton disappeared, and the signals due to RN=C*H* protons showed at 8.83 and 8.93 ppm in the ^{1}H-NMR spectrum of **5a**. The methyl proton signals exhibited three singlet lines at 0.79, 1.27 and 1.36 ppm in 1:1:2 ratio, respectively indicating that the molecule possessed the cone conformation. It also implies that the structure of **5a** is more rigid than that of **4a** when capped with the **tren** unit. FAB MS of **5a** showed a strong peak at 1185.7 m/z and the elemental analysis was pertinent to the proposed structure. Reduction of **5a** by 20 equivalents of $NaBH_4$ in CH_2Cl_2 and subsequent protonation with HCl/CH_3OH (0.74% v/v) yielded an ammonium derivative, **6a** (81 %) which showed very broad signals in the ^{1}H-NMR spectrum due to the effect of positive charges. Signals due to $ArCH_2NH_2^+CH_2$- appeared at 9.78 and 9.39 ppm with an integral ratio of 2:1. The TOF mass spectrum of **6a** showed a strong signal at m/z 1192.1 corresponding to the molecular weight of the neutralized species **7a**. Nevertheless, elemental analysis result agreed with the proposed structure of **6a**. Neutralization of **6a** with NaOH in methanol provided the neutral tripodal-amine capped benzocrown calix[4]arene, **7a** (72 %).

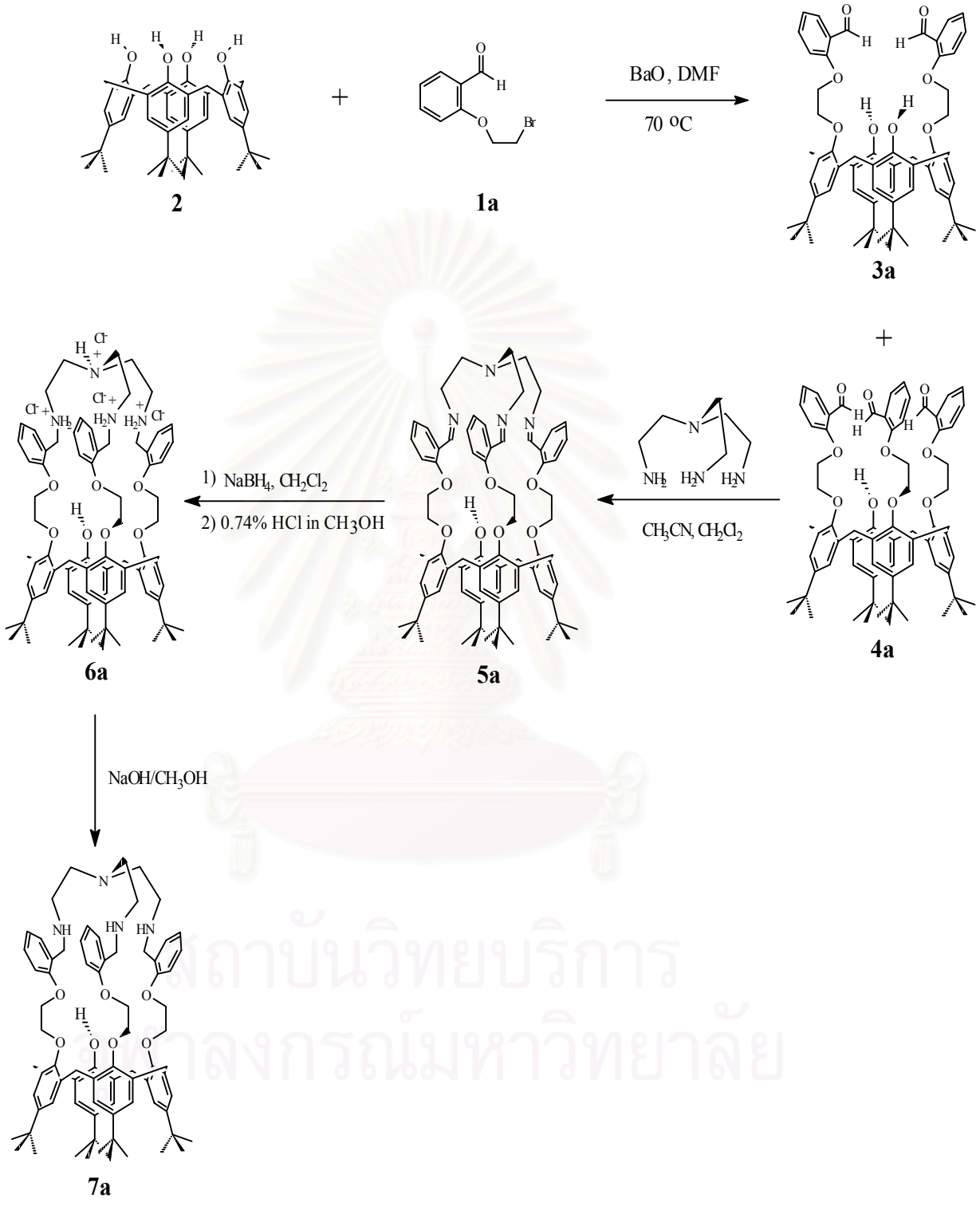

2 **1a** **3a** **4a** **5a** **6a** **7a**

Scheme 3.1 Synthesis procedure of **6a**.

3.2 X-ray studies

The solid state structure of compound **6a** was determined by X-ray crystallography (Figure 3.1). The structure was solvated by one molecule of CH_3OH and two molecules of H_2O. Two Cl^- ions were replaced by two OH^- ions. The phenyl rings of the calix[4]arene unit is in a pinched cone conformation. The structure possesses H-bonding between O(4)-H and O(2) of the calix[4]arene unit. Interestingly, one of the ethyl benzene chains connected to the **tren** unit is threaded through the cavity of the other two ethylbenzene chains. This probably resulted from a steric congestion of the capped tripodal amine and destroyed the symmetry of the molecule. This is also similar to that of calix[4](azo)crowns synthesized by Vicens and colleagues.[52] The selected bond lengths and bond angles of [**6a**-2Cl^-]$(OH^-)_2\cdot CH_3OH\cdot(H_2O)_2$ are shown in Table 3.1.

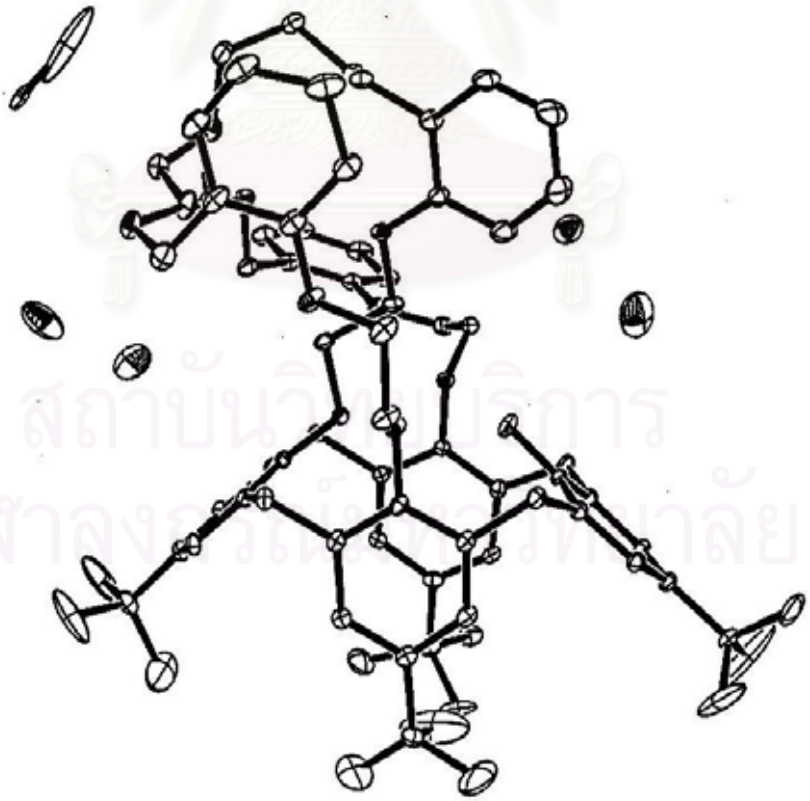

Figure 3.1 X-ray crystallography of compound [**6a**-2Cl^-]$(OH^-)_2\cdot CH_3OH\cdot(H_2O)_2$.

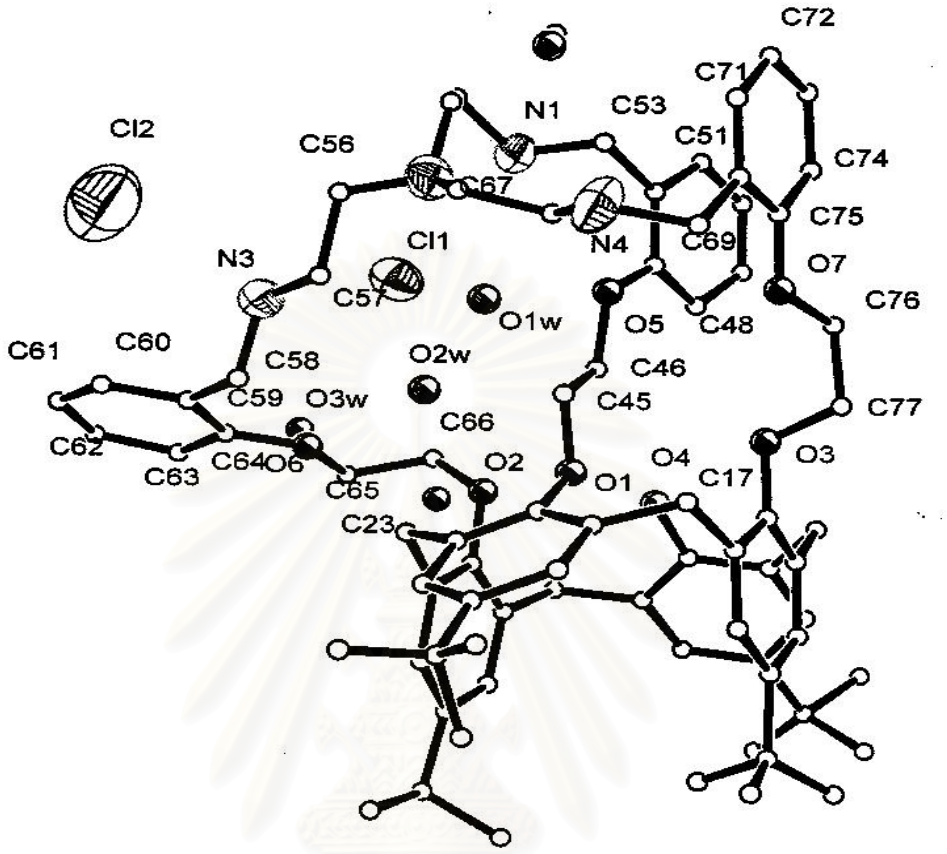

Figure 3.1 (continued) X-ray crystallography of compound [**6a**-$2Cl^-$]$(OH^-)_2 \cdot CH_3OH \cdot (H_2O)_2$.

Table 3.1 Selected bond lengths [Å] and angles [deg] for [**6a**-2Cl^-]$(OH^-)_2 \cdot CH_3OH \cdot (H_2O)_2$.

Atoms	Bond lengths (Å)	Atoms	Angles [deg]
O(1)-C(25)	1.411(5)	C(25)-O(1)-C(45)	115.9(3)
O(1)-C(45)	1.426(5)	C(26)-O(2)-C(66)	117.1(4)
O(2)-C(26)	1.394(5)	C(28)-O(3)-C(77)	112.9(4)
O(2)-C(66)	1.462(6)	C(47)-O(5)-C(46)	115.7(4)
O(3)-C(28)	1.394(6)	C(64)-O(6)-C(65)	119.1(4)
O(3)-C(77)	1.437(6)	C(75)-O(7)-C(76)	116.6(5)
O(4)-C(27)	1.369(5)	C(53)-N(1)-C(54)	115.0(4)
O(5)-C(47)	1.378(6)	C(67)-N(2)-C(56)	112.9(5)
O(5)-C(46)	1.437(6)	C(67)-N(2)-C(55)	110.7(4)
O(6)-C(64)	1.357(6)	C(56)-N(2)-C(55)	111.3(5)
O(6)-C(65)	1.423(6)	C(57)-N(3)-C(58)	112.2(5)
O(7)-C(75)	1.362(7)	C(68)-N(4)-C(69)	112.3(5)
O(7)-C(76)	1.441(7)	C(22)-C(25)-O(1)	118.6(4)
O(8)-C(79)	0.61(3)	C(18)-C(25)-O(1)	119.1(4)
N(1)-C(53)	1.480(7)	C(24)-C(26)-O(2)	118.3(4)
N(1)-C(54)	1.513(7)	O(2)-C(26)-C(4)	119.6(4)
N(2)-C(67)	1.459(7)	O(4)-C(27)-C(10)	116.1(4)
N(2)-C(56)	1.461(7)	O(4)-C(27)-C(6)	122.6(4)
N(2)-C(55)	1.470(8)	O(1)-C(45)-C(46)	106.1(4)
N(3)-C(57)	1.483(7)	O(5)-C(46)-C(45)	109.2(4)
N(3)-C(58)	1.492(7)	O(5)-C(47)-C(52)	115.7(5)
N(4)-C(68)	1.472(7)	O(5)-C(47)-C(48)	125.4(5)
N(4)-C(69)	1.545(8)	N(1)-C(53)-C(52)	109.6(4)
C(21)-C(22)	1.396(6)	N(1)-C(54)-C(55)	112.6(5)
C(22)-C(25)	1.379(6)	N(2)-C(55)-C(54)	113.2(5)
C(22)-C(23)	1.521(7)	N(2)-C(56)-C(57)	111.4(4)
C(23)-C(24)	1.529(6)	N(3)-C(57)-C(56)	111.1(5)
C(24)-C(26)	1.382(6)	O(6)-C(64)-C(59)	116.4(5)

3.3 Anion complexation studies

The ligands **6a** and **6b** contain positively charged ammonium receptors with Cl^- as counterion. They have different cavity sizes suitable for recognition studies with anions having various shapes, sizes[53] and charges[54]: spherical (F^-, Cl^-, $Br^-$and I^-), trigonal planar (NO_3^- and CO_3^{2-}), and tetrahedral (SO_4^{2-} and PO_4^{3-}).

^{1}H-NMR titration experiments are employed to study the complexation of **6a** and **6b** towards anions in DMSO-d_6 and the mixture of $CDCl_3$ and CD_3OD, respectively. Upon addition of various equivalents of anion into the solution of ligands **6a** and **6b**, the chemical shift displacement of signals of $ArCH_2NH_2^+CH_2$- and -CH_2ArH_a, respectively can be observed. Association constants between ligands and anions can be estimated from the chemical shift difference ($\Delta\delta$) in Hz and the ligand: metal ratio using a non-linear curve fitting method.[55,56]

3.3.1 Complexation studies of ligands 6a and 6b towards sodium fluoride

Upon addition of the excess of NaF to solutions of **6a** and **6b**, no chemical shift displacement in the NMR spectra was observed. The result shows that F^- cannot form complexes with **6a** and **6b**. This is probably due to the size of F^- (1.33 Å) which is smaller than the ligand cavity.

3.3.2 Complexation studies of ligands 6a and 6b towards sodium sulfate

Upon addition of the excess of Na_2SO_4 to solutions of **6a** and **6b**, signal displacement of NMR spectra for both ligands cannot be observed. This indicates that **6a** and **6b** cannot form complexes with SO_4^{2-}. This may be due to the size of SO_4^{2-} is bigger than cavity size of the ligands or the rate of complexation occurs very slowly.

3.3.3 Complexation studies of ligand 6a towards sodium bromide, sodium iodide and sodium nitrate

Upon addition of NaBr, NaI and $NaNO_3$ to the solutions of **6a**, moderate upfield shifts of the signal $ArCH_2NH_2^+CH_2$- at δ 9.39 and 9.78 ppm and slightly shifts of aromatic regions at δ 7.00 – 8.00 ppm were observed in the ^{1}H-NMR spectra. Therefore, anions must form complexes with **6a** in the cavity of the tripodally capped unit using the electrostatic interaction in case of Br^- and I^- and both electrostatic and hydrogen bonding in case of NO_3^-. The chemical shift displacements of $ArCH_2NH_2^+CH_2$- (Δδ) were collected in Table 3.2. Plots of Δδ against equivalents of anions are shown in Figures 3.2, 3.3 and 3.4 for Br^-, I^- and NO_3^-, respectively. Non-linear curve fitting method indicated that **6a** formed complexes with anions in 1:1 stoichiometry. The association constants were obtained from the resulting titration curves using a curve fitting program[57] and the values are presented in Table 3.3. It is found that **6a** forms strong complexes with Br^-, I^- and NO_3^- and the stability of the complexes varies as $I^- > NO_3^- > Br^-$. The possible structures of complexes are shown in Figure 3.5.

Table 3.2 The chemical shifts of $ArCH_2NH_2^+CH_2$- proton of **6a** upon adding anions.

Equivalents of Anions	Chemical shifts					
	NaBr		NaI		$NaNO_3$	
	δ (Hz)	Δδ (Hz)	δ (Hz)	Δδ (Hz)	δ (Hz)	Δδ (Hz)
0.00	1936.97	0.00	1944.61	0.00	1937.20	0.00
0.20	1932.54	4.43	1932.29	12.32	1937.33	0.13
0.40	1929.05	7.91	1933.62	10.99	1934.58	2.62
0.60	1931.33	5.63	1931.34	13.27	1933.37	3.83
0.80	1929.60	7.37	1924.72	19.89	1929.89	7.31
1.00	1932.32	4.64	1927.44	17.17	1933.71	3.49
1.20	1929.64	7.33	1929.69	14.92	1923.43	13.77
1.40	1925.34	11.63	1925.94	18.67	1925.58	11.62
2.00	1928.07	8.90	1923.62	20.99	1924.26	12.94
2.40	1921.80	15.17	1922.38	22.23	1922.62	14.58
3.00	1921.62	15.35	1915.29	29.32	1923.21	13.99
4.00	1921.12	15.85	1917.31	27.30	1922.35	14.85

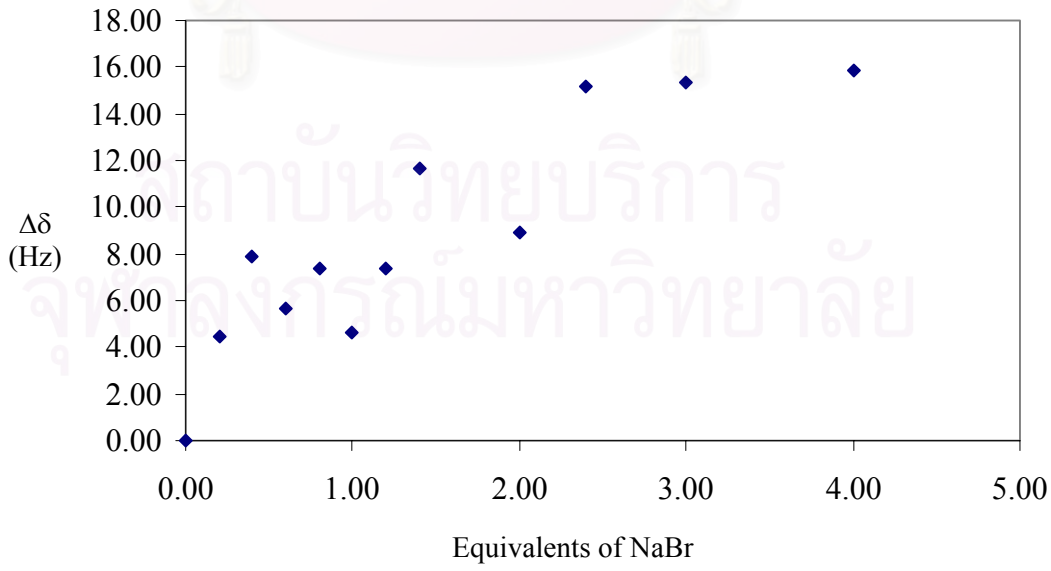

Figure 3.2 The ^{1}H-NMR titration curve of **6a** and NaBr in DMSO-d_6.

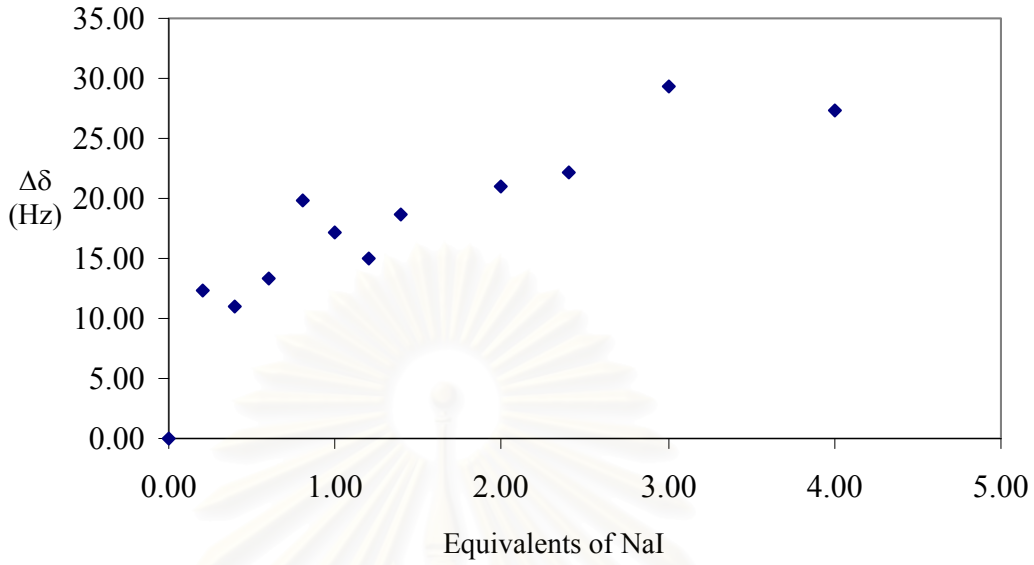

Figure 3.3 The ^{1}H-NMR titration curve of **6a** and NaI in DMSO-d_6.

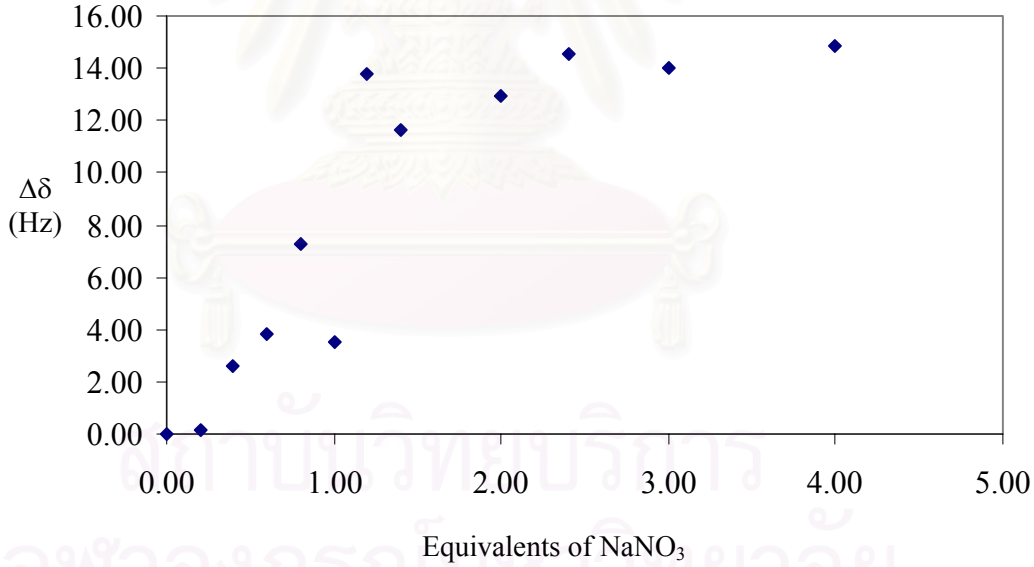

Figure 3.4 The ^{1}H-NMR titration curve of **6a** and $NaNO_3$ in DMSO-d_6.

Table 3.3 Logarithm of association constants (log K) of complexes of **6a** and various anions.

Metal cation	Anion	Log K
Na^+	I^-	2.62
Na^+	NO_3^-	2.47
Na^+	Br^-	2.23

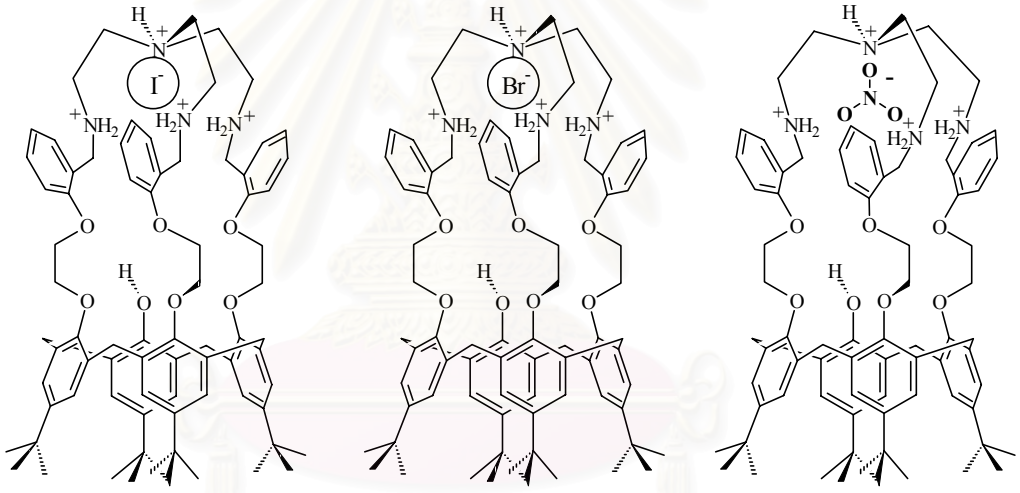

Figure 3.5 The possible structure of complexation between **6a** and various anions.

3.3.4 Complexation studies of ligand 6b towards sodium bromide, sodium iodide and sodium nitrate

Unlike **6a**, **6b** cannot dissolve in DMSO-d_6; however, **6b** can dissolve very well in $CDCl_3$ and moderately in CD_3OD. ^{1}H-NMR titration experiments of **6b** towards Br^-, I^- and NO_3^- were performed in a 1:1 mixture of $CDCl_3$ and CD_3OD. For the difference of solvent system,[58] the signal of $ArCH_2NH_2^+CH_2$- proton resonance in ligand **6b** disappeared because the protons on ammonium position exchanged with CD_3OD. Therefore, the moderate downfield shift of protons on *para* position of -CH_2ArH_a and ROArH_b (Figure 3.6) was monitored upon addition of various ratios of anions. The interaction that occurred between host **6b** and guests such as Br^-, I^- and NO_3^- was electrostatic interaction[59] and hydrogen bonding[60,61]. The chemical shifts of -CH_2ArH_{a1} proton are recorded in Table 3.4. A plot of $\Delta\delta$ against the equivalent of anions was shown in Figure 3.7. Non-linear curve fitting method indicated that **6b** formed complexes with anions in 1:1 stoichiometry. The association constants of the various anions calculated by the curve fitting method were shown in Table 3.5. It is found that the stability of anion complexes of **6b** is $I^- > NO_3^- > Br^-$. The results are similar to **6a** indicating that **6a** and **6b** possess comparable cavity size (of tripodal[62-64] ammonium unit).

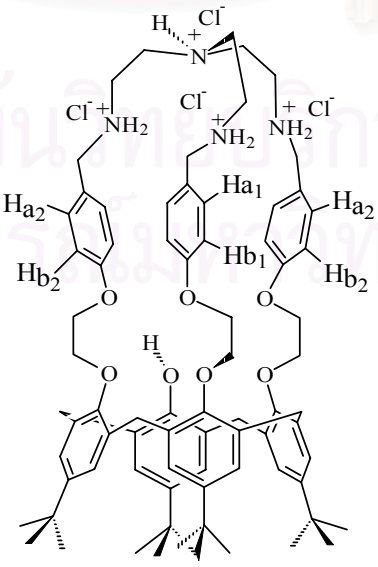

Figure 3.6 Structure of **6b** .

Table 3.4 The chemical shifts of -$CH_2Ar\mathit{H}_{a1}$ proton of **6b** upon adding anions.

Equivalents of Anions	Chemical shifts					
	NaBr		NaI		$NaNO_3$	
	δ (Hz)	Δδ (Hz)	δ (Hz)	Δδ (Hz)	δ (Hz)	Δδ (Hz)
0.00	1447.93	0.00	1449.44	0.00	1448.95	0.00
0.20	1451.90	3.97	1454.86	5.42	1448.58	0.37
0.40	1451.77	3.84	1457.23	7.79	1448.13	0.82
0.60	1457.73	9.80	1460.34	10.90	1447.59	1.36
0.80	1459.19	11.26	1461.63	12.19	1447.45	1.50
1.00	1461.61	13.68	1464.42	14.98	1446.95	2.00
1.20	1463.72	15.79	1465.51	16.07	1446.79	2.16
1.40	1464.49	16.56	1467.22	17.78	1446.54	2.41
2.00	1468.61	20.68	1471.15	21.71	1445.88	3.07
2.40	1470.55	22.62	1474.41	24.97	1445.51	3.44
3.00	1475.11	27.18	1478.64	29.20	1444.93	4.02
4.00	1479.35	31.42	1479.91	30.47	1444.57	4.38

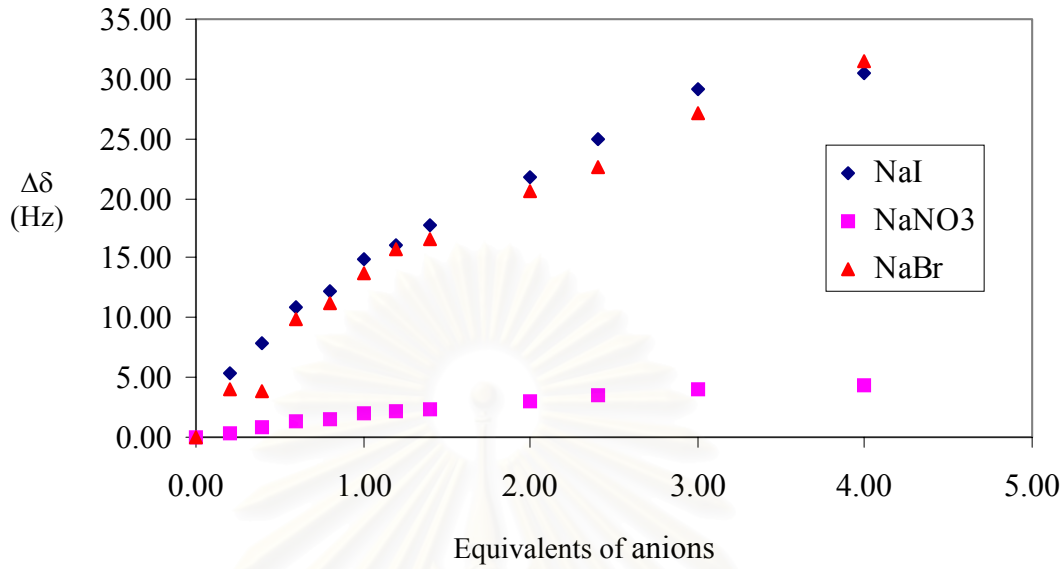

Figure 3.7 The ^{1}H-NMR titration curve of **6b** and NaBr, NaI and $NaNO_3$ in a 1:1 mixture of CD_3OD:$CDCl_3$, δ due to -$CH_2Ar\mathit{H}_{a1}$ proton.

Table 3.5 Logarithm of association constants (log K) of complexes of **6b** and various anions.

Metal cation	Anion	Log K
Na^+	I^-	2.44
Na^+	NO_3^-	2.34
Na^+	Br^-	2.28

3.3.5 Complexation studies of ligand 6a towards sodium arsenite, sodium carbonate, sodium phosphate, sodium hydrogen phosphate and sodium dihydrogen phosphate

In case of basic anions such as AsO_2^-, CO_3^{2-}, PO_4^{3-}, HPO_4^{2-} and $H_2PO_4^-$, we observed interesting phenomena when complexation studies of ligand **6a** were performed. Upon increasing the mole ratio of anions, the mixtures of the solution of **6a** and anions such as AsO_2^-, CO_3^{2-} and PO_4^{3-} precipitated white solids. Therefore, NMR titrations cannot be carried out with these anions. Unlike AsO_2^-, CO_3^{2-} and PO_4^{3-}, the solution of **6a** and HPO_4^{2-} and $H_2PO_4^-$ did not precipitate white solid. However, the chemical shift displacements of **6a** and AsO_2^-, CO_3^{2-}, HPO_4^{2-} and $H_2PO_4^-$ are similar to those of compound **7a** implying that the deprotonation of **6a** took place upon complexing AsO_2^-, CO_3^{2-}, HPO_4^{2-} and $H_2PO_4^-$.[65] Therefore, the association constants of the complexes cannot be calculated.

3.3.6 Complexation studies of ligand 6b towards sodium arsenite, sodium carbonate and sodium phosphate

Due to poor solubility of $NaAsO_2$, Na_2CO_3 and $Na_3PO_4 \cdot 12H_2O$ in CD_3OD and $CDCl_3$, anion complexation studies were carried out in vials. The reaction mixture was allowed to stir for 2 days. Then ^{1}H-NMR spectra in ($CDCl_3$) were recorded in Figures 3.8, 3.9 and 3.10. It was found that complexation occurred along with the deprotonation to give **7a**. Therefore, the association constants for these complexes cannot be calculated.

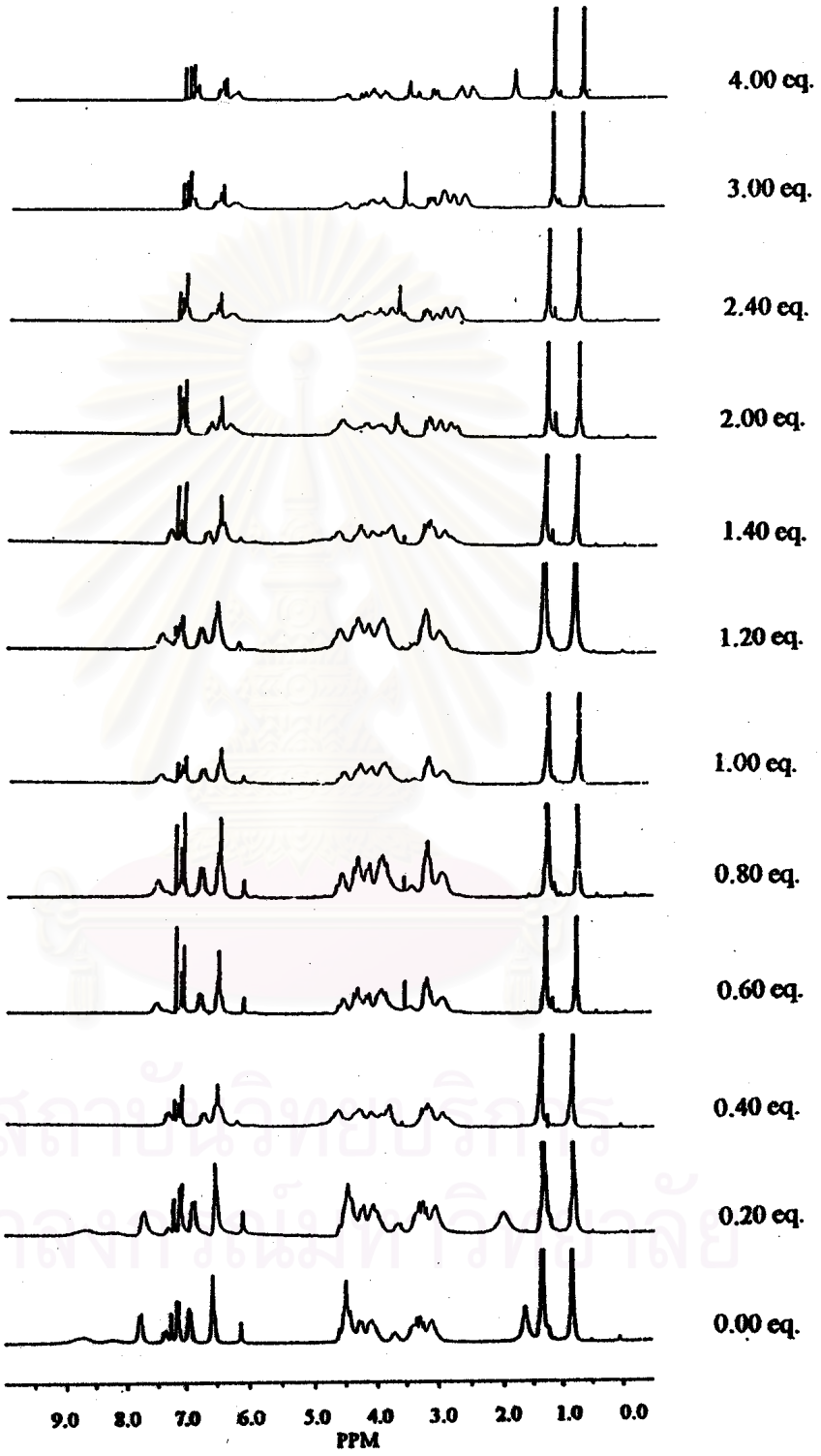

Figure 3.8 The ^{1}H-NMR spectra of **6b** with $NaAsO_2$ in $CDCl_3$.

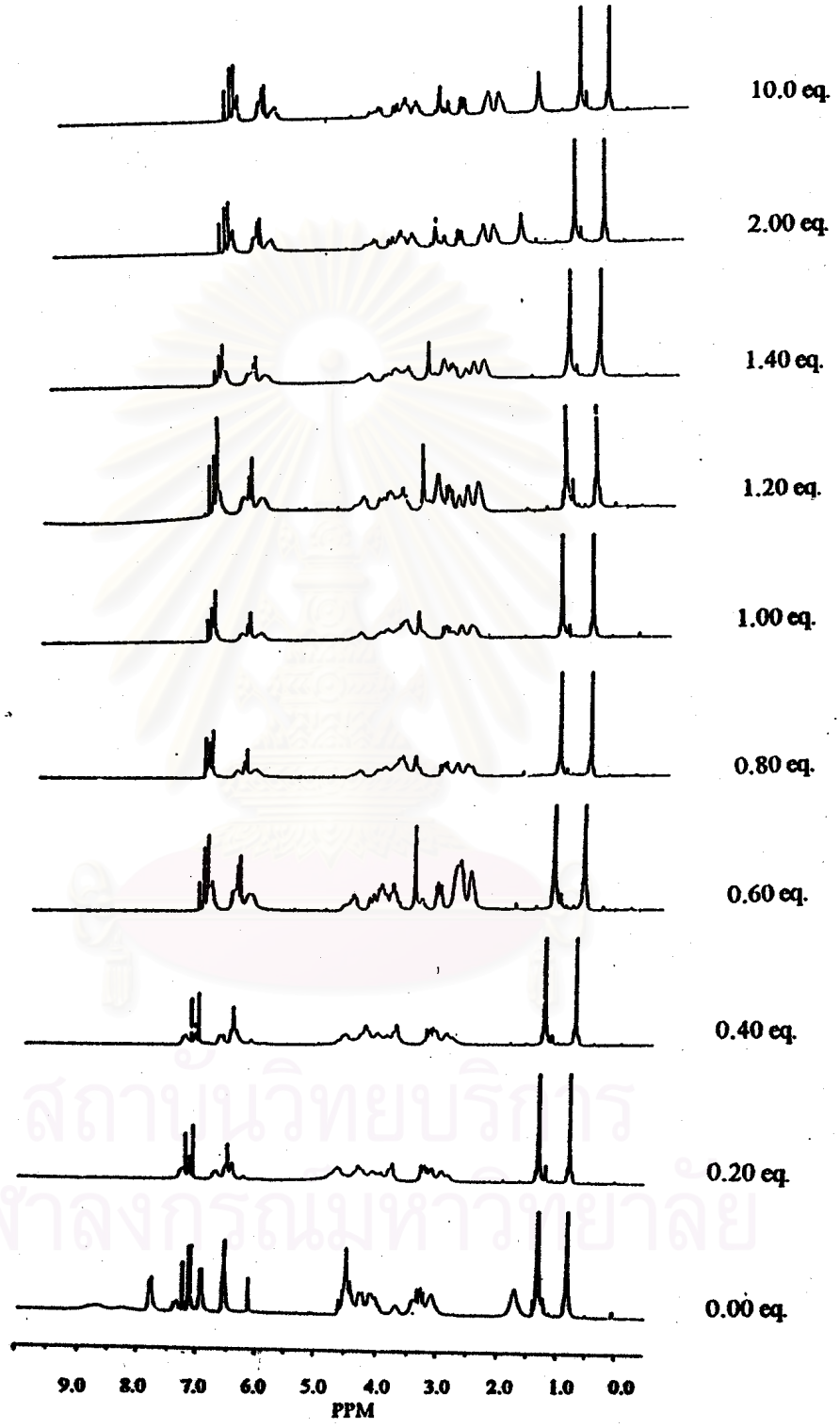

Figure 3.9 The ^{1}H-NMR spectra of **6b** with Na_2CO_3 in $CDCl_3$.

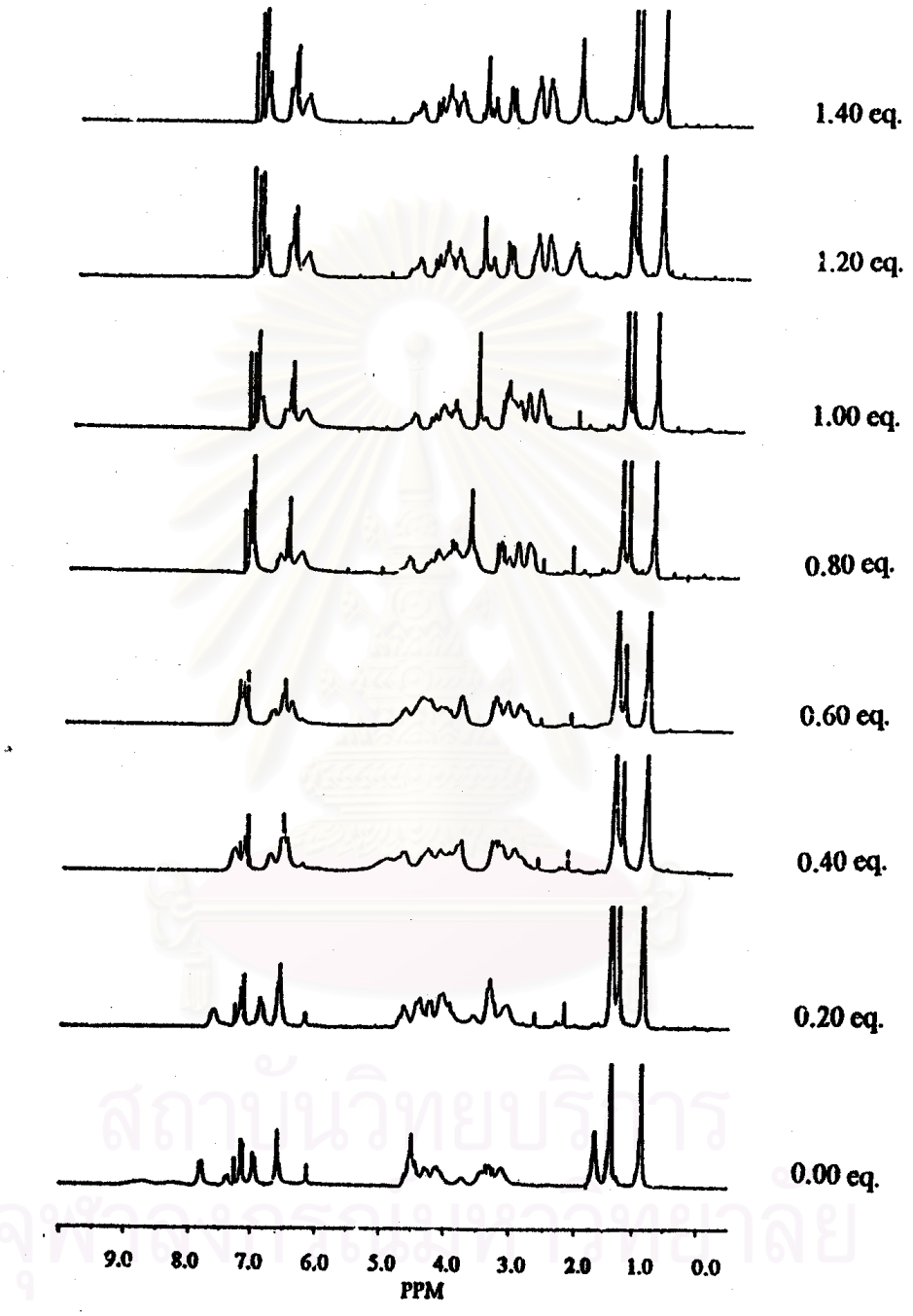

Figure 3.10 The ^{1}H-NMR spectra of **6b** with $Na_3PO_4 \cdot 12H_2O$ in $CDCl_3$.

3.3.7 Complexation studies of ligand 6b towards sodium hydrogen phosphate and sodium dihydrogen phosphate

Although addition of Na_2HPO_4 into ligand **6b** causes the displacement of the aromatic signal (δ 6.5-8.0 ppm) as shown in Figure 3.11, Na_2HPO_4 cannot be completely dissolved into solution. The association constant of the complex of **6b** and HPO_4^{2-} cannot be determined correctly with our curve-fitting program.

In addition, upon addition of excess $NaH_2PO_4 \cdot H_2O$ to the ligands **6b** solutions, no chemical shift displacement in the NMR spectra was observed. The result shows that **6b** cannot form complexes with $H_2PO_4^-$.

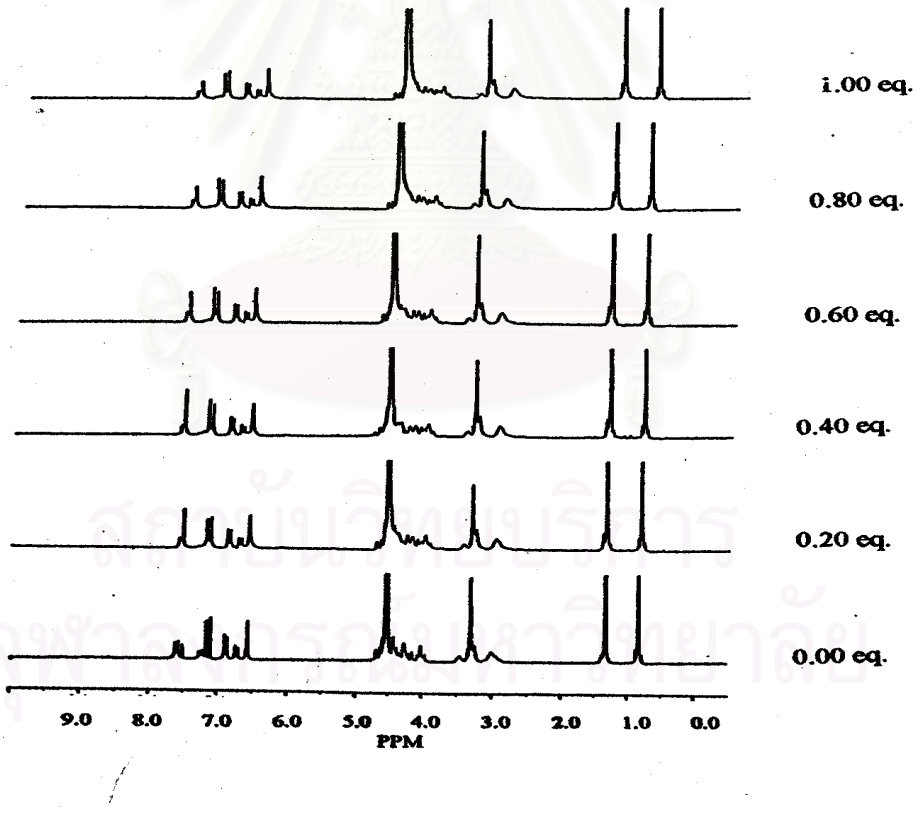

Figure 3.11 The ^{1}H-NMR spectra of **6b** with Na_2HPO_4 in $CDCl_3$ and CD_3OD.

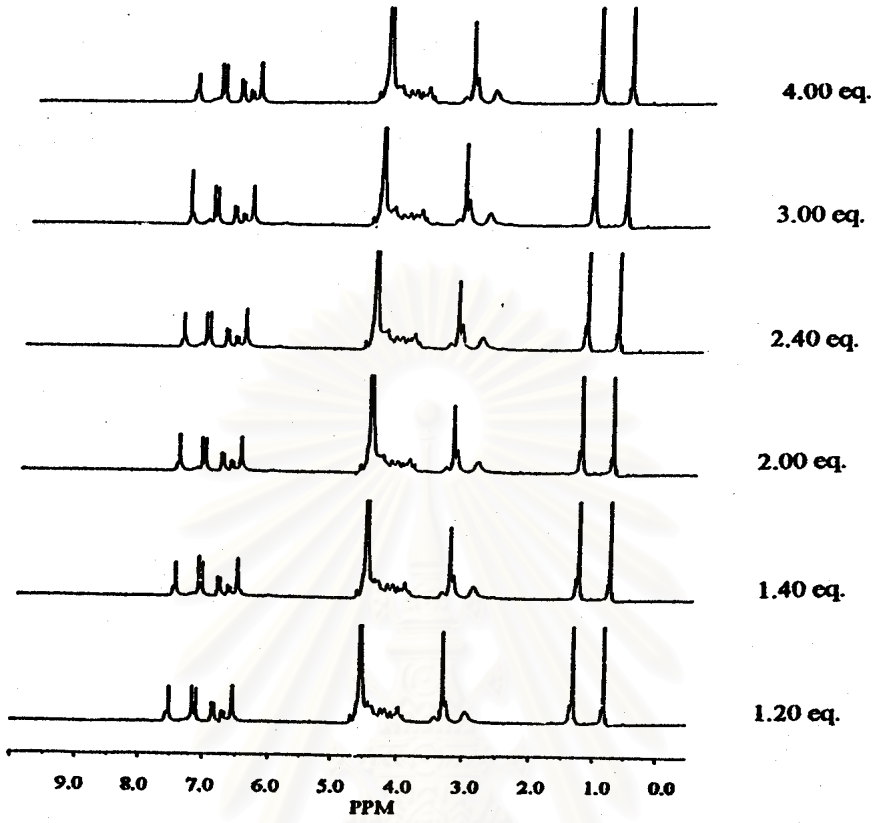

Figure 3.11 (continued) The ^{1}H-NMR spectra of **6b** with Na_2HPO_4 in $CDCl_3$ and CD_3OD.

3.3.8 Complexation studies of ligands 6a and 6b towards tetrabutylammonium bromide and tetrabutylammonium iodide

Besides a tripodal ammonium unit, a receptor for anion, structures of **6a** and **6b** composed of 6 oxygen donors rearranged into a three dimensional cage suitable for complexing alkali cations. We think that cations may affect the binding ability of **6a** and **6b** towards anions. Therefore, titration experiments using different countercations were carried out.

Upon addition of $C_{16}H_{36}BrN$ and $C_{16}H_{36}IN$ to **6a** moderate upfield shifts of the signal $ArCH_2NH_2^+CH_2$- at δ 9.39 and 9.78 ppm and to **6b** strongly downfield shifts of the signal -CH_2ArH_a and $ROArH_b$ at δ 7.38 and 6.93 ppm were observed in the ^{1}H-NMR spectra. The chemical shift displacements (Δδ) of $ArCH_2NH_2^+CH_2$- in **6a** and -CH_2ArH_{a1} in **6b** were collected in Tables 3.6 and 3.7. Plots of Δδ against equivalents of anions are shown in Figures 3.12–3.14. Non-Linear curve fitting method indicated that **6a** and **6b** formed complexes with anions in a 1:1 stoichiometry. Association constants of both ligands towards various anions are shown in Table 3.8. It is found that **6a** forms a stronger complex with Br^- but **6b** forms a stronger complex with I^-. It also implies that alkali cations must have a very important role in anion complexation of ligand **6a** while in **6b** the role of alkali cations is not so obvious. To get more information, we further study the complexation of **6a** and **6b** towards Br^- and I^- in the presence of K^+.

Table 3.6 The chemical shifts of $ArCH_2NH_2^+CH_2$- proton of **6a** upon adding anions.

Equivalents of Anions	Chemical shifts			
	$C_{16}H_{36}BrN$		$C_{16}H_{36}IN$	
	δ (Hz)	Δδ (Hz)	δ (Hz)	Δδ (Hz)
0.00	1940.99	0.00	1935.54	0.00
0.20	1940.43	0.56	1936.55	1.01
0.40	1940.29	0.70	1936.50	0.96
0.60	1933.46	7.53	1929.01	6.53
0.80	1933.77	7.22	1930.86	4.68
1.00	1935.45	5.54	1925.25	10.29
1.20	1935.06	5.93	1924.93	10.61
1.40	1930.21	10.78	1926.67	8.87
2.00	1930.72	10.27	1923.23	12.31
2.40	1929.37	11.62	1922.13	13.41
3.00	1925.33	15.66	1922.61	12.93
4.00	1924.67	16.32	1911.05	24.49

Table 3.7 The chemical shifts of -$CH_2Ar\mathit{H}_{a1}$ proton of **6b** upon adding anions.

Equivalents of Anions	Chemical shifts			
	$C_{16}H_{36}BrN$		$C_{16}H_{36}IN$	
	δ (Hz)	Δδ (Hz)	δ (Hz)	Δδ (Hz)
0.00	1448.31	0.00	1449.16	0.00
0.20	1451.47	3.16	1450.06	0.90
0.40	1454.20	5.89	1454.37	5.21
0.60	1456.03	7.72	1457.74	8.58
0.80	1458.05	9.74	1460.32	11.16
1.00	1460.38	12.07	1461.64	12.48
1.20	1462.29	13.98	1462.60	13.44
1.40	1462.92	14.61	1464.29	15.13
2.00	1465.37	17.06	1467.79	18.63
2.40	1468.20	19.89	1469.36	20.2
3.00	1470.40	22.09	1471.34	22.18
4.00	1473.41	25.10	1474.62	25.46

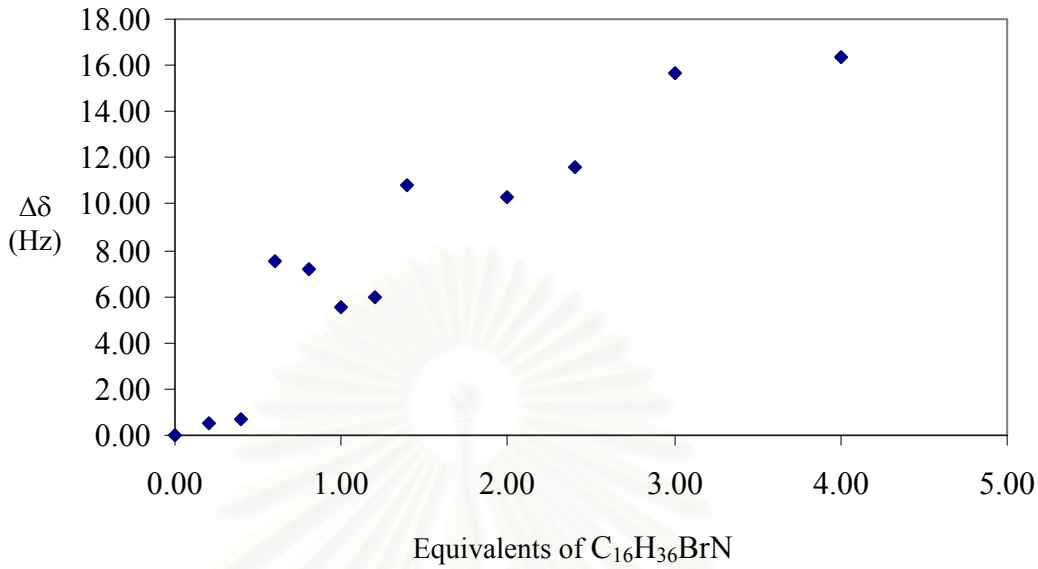

Figure 3.12 The ^{1}H-NMR titration curve of **6a** towards $C_{16}H_{36}BrN$ in DMSO-d_6.

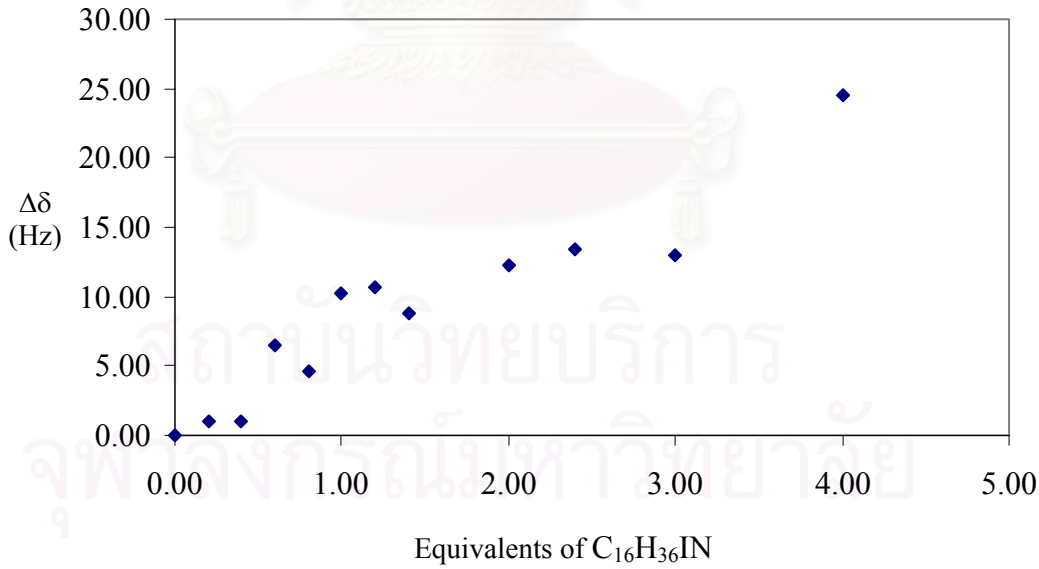

Figure 3.13 The ^{1}H-NMR titration curve of **6a** towards $C_{16}H_{36}IN$ in DMSO-d_6.

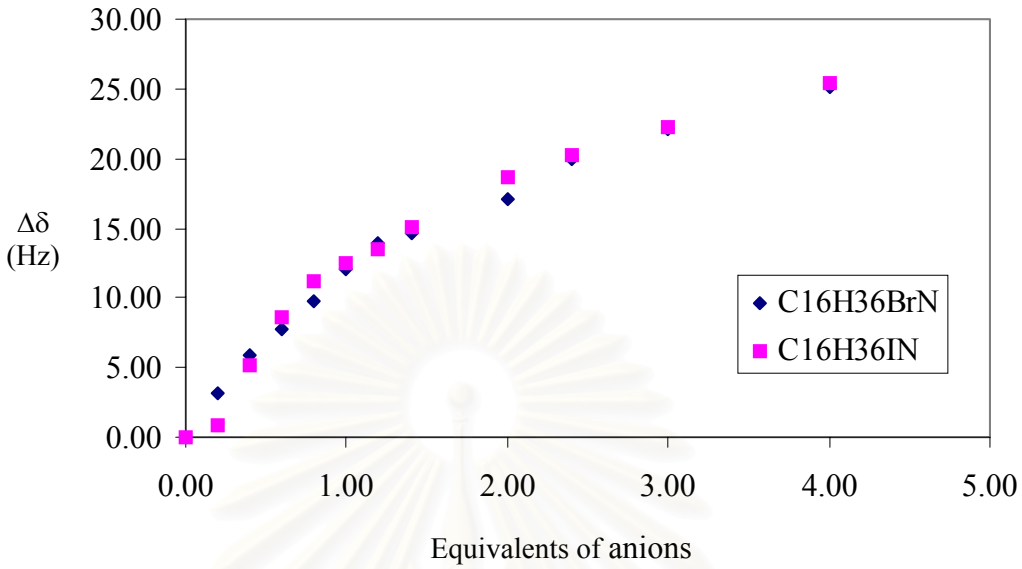

Figure 3.14 The ^{1}H-NMR titration curve of **6b** towards $C_{16}H_{36}BrN$ and $C_{16}H_{36}IN$ in a 1:1 mixture of CD_3OD:$CDCl_3$, δ due to -$CH_2Ar\mathit{H}_{a1}$ proton.

Table 3.8 The value of Log K of complexes of **6a** and **6b** with $C_{16}H_{36}BrN$ and $C_{16}H_{36}IN$.

Counter cation	Anion	Log K	
		6a	**6b**
$^{n}Bu_4N^+$	I^-	1.78	2.40
$^{n}Bu_4N^+$	Br^-	2.13	2.38

3.3.9 Complexation studies of ligands 6a and 6b towards potassium bromide and potassium iodide

Upon addition of KBr and KI to **6a** moderate upfield shifts of the signal $ArCH_2NH_2^+CH_2$- at δ 9.39 and 9.78 ppm and to **6b** downfield shifts of the signal -CH_2ArH_a and $ROArH_b$ at δ 7.38 and 6.93 ppm were observed in the ^{1}H-NMR spectra. The chemical shift displacements (Δδ) of $ArCH_2NH_2^+CH_2$- in **6a** and -CH_2ArH_{a1} in **6b** are collected in Tables 3.9 and 3.10. Plots of Δδ against equivalents of anions are shown in Figures 3.15–3.17. Non-Linear curve fitting method indicated that **6a** and **6b** formed complexes with anions in 1:1 stoichiometry. The association constants of **6a** and **6b** with various anions are shown in Table 3.11. It is found that both **6a** and **6b** form a stronger complex with I^-. This result is consistent with the result obtained from using Na^+ as counter cation.

Table 3.9 The chemical shifts of $ArCH_2NH_2^+CH_2$- proton of **6a** upon adding anions.

Equivalents of Anions	Chemical shifts			
	KBr		KI	
	δ (Hz)	Δδ (Hz)	δ (Hz)	Δδ (Hz)
0.00	1945.68	0.00	1942.58	0.00
0.20	1939.16	6.52	1937.58	5.00
0.40	1936.30	9.38	1935.66	6.92
0.60	1940.75	4.93	1932.42	10.16
0.80	1935.82	9.86	1935.68	6.90
1.00	1936.88	8.80	1929.60	12.98
1.20	1922.59	23.09	1929.98	12.60
1.40	1923.49	22.19	1929.85	12.73
2.00	1921.26	24.42	1921.85	20.73
2.40	1923.06	22.62	1923.07	19.51
3.00	1923.08	22.60	1923.88	18.70
4.00	1920.49	25.19	1922.88	19.70

Table 3.10 The chemical shifts of **-**$CH_2Ar\mathit{H}_{a1}$ proton of **6b** upon adding anions.

Equivalents of Anions	Chemical shifts			
	KBr		KI	
	δ (Hz)	Δδ (Hz)	δ (Hz)	Δδ (Hz)
0.00	1448.92	0.00	1449.37	0.00
0.20	1452.27	3.35	1453.15	3.78
0.40	1455.33	6.41	1456.93	7.56
0.60	1458.30	9.38	1460.17	10.80
0.80	1459.81	10.89	1463.81	14.44
1.00	1461.80	12.88	1466.49	17.12
1.20	1465.32	16.40	1469.31	19.94
1.40	1467.38	18.46	1471.73	22.36
2.00	1473.66	24.74	1476.41	27.04
2.40	1477.32	28.4	1480.00	30.63
3.00	1480.49	31.57	1485.77	36.40
4.00	1486.18	37.26	1488.43	39.06

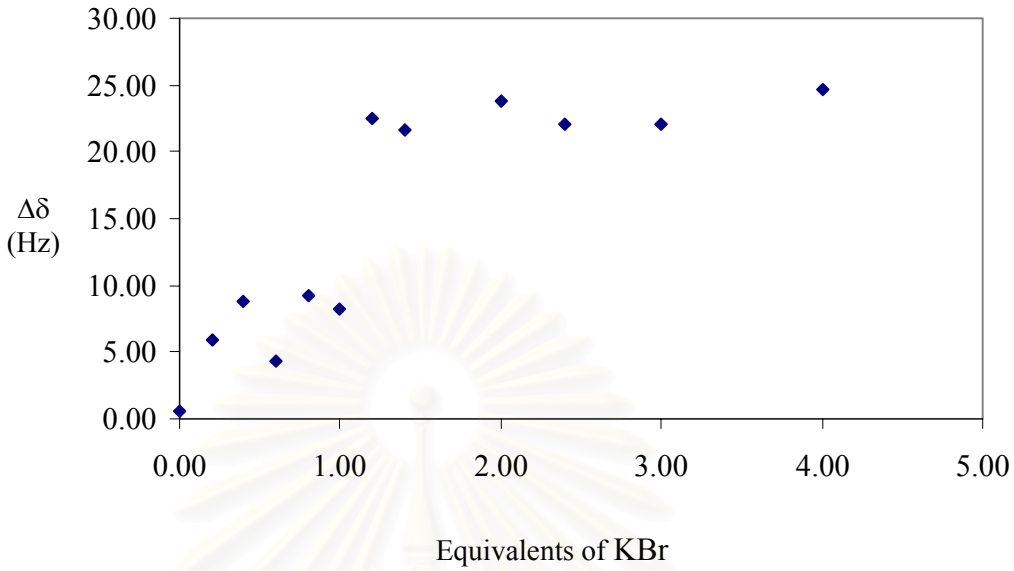

Figure 3.15 The ^{1}H-NMR titration curve of **6a** towards KBr in DMSO-d_6.

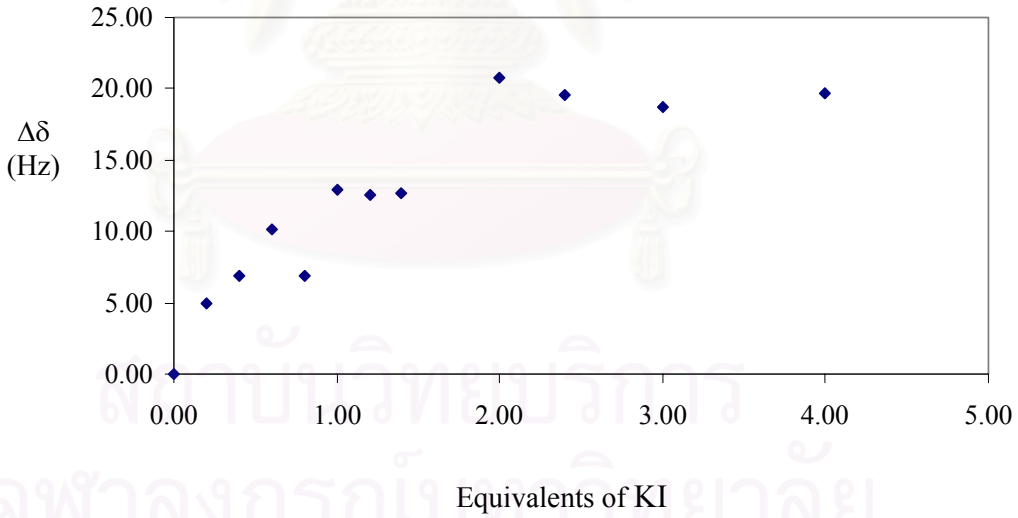

Figure 3.16 The ^{1}H-NMR titration curve of **6a** towards KI in DMSO-d_6.

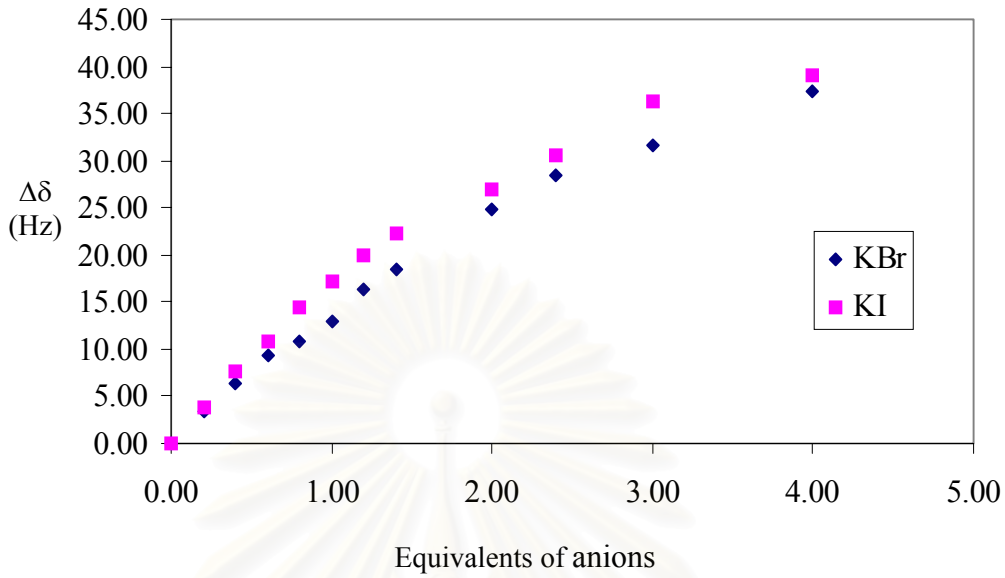

Figure 3.17 The ^{1}H-NMR titration curve of **6b** towards KBr and KI in a 1:1 mixture of CD_3OD:$CDCl_3$, δ due to -$CH_2Ar\mathit{H}_{a1}$ proton.

.

Table 3.11 The value of Log K's of complexes of **6a** and **6b** with KBr and KI.

Metal cation	Anion	Log K	
		6a	**6b**
K^+	I^-	2.19	2.35
K^+	Br^-	2.14	2.22

3.4 Effect of alkali cations towards anion complexation of 6a and 6b

Table 3.12 summarizes association constants of complexes between ligands **6a** and **6b** and $Br^-$and I^- with various countercations.

Table 3.12 The values of log K's of complexes of **6a** and **6b** with Br^- and I^-.

Metal cation	Anion	Log K	
		6a	**6b**
None*	Br^-	2.13	2.38
Na^+	Br^-	2.23	2.28
K^+	Br^-	2.14	2.22
None*	I^-	1.78	2.40
Na^+	I^-	2.62	2.44
K^+	I^-	2.19	2.35

* using $^nBu_4N^+$ as countercation

The results indicate that both ligands can bind I^- and Br^- ions with moderate stability in the presence of alkali countercations. Ligands **6a** and **6b** form the most stable complex with I^- in the presence of Na^+. However, without alkali cations, the stability constant of the complex of **6a** and I^- decreases dramatically while that of **6b** is almost unchanged. The result shows that alkali cations promote the complexation of **6a** towards anions. Contemplating at the crystal structure of ligand **6a**, one can obviously sees that **6a** has to reorganize its donor atom to accommodate such a big anion like I^-. This can be furnished by alkali cation which can reside in the cavity of 6 oxygen atoms and induces the structural reorganization of **6a** to be more appropriate for binding I^- as illustrated in Scheme 3.2.

Scheme 3.2 Structural rearrangement of **6a** induced by the presence of alkali ions.

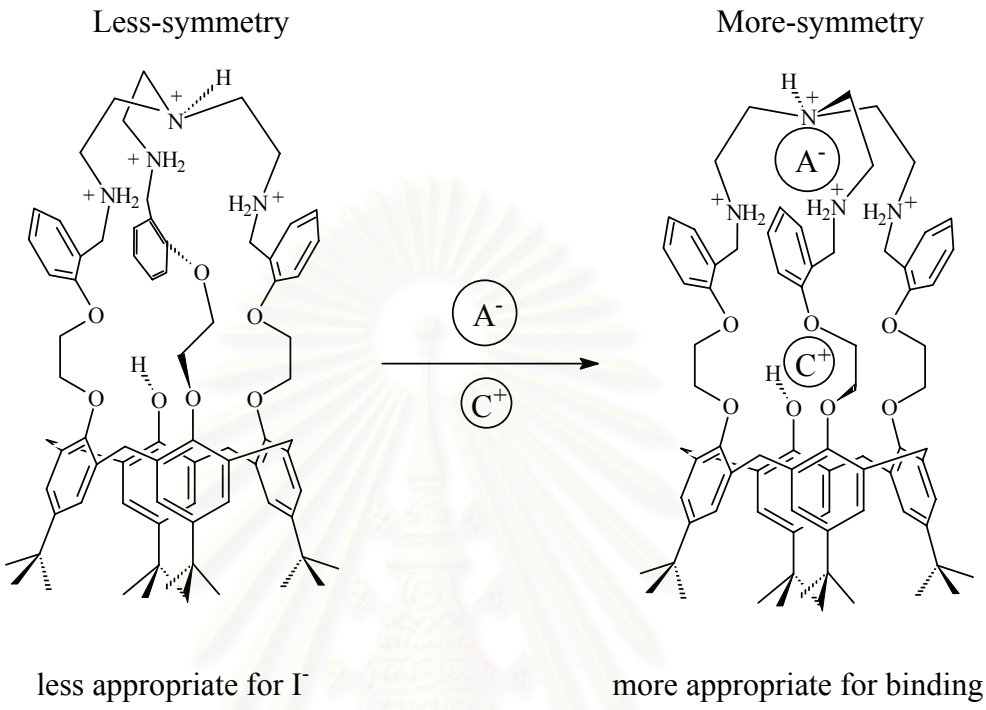

Compound **6b** can bind I^- with high stability no matter what cations involve. The result implies that the structure of **6b** must be more symmetrical as shown in Figure 3.18 and it is agreeable with 2D-NMR results (NOSEY and COSY).[47]

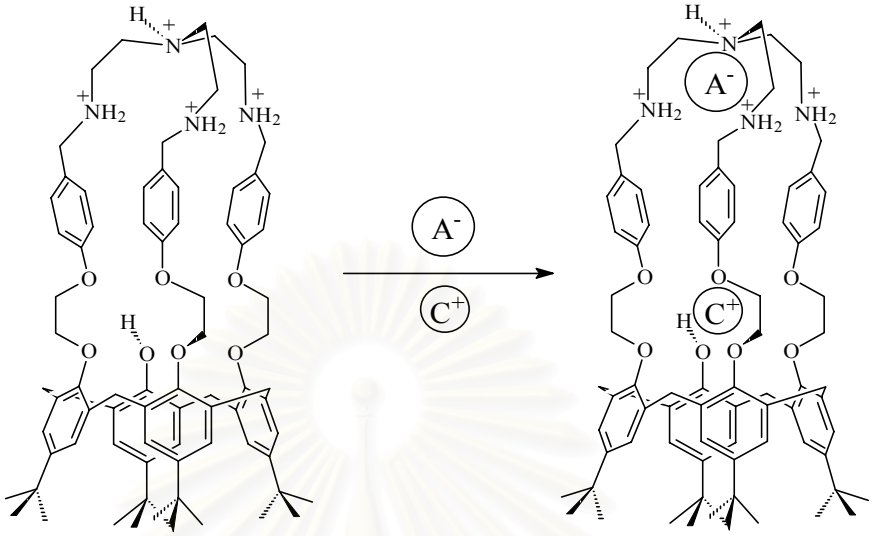

Figure 3.18 Possible structure of ligand **6b** with cation and anion complexes.

CHAPTER IV

CONCLUSION

The ligands, 25,26,27-*N,N′,N″*-tri-((2-ethoxy)benzyl)ethylenetetraamine-*p*-*tert*-butylcalix[4]arene·4HCl, **6a** and 25,26,27-*N,N′,N″*-tri-((4-ethoxy)benzyl) ethylenetetraamine-*p*-*tert*-butylcalix[4]arene·4HCl, **6b**, have been synthesized. The ligand **6a** was achieved by a substitution reaction of bromoaldehyde, **1a** and *p*-*tert*-butylcalix[4]arene, **2** to give dialdehyde, **3a** (25 %) and trialdehyde, **4a** (21 %). The condensation between **3a** and tris(2-amino)ethylamine gave the Schiff base, **5a** (95 %). Reduction of **5a** with $NaBH_4$ and subsequent protonation with HCl/CH_3OH afforded the ammonium derivative, **6a** (81 %). Preparation of **6b** was carried out in the same manner as **6a**.[47] The ligands **6a** and **6b** were then neutralized with $NaOH/CH_3OH$ to obtain the neutral ligands, **7a** and **7b**, in 72 % yields.

We have studied anion complexation of **6a** and **6b** with various anions such as F^-, Br^-, I^-, NO_3^-, SO_4^{2-}, CO_3^{2-}, PO_4^{3-}, AsO_2^-, HPO_4^{2-} and $H_2PO_4^-$ using Na^+ countercation. The results are summarized in Tables 4.1 and 4.2. Both **6a** and **6b** can generally from complexes with Br^-, I^- and NO_3^- in a different extent in the presence of alkali ions: $I^- > NO_3^- > Br^-$.

Table 4.1 Summary of complexation studies of **6a** and **6b** towards anions.

Anions[a]	Ligand **6a** (DMSO-d_6)	Ligand **6b** ($CD_3OD/CDCl_3$)
F^-	X	X
SO_4^{2-}	X	X
Br^-	√	√
I^-	√	√
NO_3^-	√	√
CO_3^{2-}	neutral form[b]	neutral form[b]
PO_4^{3-}	neutral form[b]	neutral form[b]
AsO_2^-	neutral form[b]	neutral form[b]
HPO_4^{2-}	neutral form[b]	√[c]
$H_2PO_4^-$	neutral form[b]	X

X no complexation, √ complexation occurs

[a] using sodium salts

[b] neutral forms occur and association constants cannot be calculated

[c] Na_2HPO_4 was not completely dissolved

Table 4.2 Summary of association constants of ligands **6a** and **6b** towards various anions.

Metal	Anion	Log K	
		Ligand **6a**	Ligand **6b**
None*	Br^-	2.1256	2.3835
Na^+	Br^-	2.2316	2.2818
K^+	Br^-	2.1378	2.2179
None*	I^-	1.7829	2.4039
Na^+	I^-	2.6154	2.4378
K^+	I^-	2.1937	2.3480
Na^+	NO_3^-	2.4666	2.3389

* Using tetrabutylammonium as countercation.

From the results, three factors have involved in anion complexation of compounds **6a** and **6b**: cavity size of the ligands and effect from cationic size,[15] anionic size and interactions[15,66] and basicity of anions.

1. Cavity size of ligands and effects from cationic size

Both **6a** and **6b** formed rather strong complexes with I^- in the presence of alkali metal ions. This implies that the cavity in **6a** and **6b** is suitable for binding I^-. However, without metal ions, the stability of the complex between **6a** and I^- decreased dramatically. The structure of **6a** must be rearranged in the presence of alkali ions to be able to accommodate I^-. For **6b**, there is no implicit effect of countercations suggesting that the cavity of **6b** is essentially big enough to accommodate I^-.

2. Anionic size and interactions

Although NO_3^- has a smaller size than I^- and Br^-, it forms complexes with **6a** and **6b** with quite high stability constants. This may result from cooperative electrostatic and hydrogen bonding interactions. Br^- and I^- form complexes with **6a** and **6b** with only electrostatic interaction, and the size of I^- matches the cavity size of **6a** and **6b** (in the presence of alkali cations).

3. Basicity of anions

In case of basic anionic guests such as AsO_2^-, CO_3^{2-} and PO_4^{3-}, two phenomena have occurred. The first one is complexation and the second one is deprotonation. We, therefore, cannot calculate the stability constants of these complexes. This is the most crucial defect of anion hosts using ammonium receptors.

The suggestion for future work:

From the aforementioned results and discussion, future works are suggested as follows:

1. Both the crystal structures of the complexes of **6a** and **6b** with cations and anions should be determined by single crystal X-ray crystallography.
2. Solvent extraction of both ligands towards anions should be studied.
3. The kinetic studies of both ligands should be carried out to identify the mechanism of complexation.
4. The possibility of using calix[4]arene derivatives as anion sensors should be explored.
5. Construction of neutral anion receptor using urea or thiourea derivative should be explored.

REFERENCES

1. Lenh, J.-M. *Angew .Chem .Int. Ed. Engl.* **1988**, *27*, 89.
2. Dietrich, B.; Guilhem, J.; Lenh, J.-M.; Pascard, C.; Sonveaux, E. *Helvetica Chimica Acta*. **1984**, *67*, 91.
3. Beer, P. D.; Smith, D. K. *Progress in Inorganic Chemistry*, Karlin, K.D., Ed. New York: John Wiley & Sons, **1997**, Vol 46.
4. Fenniri, H.; Hosseini, M. W.; Lenh, J. M. *Helvetica Chimica Acta*. **1997**, *80*, 786.
5. Calladine, C. R.; Drew, H. R. *Understanding DNA : The molecule and how it works*. 2nd ed. New York: Academic Press, **1997**.
6. Beer, P. D. *J. Chem. Soc., Chem. Commun*. **1996**, 689.
7. Dietrich, B. *Inclusion Compounds*, Atwood, J. L.; Davies, J. E. D.; MacNicol, D. D., Eds. New York: Academic, **1984**, Vol. 2, p. 373.
8. Harrison, R. M. *Pollution: Causes Effects and Control*. London: Royal Society of Chemistry, **1983**.
9. Quinton, P. M. *FASEB J.* **1990**, *4*, 2709.
10. Watson, C.A., Ed. *Offical and Standardized Methods of Analysis*. Cambridge, UK: The Royal Society of Chemistry, **1994**, Vol. 3.
11. Renkawek, K.; Bosman, G. J. C. G. M. *Neuroreport* **1995**, *6*, 929.
12. Schmidtchen, F.P.; Berger, M. *Chem. Rev*. **1997**, *97*, 1609.
13. Huber, W. *Titration in Nonaqueous Solvents*. New York: Academic Press Inc., **1967**, p.215.
14. Vogtle, F. *Angew. Chem., Int. Ed. Engl.* **1985**, *24*, 728.
15. Steed, J. W.; Atwood, J. L. *Supramolecular Chemistry*. New York: John Wiley Ed., **2000**, p.3.
16. Bianchi, A.; Bowman-James, K.; Garcia-Espana, E. *Supramolecular Chemistry of Anions*. New York: Wiley, **1997**.
17. Gale, P. A. *Coordination Chemistry Reviews* **2000**, *199*, 181.
18. Scheerder, J.; Engbersen, J. F. J.; Reinhoudt, D. N. *Recl. Trav. Chim. Pays-Bas* **1996**, *115*, 307.

19. Papoyan, G.; Gu, K.; Wiorkiewicz-Kuczera, J.; Kuczera, K.; Bowman-James, K. *J. Am. Chem. Soc.* **1996**, *118*, 1354.

20. Boudon, S.; Decian, A.; Fischer, J.; Hosseini, M.W.; Lehn, J.-M.; Wipff, G. *J. Coord. Chem.*, **1991**, *23*, 113.

21. Ichikawa, K.; Hossain, M. A. *Chem. Commun.* **1996**, 1721.

22. Schmidtchen, F. P. *Angew. Chem., Int. Ed. Engl.* **1977**, *16*, 720.

23. Ichikawa, K.; Yamamoto, A.; Hossain, M.A. *Chem. Lett.* **1993**, 2177.

24. Ichikawa, K.; Hossain, M. A.; Tarura T.; Kamo, N. *Supramol. Chem.* **1995**, *5*, 219.

25. Hossain, M. A.; Ichikawa, K. *Tetrahedron Lett.* **1994**, *35*, 8393.

26. Hannon, C. L.; Anslyn, E.V. *The Guanidium Group: Its Biological Role; Synthetic Analogs* in *Bioorganic Chemistry Frontiers*, Dugas, H.; Schmidtchen, F.P. Eds. Heidelberg: Springer, **1993**, p.193.

27. Schmidtchen, F. P. *Tetrahedron Lett.* **1989**, *30*, 4493.

28. Sessler, J. L.; Cyr, M.; Furuta, H.; Král, V.; Mody, T.; Morishima, T.; Shionoya, M.; Weghorn, S. *Pure & Appl. Chem.* **1993**, *65*, 393.

29 Sessler, J. L.; Cyr, M. J.; Lynch, V.; McGhee, E.; Ibers, J. A. *J. Am. Chem. Soc.* **1990**, 112, 2810.

30. Shionoya, M.; Furuta, H.; Lynch, V; Harriman, A.; Sessler, J. L. J. *J. Am. Chem. Soc.* **1992***, 114,* 5714.

31. Beer, P. D.; Hesek, D.; Kingston, J. E.; Smith, D. K.; Stokes, S. E. *Organometallics* **1995**, *14*, 3288.

32. Atwood, J L.; Holman, K. T.; Steed, J. W. *Chem.Commun.* **1996**, 1401.

33. Beer, P. D. *Acc. Chem. Res.* **1998**, *31*, 71.

34. Beer, P. D.; Chen, Z.; Golden, A. J.; Grieve, A.; Hesek, D.; Szemes, F.; Wear, D. *J. Chem. Soc., Chem. Commun*. **1994**, 1269.

35. Antonisse, M. M. G.; Reinhoudt, D. N. *Chem. Commun.* **1998**, 443.

36. Dietrich, B. *Pure & Appl. Chem.* **1993**, *65*, 1457.

37. Snellink-Ruël, B. H. M.; Antonisse, M. G.; Engbersen, J. F. J.; Timmerman, P.; Reinhoudt, D. N. *Eur. J. Org. Chem.* **2000**, 165.

38. Kang, S. O.; Nam, K. C. *Bull. Korean. Chem. Soc.* **2000**, *21*, 461.

39. Beer, P. D.; Gale, P. A.; Smith, D. K. *Supramolecular Chemistry*. Oxford, **1999**.

40. Poster, J.; Lachmann, H. *Spectrometric Titrations*. Weinhein. VCH, **1989**.

41. Conors, K.A. *Binding Constants*. Chichester: John Wiley & Sons, **1987**.

42. Hynes, M. J. *J. Chem. Soc., Dalton Trans.* **1993**, 311.

43. Perrin, D. D.; Armarego, W. L. F. *Purification of Laboratory Chemicals*; 3rd ed. Oxford: Pergamon Press, **1988**, p.157-158.

44. a) Loon, J.-D.; Verboom, W.; Reinhoudt, D.N. *Organic Preparation and procedures Inc.* **1992**, *24*, 437.

b) Shinkai, S. *Tetrahedron* **1993**, *49*, 8933.

c) Bohmer, V. *Angew. Chem. Int. Ed. Engl.* **1995**, *34*, 713.

45. Gutsche, C. D.; Iqbal, M. *Org. Synth.* **1989**, *68*, 234.

46. Pochini, A.; Ungaro, R. *In Comprehensive Supramolecular Chemistry*, Vogtle, F. Ed. Oxford: Pergamon Press, **1996**, Vol 2, p.103.

47. Thavornyutikarn, P.; Tuntulani, T. manuscript in preparation.

48. Seangprasertkit, R.; Asfari, Z.; Vicens, J. *J.Org.Chem.* **1994**, *59*, 1741.

49. Sessler, J. L.; Kral, V.; Furuta, H. *J. Am. Chem. Soc.* **1992**, *114*, 8704.

50. Lenh, J.-M. *Supramolecular Chemistry: Concepts and Perspectives.* Weinhein, VCH, **1995**.

51. Tuntulani, T.; Ruangpornvisuti, V.; Tantikunwattana, N.; Ngampaiboonsombat, O.; Seangprasertkij-Magee, R. *Tetrahedron Letters* **1997**. *38*, 3985.

52. Oueslati, I.; Abidi, R.; Amri, H.; Thuéry, P.; Nierlich, M.; Asfari, Z.; Vicens, J. *Tetrahedron Lett*. **2001**, *42*, 1685.

53. Fabbrizzi, L.; Poggi, A. *Chem. Soc. Rev.* **1995**, 197.

54. Jairajpuri, M. A.; Azam, N.; Baburaj, K.; Bulliraju, E.; Durani, S. *Biochemistry* **1998**, *37*, 10780.

55. Beer, P. D.; Hazlewood, C.; Hesek, D.; Hodacova, J.; Stokes, S. E. *J. Chem. Soc. Dalton Trans.* **1993**, 1327.

56. Uno, M.; Takahashi, S. *Chemistry Lett.* **1996**, 839.

57. Beer, P. D.; Drew, M. G. B.; Knubley, R. J.; Ogden, M. I. *J. Chem. Soc., Dalton Trans.* **1995**, 3117.

58. Beer, P. D.; Graydon, A. R.; Jonhson, A. O. M.; Smith, D. K. *Inorg. Chem.* **1997**, *36*, 2112.

59. Schneider, H.-J.; Blatter, T.; Eliseev, A.; Rűdiger, V.; Raevsky, O. A. *Pure & Appl. Chem.* **1993**, *65*, 2329.

60. Beer, P. D.; Drew, M. G. B.; Graydon, A. R., Smith, D. K., Stokes, S. E. *J. Chem Soc. Dalton Trans.* **1995**, 403.

61. Schmidtchen, F.P.; Műller, G. *J. Chem. Soc., Chem. Commn.* **1984**, 1115.

62. Raposo, C.; Almaraz, M.; Martín, M.; Weinrich, V.; Mussóns, M. L.; Alcázar, V. *Chem. Lett.* **1995**, 759.

63. Beer, P. D.; Hopkins, P. K.; McKinney, J. D. *Chem. Commun.* **1999**, 1253.

64. Sato, K.; Arai, S.; Yamagishi, T. *Tetrahedron Lett.* **1999**, *40*, 5219.

65. Rojsajjakul, T.; Veravong, S.; Tumcharern, G.; Seangprasertkij-Magee, R.; Tuntulani, T. *Tetrahedron* **1997**, *53*, 4669.

66. Jeffrey, G. A. *An Introduction to Hydrogen Bonding.* Oxford: Oxford University Press, **1997**.

APPENDICES

APPENDIX A

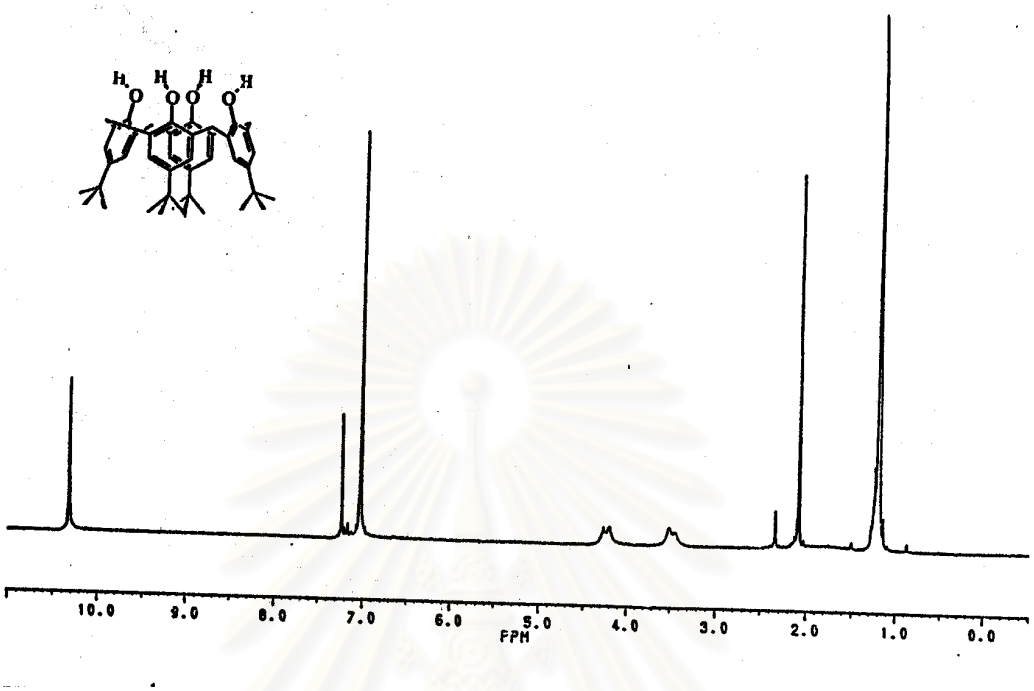

Figure A.1 ^{1}H-NMR ($CDCl_3$) spectrum of *p-tert*-butylcalix[4]arene, **2**.

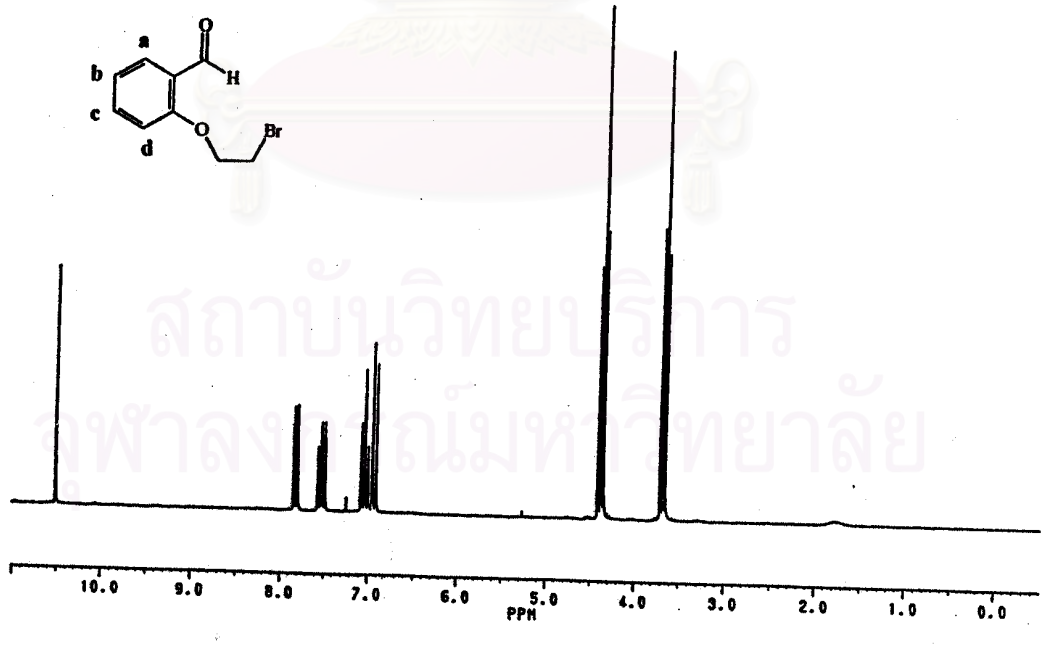

Figure A.2 ^{1}H-NMR ($CDCl_3$) spectrum of 2-(2′-bromoethoxy)benzaldehyde, **1a**.

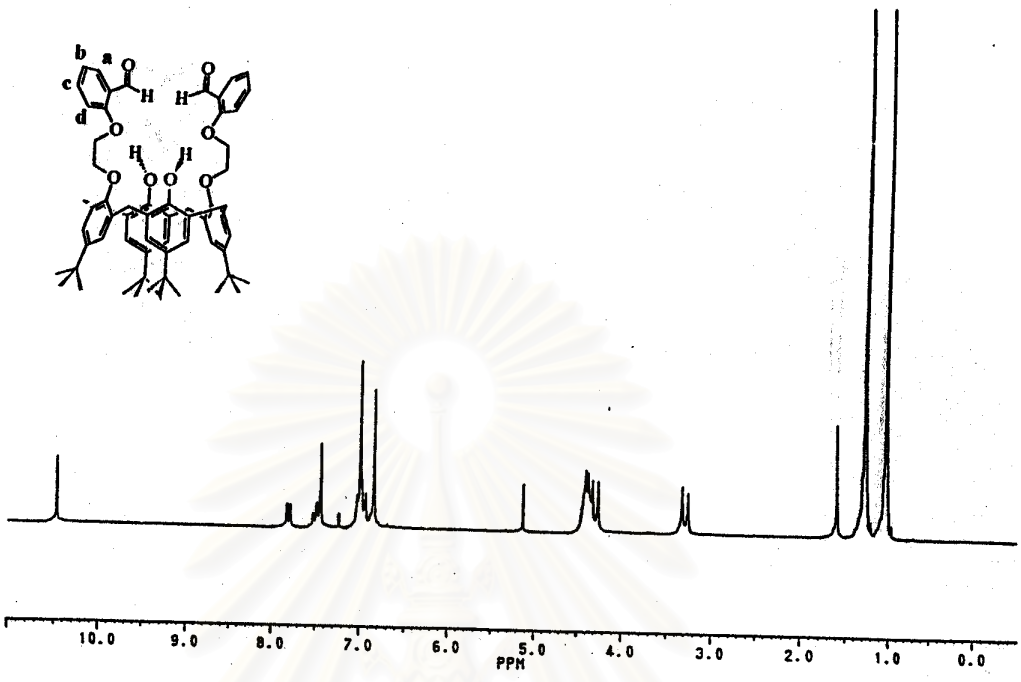

Figure A.3 ^{1}H-NMR ($CDCl_3$) spectrum of 25, 27-di((2-ethoxy)benzaldehyde-*p-tert*-butylcalix[4]arene, **3a**.

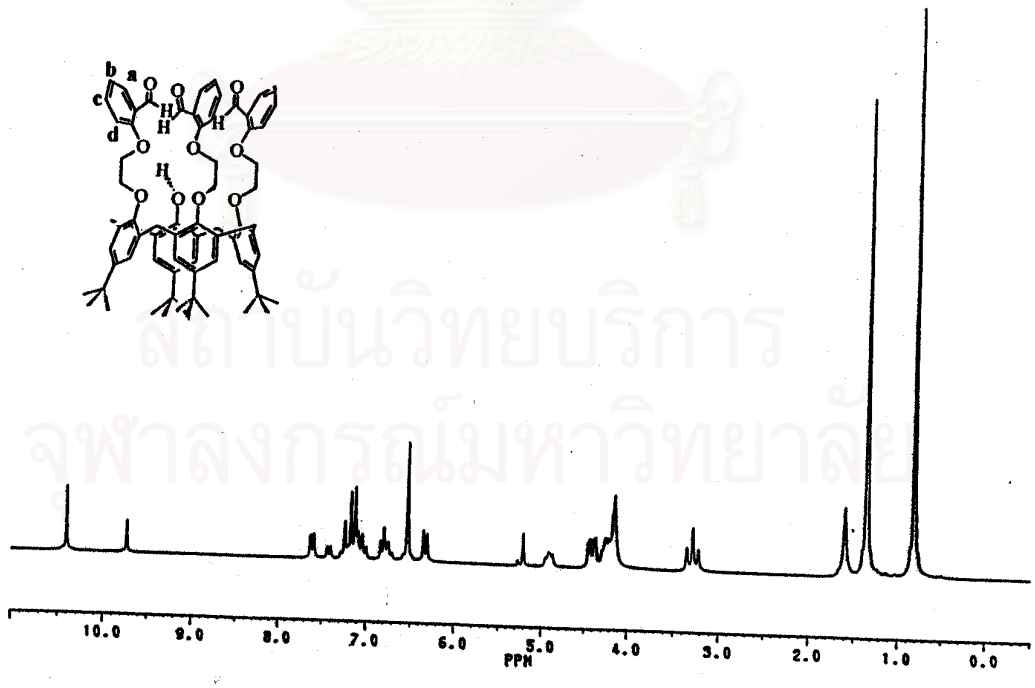

Figure A.4 ^{1}H-NMR ($CDCl_3$) spectrum of 25,26,27-tri((2-ethoxy)benzaldehyde-*p-tert*-butylcalix[4]arene, **4a**.

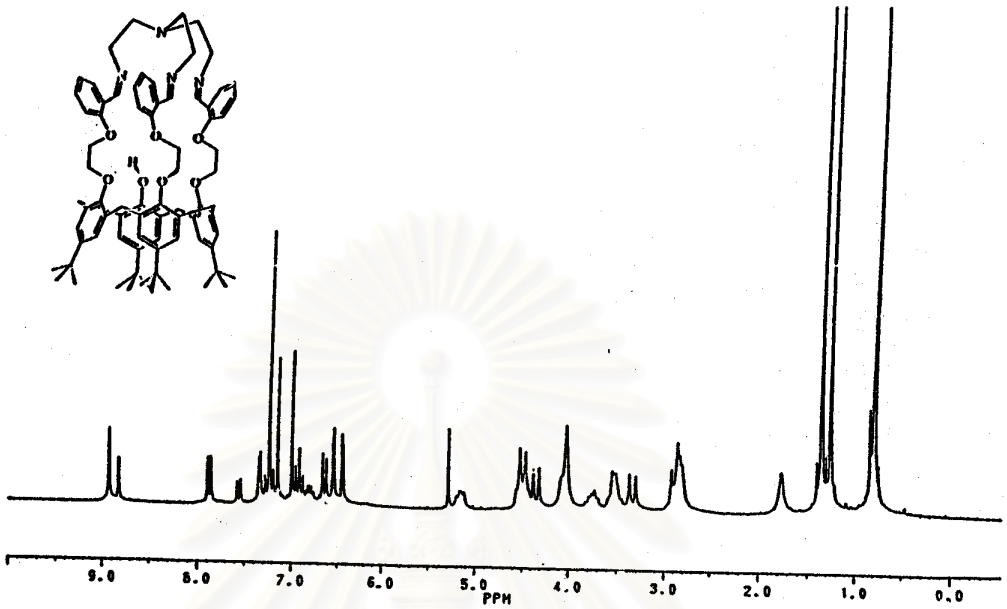

Figure A.5 ^{1}H-NMR ($CDCl_3$) spectrum of 25,26,27-*N,N′,N″*-tri-((2-ethoxy)benzyl) ethylenetriimine-*p-tert*-butylcalix[4]arene, **5a**.

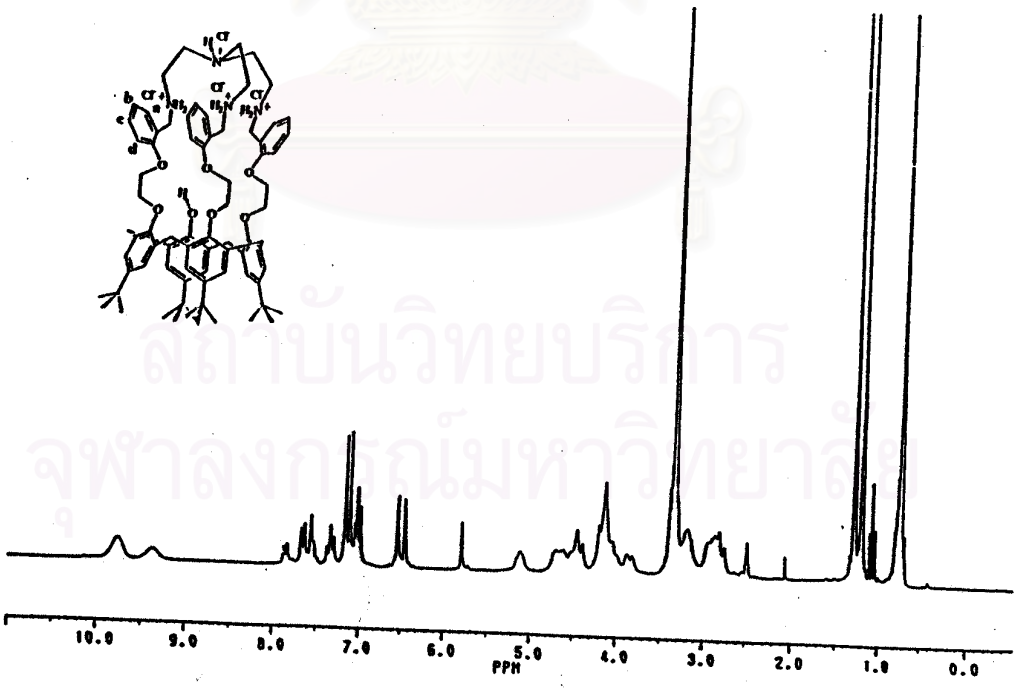

Figure A.6 ^{1}H-NMR (DMSO-d_6) spectrum of 25,26,27-*N,N′,N″*-tri((2-ethoxy)benzyl) ethylenetetraamine-*p-tert*-butylcalix[4]arene·4HCl, **6a**.

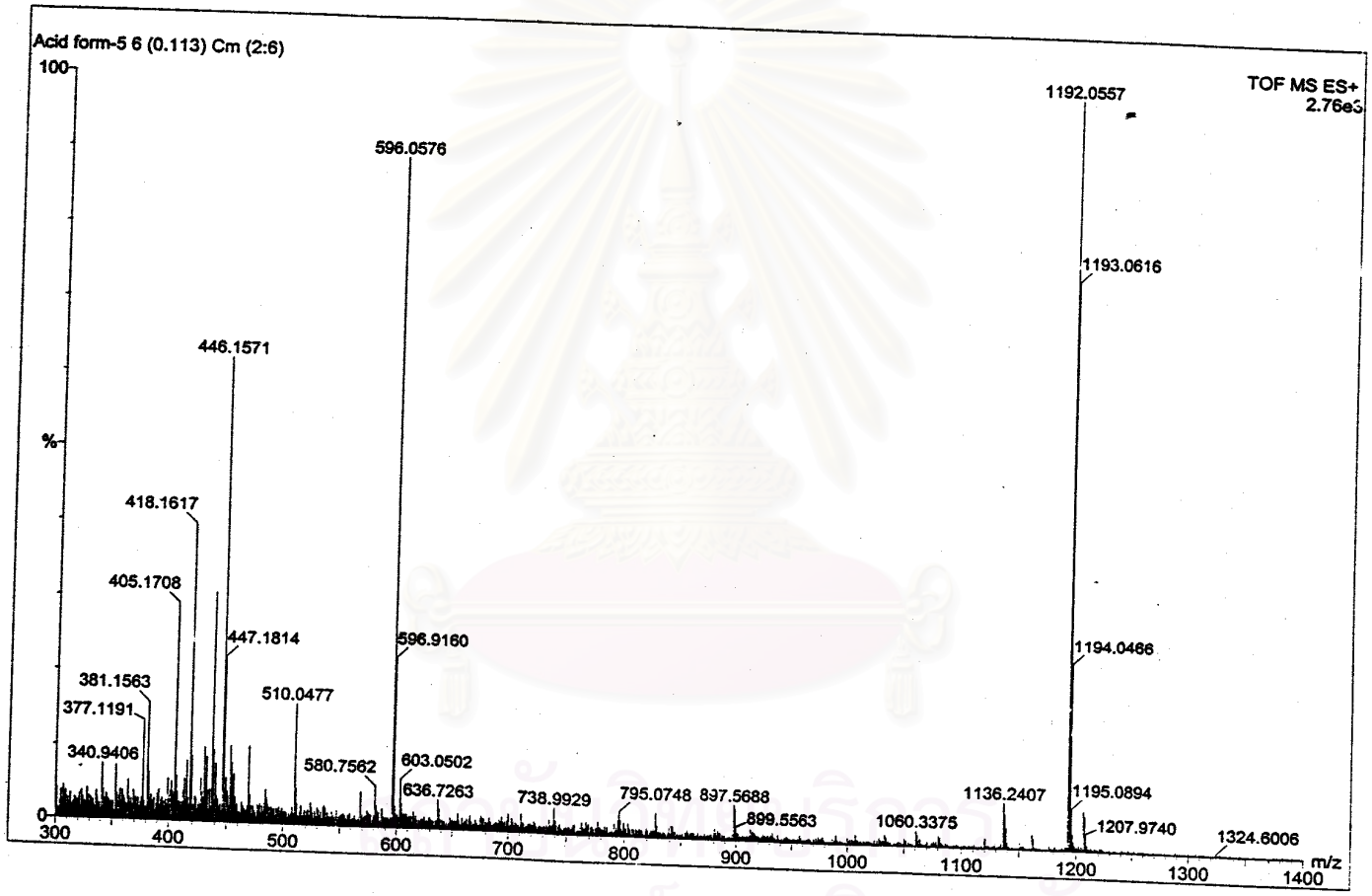

Figure A.7 TOF-MS of 26,27-*N,N′,N″*-tri((2-ethoxy)benzyl)ethylenetetraamine-*p-tert*-butylcalix[4]arene·4HCl, **6a**.

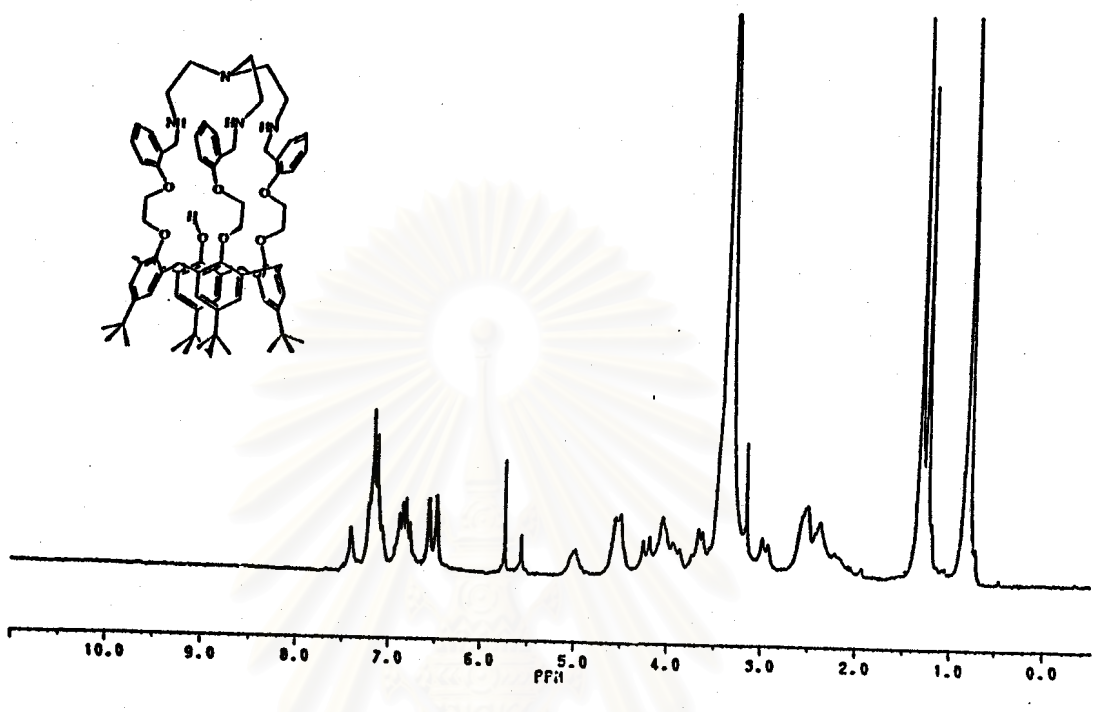

Figure A.8 ^{1}H-NMR (DMSO-d_6) spectrum of 25,26,27-*N,N′,N″*-tri((2-ethoxy)benzyl) ethylenetetraamine-*p-tert*-butylcalix[4]arene, **7a**.

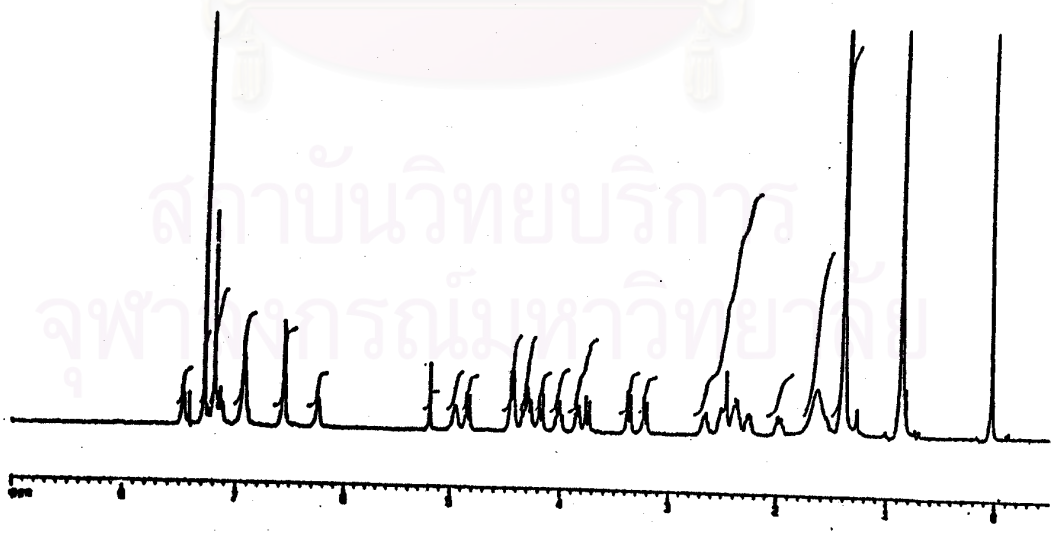

Figure A.9 ^{1}H-NMR (400 MHz, $CDCl_3$) spectrum of 25,26,27-*N,N′,N″*-tri((2-ethoxy) benzyl)ethylenetetraamine-*p-tert*-butylcalix[4]arene, **7a**.

APPENDIX B

Table B.1 Atomic coordinates ($x10^4$) and equivalent isotropic displacement parameters ($A^2 \times 10^3$) for [**6a**-$2Cl^-$]$(OH^-)_2 \cdot CH_3OH \cdot (H_2O)_2$.

	x	y	z	U(eq)
Cl(1)	152(1)	1141(1)	4840(1)	72(1)
Cl(2)	-526(1)	2677(3)	2698(2)	191(2)
O(1)	1370(1)	1961(2)	5308(1)	44(1)
O(2)	934(1)	2450(2)	6015(1)	48(1)
O(1W)	1167(2)	1580(6)	2821(5)	197(7)
O(3)	1854(1)	458(2)	5750(1)	52(1)
O(2W)	1049(5)	2489(17)	3532(6)	540(30)
O(4)	1472(1)	1417(2)	6602(1)	62(1)
O(3W)	-207(2)	2785(6)	6618(4)	152(5)
O(5)	929(1)	14(2)	5106(1)	60(1)
O(4W)	402(3)	2454(12)	7428(4)	281(9)
O(6)	305(1)	3233(2)	5249(1)	56(1)
O(7)	1619(1)	-770(2)	4827(2)	74(1)
O(8)	748(2)	-842(3)	2176(2)	76(2)
N(1)	271(1)	-671(3)	4448(2)	58(1)
N(2)	325(1)	420(3)	3527(2)	63(1)
N(3)	19(1)	2404(3)	3869(2)	61(1)
N(4)	1106(1)	-49(4)	3293(2)	80(2)
C(1)	1311(1)	4484(3)	5955(2)	49(1)
C(2)	1439(1)	4713(3)	6525(2)	57(1)
C(3)	1413(1)	4136(3)	6911(2)	55(1)
C(4)	1253(1)	3354(3)	6768(2)	47(1)
C(5)	1257(1)	2728(3)	7221(2)	54(1)
C(6)	1570(1)	2240(3)	7461(2)	46(1)
C(7)	1777(1)	2373(3)	8007(2)	46(1)
C(8)	2066(1)	1937(3)	8250(2)	49(1)

Table B.1 (continued) Atomic coordinates ($x10^4$) and equivalent isotropic displacement parameters ($A^2 \times 10^3$) for [**6a**-$2Cl^-$]$(OH^-)_2 \cdot CH_3OH \cdot (H_2O)_2$.

	x	y	z	U(eq)
C(9)	2148(1)	1349(3)	7906(2)	50(1)
C(10)	1955(1)	1195(3)	7350(2)	47(1)
C(11)	2071(1)	654(3)	6968(2)	53(1)
C(12)	2182(1)	1221(3)	6571(2)	45(1)
C(13)	2387(1)	1889(3)	6787(2)	54(1)
C(14)	2469(1)	2483(3)	6455(2)	52(1)
C(15)	2331(1)	2396(3)	5885(2)	51(1)
C(16)	2122(1)	1727(3)	5636(2)	48(1)
C(17)	1944(1)	1718(3)	5003(2)	52(1)
C(18)	1732(1)	2488(3)	4832(2)	45(1)
C(19)	1825(1)	3155(3)	4563(2)	51(1)
C(20)	1658(1)	3919(3)	4458(2)	57(1)
C(21)	1391(1)	4002(3)	4643(2)	49(1)
C(22)	1291(1)	3353(3)	4921(2)	42(1)
C(23)	1018(1)	3508(3)	5158(2)	46(1)
C(24)	1146(1)	3727(3)	5785(2)	41(1)
C(25)	1458(1)	2603(3)	5000(2)	40(1)
C(26)	1106(1)	3195(3)	6191(2)	38(1)
C(27)	1663(1)	1624(3)	7138(2)	46(1)
C(28)	2059(1)	1128(3)	5990(2)	44(1)
C(29)	1778(2)	4645(4)	4184(3)	80(2)
C(30)	2006(6)	5133(14)	4657(7)	430(30)
C(31)	1962(4)	4402(7)	3831(7)	211(11)
C(32)	1513(3)	5190(7)	3860(6)	210(10)
C(33)	1586(2)	5594(4)	6699(3)	77(2)
C(34)	1937(2)	5485(6)	7114(5)	103(5)

Table B.1 (continued) Atomic coordinates ($x10^4$) and equivalent isotropic displacement parameters ($A^2 \times 10^3$) for [**6a**-$2Cl^-$]$(OH^-)_2 \cdot CH_3OH \cdot (H_2O)_2$.

	x	y	z	U(eq)
C(35)	1572(2)	6137(5)	6208(4)	125(5)
C(36)	1380(2)	6048(5)	7023(4)	80(4)
C(37)	2293(1)	2089(4)	8850(2)	61(2)
C(38)	2629(2)	2087(9)	8905(4)	219(11)
C(39)	2182(5)	2717(12)	9128(5)	390(20)
C(40)	2315(3)	1250(7)	9198(4)	153(9)
C(41)	2917(5)	3077(10)	7267(8)	350(20)
C(42)	2782(6)	3731(12)	6372(6)	380(20)
C(43)	2480(5)	3818(11)	6897(12)	370(30)
C(44)	2675(2)	3245(4)	6720(3)	70(2)
C(45)	1159(1)	1328(3)	4982(2)	54(1)
C(46)	1083(1)	763(3)	5392(2)	57(1)
C(47)	915(1)	-651(3)	5449(2)	65(2)
C(48)	1066(2)	-682(5)	6026(3)	111(3)
C(49)	1048(3)	-1418(6)	6315(4)	158(5)
C(50)	865(2)	-2067(5)	6062(4)	140(4)
C(51)	707(2)	-2033(4)	5500(3)	85(2)
C(52)	727(1)	-1325(3)	5182(2)	63(2)
C(53)	536(1)	-1295(3)	4555(2)	63(2)
C(54)	25(2)	-688(4)	3859(2)	72(2)
C(55)	170(2)	-411(4)	3413(2)	73(2)
C(56)	84(1)	1093(4)	3384(2)	66(2)
C(57)	234(2)	1935(4)	3626(2)	68(2)
C(58)	154(1)	3247(4)	4086(2)	64(2)
C(59)	-52(1)	3668(3)	4377(3)	56(1)
C(60)	-340(2)	4088(4)	4061(3)	77(2)

Table B.1 (continued) Atomic coordinates ($x10^4$) and equivalent isotropic displacement parameters ($A^2 \times 10^3$) for [**6a**-$2Cl^-$]$(OH^-)_2 \cdot CH_3OH \cdot (H_2O)_2$.

	x	y	z	U(eq)
C(61)	-537(2)	4460(4)	4305(4)	90(2)
C(62)	-456(2)	4451(4)	4879(4)	85(2)
C(63)	-167(1)	4060(3)	5224(3)	70(2)
C(64)	28(1)	3647(3)	4960(2)	53(1)
C(65)	389(1)	3140(4)	5843(2)	59(1)
C(66)	608(1)	2401(3)	6057(2)	58(1)
C(67)	567(2)	508(4)	3247(2)	69(2)
C(68)	881(2)	122(4)	3606(2)	77(2)
C(69)	1417(2)	-504(5)	3659(3)	93(2)
C(71)	1152(2)	-1920(6)	3586(3)	97(2)
C(72)	1073(2)	-2618(6)	3791(4)	112(3)
C(73)	1165(2)	-2748(5)	4397(4)	110(3)
C(74)	1351(2)	-2127(4)	4744(3)	82(2)
C(75)	1439(1)	-1407(4)	4513(3)	71(2)
C(76)	1787(2)	-947(4)	5414(3)	80(2)
C(77)	2026(2)	-265(3)	5657(3)	75(2)
C(78)	1335(2)	-1296(5)	3920(3)	77(2)
C(79)	684(4)	-1050(11)	2314(6)	450(30)

U(eq) is defined as one third of the trace of the orthogonalized Uij tensor.

Table B.2 Bond lengths [Å] for [**6a**-2Cl^-]$(OH^-)_2 \cdot CH_3OH \cdot (H_2O)_2$.

Atoms	Bond lengths (Å)	Atoms	Bond lengths (Å)
O(1)-C(25)	1.411(5)	C(4)-C(5)	1.509(7)
O(1)-C(45)	1.426(5)	C(5)-C(6)	1.514(7)
O(2)-C(26)	1.394(5)	C(6)-C(7)	1.385(6)
O(2)-C(66)	1.462(6)	C(6)-C(27)	1.416(7)
O(3)-C(28)	1.394(6)	C(7)-C(8)	1.391(7)
O(3)-C(77)	1.437(6)	C(8)-C(9)	1.398(7)
O(4)-C(27)	1.369(5)	C(8)-C(37)	1.525(7)
O(5)-C(47)	1.378(6)	C(9)-C(10)	1.394(6)
O(5)-C(46)	1.437(6)	C(10)-C(27)	1.389(7)
O(6)-C(64)	1.357(6)	C(10)-C(11)	1.500(7)
O(6)-C(65)	1.423(6)	C(11)-C(12)	1.537(7)
O(7)-C(75)	1.362(7)	C(12)-C(13)	1.379(7)
O(7)-C(76)	1.441(7)	C(12)-C(28)	1.389(6)
O(8)-C(79)	0.61(3)	C(13)-C(14)	1.387(7)
N(1)-C(53)	1.480(7)	C(14)-C(15)	1.367(7)
N(1)-C(54)	1.513(7)	C(14)-C(44)	1.524(8)
N(2)-C(67)	1.459(7)	C(15)-C(16)	1.407(7)
N(2)-C(56)	1.461(7)	C(16)-C(28)	1.394(7)
N(2)-C(55)	1.470(8)	C(16)-C(17)	1.523(6)
N(3)-C(57)	1.483(7)	C(17)-C(18)	1.508(7)
N(3)-C(58)	1.492(7)	C(18)-C(19)	1.389(7)
N(4)-C(68)	1.472(7)	C(18)-C(25)	1.408(7)
N(4)-C(69)	1.545(8)	C(19)-C(20)	1.397(7)
C(1)-C(24)	1.397(6)	C(20)-C(21)	1.398(7)
C(1)-C(2)	1.403(7)	C(20)-C(29)	1.526(8)
C(2)-C(3)	1.369(7)	C(21)-C(22)	1.396(6)
C(2)-C(33)	1.543(8)	C(22)-C(25)	1.379(6)
C(3)-C(4)	1.414(7)	C(22)-C(23)	1.521(7)

Table B.2 (continued) Bond lengths [Å] for [**6a**-2Cl^-]$(OH^-)_2$·CH_3OH·$(H_2O)_2$.

Atoms	Bond lengths (Å)	Atoms	Bond lengths (Å)
C(4)-C(26)	1.404(6)	C(23)-C(24)	1.529(6)
C(24)-C(26)	1.382(6)	C(52)-C(53)	1.519(8)
C(29)-C(31)	1.435(12)	C(54)-C(55)	1.525(8)
C(29)-C(32)	1.459(11)	C(56)-C(57)	1.526(8)
C(29)-C(30)	1.492(16)	C(58)-C(59)	1.495(8)
C(33)-C(35)	1.494(10)	C(59)-C(64)	1.391(8)
C(33)-C(34)	1.548(10)	C(59)-C(60)	1.409(7)
C(33)-C(36)	1.578(10)	C(60)-C(61)	1.351(10)
C(37)-C(39)	1.394(13)	C(61)-C(62)	1.369(10)
C(37)-C(38)	1.429(11)	C(62)-C(63)	1.416(9)
C(37)-C(40)	1.582(11)	C(63)-C(64)	1.406(8)
C(41)-C(44)	1.454(15)	C(65)-C(66)	1.500(7)
C(42)-C(44)	1.363(14)	C(67)-C(68)	1.498(8)
C(43)-C(44)	1.420(15)	C(69)-C(78)	1.519(10)
C(45)-C(46)	1.489(7)	C(71)-C(72)	1.317(12)
C(47)-C(52)	1.382(7)	C(71)-C(78)	1.372(10)
C(47)-C(48)	1.382(8)	C(72)-C(73)	1.458(12)
C(48)-C(49)	1.395(10)	C(73)-C(74)	1.389(10)
C(49)-C(50)	1.330(11)	C(74)-C(75)	1.395(10)
C(50)-C(51)	1.354(11)	C(75)-C(78)	1.421(9)
C(51)-C(52)	1.401(8)	C(76)-C(77)	1.490(8)

Table B.3 Angles [deg] for [**6a**-2Cl^-]$(OH^-)_2 \cdot CH_3OH \cdot (H_2O)_2$.

Atoms	Angles [deg]	Atoms	Angles [deg]
C(25)-O(1)-C(45)	115.9(3)	C(22)-C(23)-C(24)	112.2(4)
C(26)-O(2)-C(66)	117.1(4)	C(26)-C(24)-C(1)	118.7(4)
C(28)-O(3)-C(77)	112.9(4)	C(26)-C(24)-C(23)	122.1(4)
C(47)-O(5)-C(46)	115.7(4)	C(1)-C(24)-C(23)	119.2(4)
C(64)-O(6)-C(65)	119.1(4)	C(22)-C(25)-C(18)	122.1(4)
C(75)-O(7)-C(76)	116.6(5)	C(22)-C(25)-O(1)	118.6(4)
C(53)-N(1)-C(54)	115.0(4)	C(18)-C(25)-O(1)	119.1(4)
C(67)-N(2)-C(56)	112.9(5)	C(24)-C(26)-O(2)	118.3(4)
C(67)-N(2)-C(55)	110.7(4)	C(24)-C(26)-C(4)	122.0(4)
C(56)-N(2)-C(55)	111.3(5)	O(2)-C(26)-C(4)	119.6(4)
C(57)-N(3)-C(58)	112.2(5)	O(4)-C(27)-C(10)	116.1(4)
C(68)-N(4)-C(69)	112.3(5)	O(4)-C(27)-C(6)	122.6(4)
C(24)-C(1)-C(2)	121.8(5)	C(10)-C(27)-C(6)	121.4(4)
C(3)-C(2)-C(1)	116.9(5)	C(12)-C(28)-C(16)	120.9(4)
C(3)-C(2)-C(33)	122.1(5)	C(12)-C(28)-O(3)	120.4(4)
C(1)-C(2)-C(33)	120.9(5)	C(16)-C(28)-O(3)	118.6(4)
C(2)-C(3)-C(4)	124.1(5)	C(31)-C(29)-C(32)	108.5(8)
C(26)-C(4)-C(3)	116.0(4)	C(31)-C(29)-C(30)	105.8(14)
C(26)-C(4)-C(5)	123.4(4)	C(32)-C(29)-C(30)	109.3(14)
C(3)-C(4)-C(5)	120.6(4)	C(31)-C(29)-C(20)	115.2(6)
C(4)-C(5)-C(6)	115.0(4)	C(32)-C(29)-C(20)	112.0(6)
C(7)-C(6)-C(27)	117.4(4)	C(30)-C(29)-C(20)	105.8(7)
C(7)-C(6)-C(5)	121.4(4)	C(35)-C(33)-C(2)	113.0(6)
C(27)-C(6)-C(5)	121.2(4)	C(35)-C(33)-C(34)	112.4(7)
C(6)-C(7)-C(8)	123.8(4)	C(2)-C(33)-C(34)	108.4(6)
C(7)-C(8)-C(9)	116.2(4)	C(35)-C(33)-C(36)	106.8(7)
C(7)-C(8)-C(37)	123.5(4)	C(2)-C(33)-C(36)	107.9(5)
C(9)-C(8)-C(37)	120.4(4)	C(34)-C(33)-C(36)	108.0(6)

Table B.3 (continued) Angles [deg] for [**6a**-2Cl^-]$(OH^-)_2 \cdot CH_3OH \cdot (H_2O)_2$.

Atoms	Angles [deg]	Atoms	Angles [deg]
C(3)-C(2)-C(33)	122.1(5)	C(39)-C(37)-C(38)	118.0(11)
C(39)-C(37)-C(8)	113.1(6)	N(3)-C(58)-C(59)	110.7(5)
C(38)-C(37)-C(8)	113.7(6)	C(64)-C(59)-C(60)	118.2(5)
C(39)-C(37)-C(40)	107.1(11)	C(64)-C(59)-C(58)	121.6(4)
C(38)-C(37)-C(40)	94.2(7)	C(60)-C(59)-C(58)	120.2(6)
C(8)-C(37)-C(40)	108.3(5)	C(61)-C(60)-C(59)	122.2(7)
C(42)-C(44)-C(43)	102.0(12)	C(60)-C(61)-C(62)	119.8(6)
C(42)-C(44)-C(41)	114.7(12)	C(61)-C(62)-C(63)	121.1(6)
C(43)-C(44)-C(41)	98.2(11)	C(64)-C(63)-C(62)	118.1(6)
C(42)-C(44)-C(14)	116.7(6)	O(6)-C(64)-C(59)	116.4(5)
C(43)-C(44)-C(14)	108.6(8)	O(6)-C(64)-C(63)	123.0(5)
C(41)-C(44)-C(14)	113.9(6)	C(59)-C(64)-C(63)	120.6(5)
O(1)-C(45)-C(46)	106.1(4)	O(6)-C(65)-C(66)	111.7(4)
O(5)-C(46)-C(45)	109.2(4)	O(2)-C(66)-C(65)	116.9(4)
O(5)-C(47)-C(52)	115.7(5)	N(2)-C(67)-C(68)	109.5(5)
O(5)-C(47)-C(48)	125.4(5)	N(4)-C(68)-C(67)	113.1(5)
C(52)-C(47)-C(48)	118.8(5)	C(78)-C(69)-N(4)	110.9(6)
C(47)-C(48)-C(49)	119.3(7)	C(72)-C(71)-C(78)	123.0(8)
C(50)-C(49)-C(48)	122.0(8)	C(71)-C(72)-C(73)	120.9(8)
C(49)-C(50)-C(51)	119.1(7)	C(74)-C(73)-C(72)	117.2(9)
C(50)-C(51)-C(52)	121.5(6)	C(73)-C(74)-C(75)	120.4(7)
C(47)-C(52)-C(51)	119.0(6)	O(7)-C(75)-C(74)	123.7(6)
C(47)-C(52)-C(53)	120.9(5)	O(7)-C(75)-C(78)	116.0(6)
C(51)-C(52)-C(53)	120.1(5)	C(74)-C(75)-C(78)	120.3(6)
N(1)-C(53)-C(52)	109.6(4)	O(7)-C(76)-C(77)	109.0(5)
N(1)-C(54)-C(55)	112.6(5)	O(3)-C(77)-C(76)	108.4(5)
N(2)-C(55)-C(54)	113.2(5)	C(71)-C(78)-C(75)	118.1(8)
N(2)-C(56)-C(57)	111.4(4)	C(71)-C(78)-C(69)	120.6(7)
N(3)-C(57)-C(56)	111.1(5)	C(75)-C(78)-C(69)	121.3(6)

Symmetry transformations used to generate equivalent atoms.

Table B.4 Anisotropic displacement parameters (A^2 x 10^3) for [**6a**-2Cl^-]$(OH^-)_2$·CH_3OH·$(H_2O)_2$.

	U11	U22	U33	U23	U13	U12
Cl(1)	91(1)	62(1)	68(1)	-5(1)	30(1)	-1(1)
Cl(2)	160(3)	218(4)	158(3)	-5(2)	4(2)	30(3)
O(1)	54(2)	38(2)	39(2)	1(1)	13(2)	-5(2)
O(2)	42(2)	44(2)	54(2)	2(2)	10(2)	-2(2)
O(1W)	107(6)	215(10)	275(14)	125(9)	71(7)	10(5)
O(3)	64(2)	38(2)	49(2)	-4(2)	10(2)	6(2)
O(2W)	480(30)	800(50)	182(13)	143(19)	-105(15)	-450(30)
O(4)	72(3)	56(2)	40(2)	-7(2)	-5(2)	11(2)
O(3W)	132(8)	196(10)	134(8)	-34(6)	54(6)	-26(6)
O(5)	71(2)	40(2)	58(2)	-6(2)	8(2)	-17(2)
O(4W)	179(10)	480(20)	165(9)	73(10)	34(7)	56(11)
O(6)	49(2)	64(2)	53(2)	3(2)	14(2)	15(2)
O(7)	79(3)	62(3)	62(2)	-15(2)	-2(2)	11(2)
O(8)	93(4)	73(3)	45(3)	-26(2)	1(3)	8(3)
N(1)	55(3)	57(3)	51(3)	-3(2)	4(2)	8(2)
N(2)	66(3)	65(3)	59(3)	-5(2)	22(2)	9(2)
N(3)	53(3)	55(3)	69(3)	-13(2)	13(2)	5(2)
N(4)	50(3)	121(5)	62(3)	-7(3)	10(2)	17(3)
C(1)	43(3)	43(3)	64(3)	0(2)	21(2)	1(2)
C(2)	50(3)	47(3)	73(4)	-8(3)	20(3)	-5(2)
C(3)	50(3)	59(3)	49(3)	-11(3)	6(2)	1(3)
C(4)	37(3)	52(3)	48(3)	-2(2)	9(2)	3(2)
C(5)	42(3)	70(4)	47(3)	1(2)	10(2)	9(2)
C(6)	44(3)	49(3)	42(3)	3(2)	10(2)	1(2)
C(7)	47(3)	48(3)	39(3)	-8(2)	11(2)	-1(2)
C(8)	53(3)	42(3)	45(3)	-4(2)	5(2)	-4(2)

Table B.4 (continued) Anisotropic displacement parameters (A^2 x 10^3) for [**6a**-$2Cl^-$] $(OH^-)_2 \cdot CH_3OH \cdot (H_2O)_2$.

	U11	U22	U33	U23	U13	U12
C(9)	51(3)	46(3)	40(3)	8(2)	-2(2)	3(2)
C(10)	55(3)	37(3)	43(3)	4(2)	9(2)	2(2)
C(11)	71(4)	36(3)	44(3)	4(2)	8(2)	9(2)
C(12)	52(3)	34(2)	44(3)	0(2)	9(2)	14(2)
C(13)	58(3)	49(3)	46(3)	-2(2)	4(2)	7(3)
C(14)	50(3)	42(3)	61(3)	-7(2)	14(3)	3(2)
C(15)	60(3)	43(3)	55(3)	0(2)	26(3)	10(2)
C(16)	52(3)	46(3)	44(3)	1(2)	14(2)	16(2)
C(17)	63(3)	46(3)	48(3)	-2(2)	22(2)	7(2)
C(18)	51(3)	45(3)	37(2)	0(2)	12(2)	4(2)
C(19)	51(3)	57(3)	49(3)	8(2)	22(2)	10(2)
C(20)	64(4)	54(3)	52(3)	8(2)	20(3)	0(3)
C(21)	60(3)	39(3)	48(3)	8(2)	17(2)	7(2)
C(22)	40(3)	46(3)	35(2)	5(2)	9(2)	3(2)
C(23)	41(3)	43(3)	47(3)	10(2)	7(2)	7(2)
C(24)	36(2)	42(3)	43(3)	-1(2)	10(2)	5(2)
C(25)	42(3)	38(3)	37(2)	0(2)	7(2)	-1(2)
C(26)	29(2)	37(3)	44(3)	3(2)	7(2)	3(2)
C(27)	52(3)	42(3)	34(2)	-1(2)	1(2)	-9(2)
C(28)	46(3)	39(3)	42(3)	-1(2)	7(2)	9(2)
C(29)	85(5)	75(4)	87(5)	29(4)	39(4)	-1(4)
C(30)	600(40)	390(30)	183(18)	76(17)	-10(20)	-400(30)
C(31)	285(19)	129(10)	330(20)	110(11)	250(18)	53(10)
C(32)	170(12)	172(12)	350(20)	192(14)	169(14)	85(9)
C(33)	74(4)	62(4)	89(5)	-20(3)	21(4)	-21(3)
C(34)	51(6)	75(7)	161(10)	-46(6)	7(5)	-23(4)

Table B.4 (continued) Anisotropic displacement parameters (A^2 x 10^3) for [**6a**-$2Cl^-$] $(OH^-)_2 \cdot CH_3OH \cdot (H_2O)_2$.

	U11	U22	U33	U23	U13	U12
C(35)	154(9)	89(7)	143(9)	-7(5)	65(7)	-51(6)
C(36)	77(6)	53(5)	105(7)	-35(4)	23(5)	0(4)
C(37)	60(4)	71(4)	41(3)	-15(3)	3(3)	-3(3)
C(38)	64(7)	410(30)	148(11)	-154(13)	-5(6)	-36(9)
C(39)	370(30)	420(30)	178(14)	-210(17)	-180(16)	270(20)
C(40)	219(17)	130(11)	43(6)	24(6)	-46(7)	-37(9)
C(41)	330(30)	185(17)	320(30)	55(14)	-170(20)	-171(19)
C(42)	590(50)	380(30)	172(15)	-136(16)	149(19)	-420(30)
C(43)	290(30)	260(20)	630(60)	-330(30)	250(30)	-140(20)
C(44)	83(4)	46(3)	76(4)	-6(3)	23(4)	-10(3)
C(45)	66(3)	40(3)	43(3)	-2(2)	0(2)	-11(2)
C(46)	61(3)	45(3)	59(3)	-8(2)	13(3)	-14(2)
C(47)	70(4)	45(3)	63(4)	7(3)	0(3)	-11(3)
C(48)	122(6)	80(5)	83(5)	25(4)	-30(4)	-44(4)
C(49)	191(10)	118(7)	98(6)	58(6)	-42(6)	-57(7)
C(50)	147(8)	79(6)	142(8)	54(5)	-21(7)	-33(5)
C(51)	84(5)	39(3)	114(6)	10(3)	9(4)	-7(3)
C(52)	63(4)	42(3)	73(4)	0(3)	8(3)	6(3)
C(53)	69(4)	43(3)	70(4)	-13(3)	14(3)	-9(3)
C(54)	75(4)	76(4)	60(4)	-15(3)	14(3)	-9(3)
C(55)	80(4)	73(4)	61(4)	-9(3)	16(3)	-4(3)
C(56)	60(4)	75(4)	56(3)	-8(3)	10(3)	11(3)
C(57)	64(4)	73(4)	65(4)	0(3)	19(3)	11(3)
C(58)	54(3)	67(4)	59(3)	3(3)	4(3)	0(3)
C(59)	42(3)	37(3)	79(4)	-2(2)	6(3)	4(2)
C(60)	60(4)	57(4)	87(4)	2(3)	-10(3)	8(3)

Table B.4 (continued) Anisotropic displacement parameters (A^2 x 10^3) for [**6a**-2Cl^-] $(OH^-)_2 \cdot CH_3OH \cdot (H_2O)_2$.

	U11	U22	U33	U23	U13	U12
C(61)	54(4)	66(4)	125(7)	-16(4)	-2(4)	19(3)
C(62)	56(4)	55(4)	142(7)	-20(4)	32(4)	10(3)
C(63)	49(3)	58(4)	100(5)	-10(3)	23(3)	4(3)
C(64)	42(3)	41(3)	72(4)	2(2)	15(3)	7(2)
C(65)	46(3)	67(4)	64(4)	-7(3)	19(3)	-5(3)
C(66)	53(3)	65(4)	51(3)	8(3)	11(3)	-16(3)
C(67)	74(4)	70(4)	66(4)	3(3)	27(3)	14(3)
C(68)	73(4)	102(5)	56(4)	-15(3)	22(3)	14(4)
C(69)	63(4)	123(6)	86(5)	-9(4)	18(4)	15(4)
C(71)	95(6)	85(6)	95(5)	-32(5)	10(4)	12(5)
C(72)	99(6)	97(7)	114(7)	-53(5)	-1(5)	11(5)
C(73)	91(6)	76(5)	147(8)	-33(5)	17(5)	12(4)
C(74)	87(5)	57(4)	89(5)	-19(3)	13(4)	10(3)
C(75)	59(4)	66(4)	76(4)	-30(3)	6(3)	12(3)
C(76)	91(5)	52(4)	72(4)	-17(3)	-7(3)	28(3)
C(77)	76(4)	42(3)	81(4)	-17(3)	-8(3)	22(3)
C(78)	59(4)	95(5)	67(4)	-33(4)	8(3)	22(3)
C(79)	390(30)	670(50)	110(12)	-230(20)	-158(15)	470(40)

The anisotropic displacement factor exponent takes the form: $-2pi^2[h^2a^2*U11 + ... + 2hka*b*U12]$.

APPENDIX C

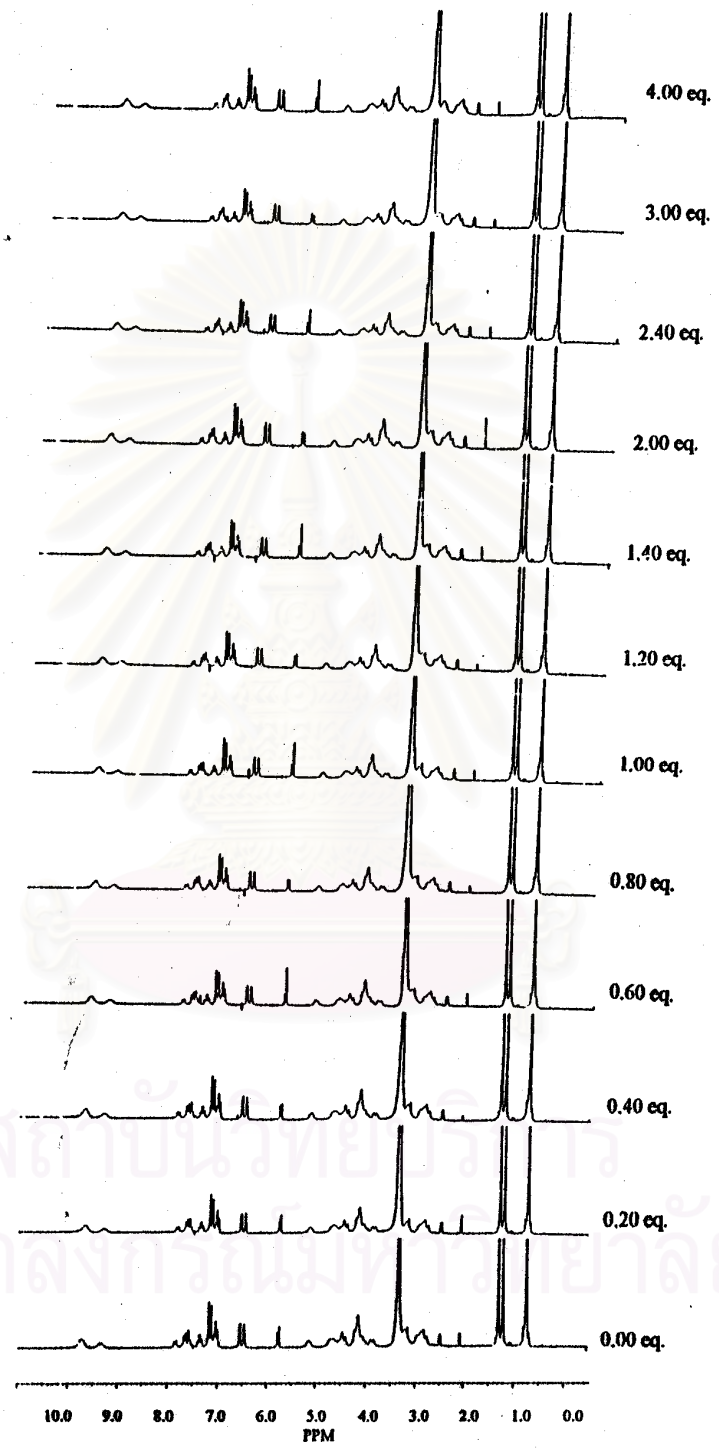

Figure C.1 ^{1}H-NMR (DMSO-d_6) spectra of complexation between **6a** and NaI at 0.00-4.00 ratios.

Figure C.2 ^{1}H-NMR (DMSO-d_6) spectra of complexation between **6a** and $NaNO_3$ at 0.00-4.00 ratios.

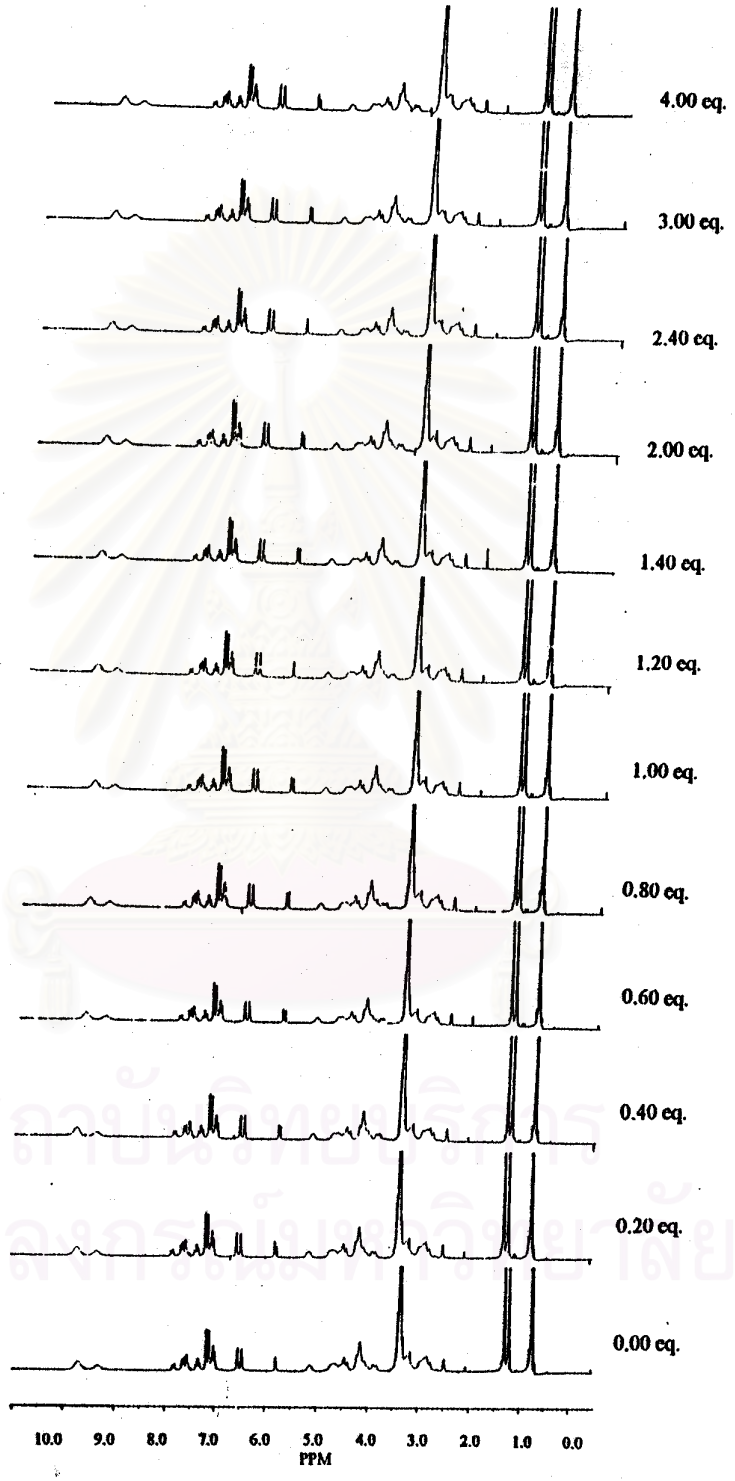

Figure C.3 ^{1}H-NMR (DMSO-d_6) spectra of complexation between **6a** and NaBr at 0.00-4.00 ratios.

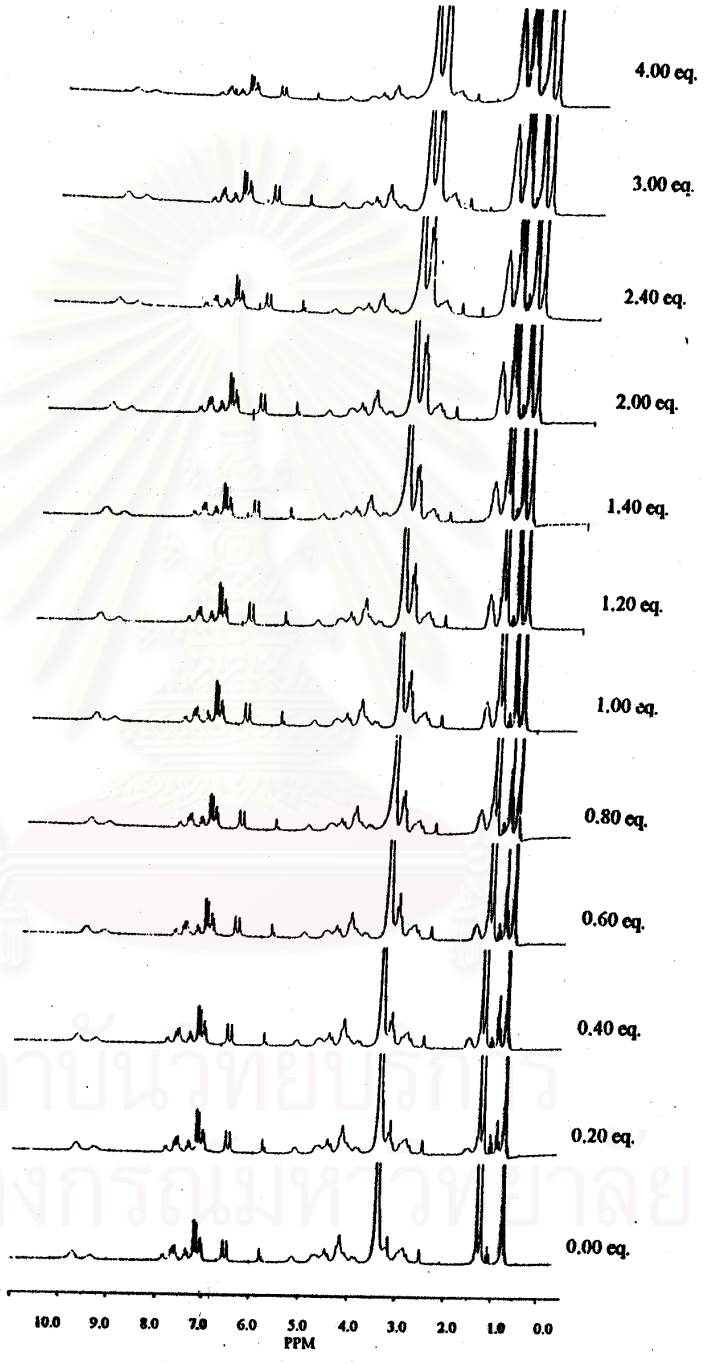

Figure C.4 ^{1}H-NMR (DMSO-d_6) spectra of complexation between **6a** and $C_{16}H_{36}IN$ at 0.00-4.00 ratios.

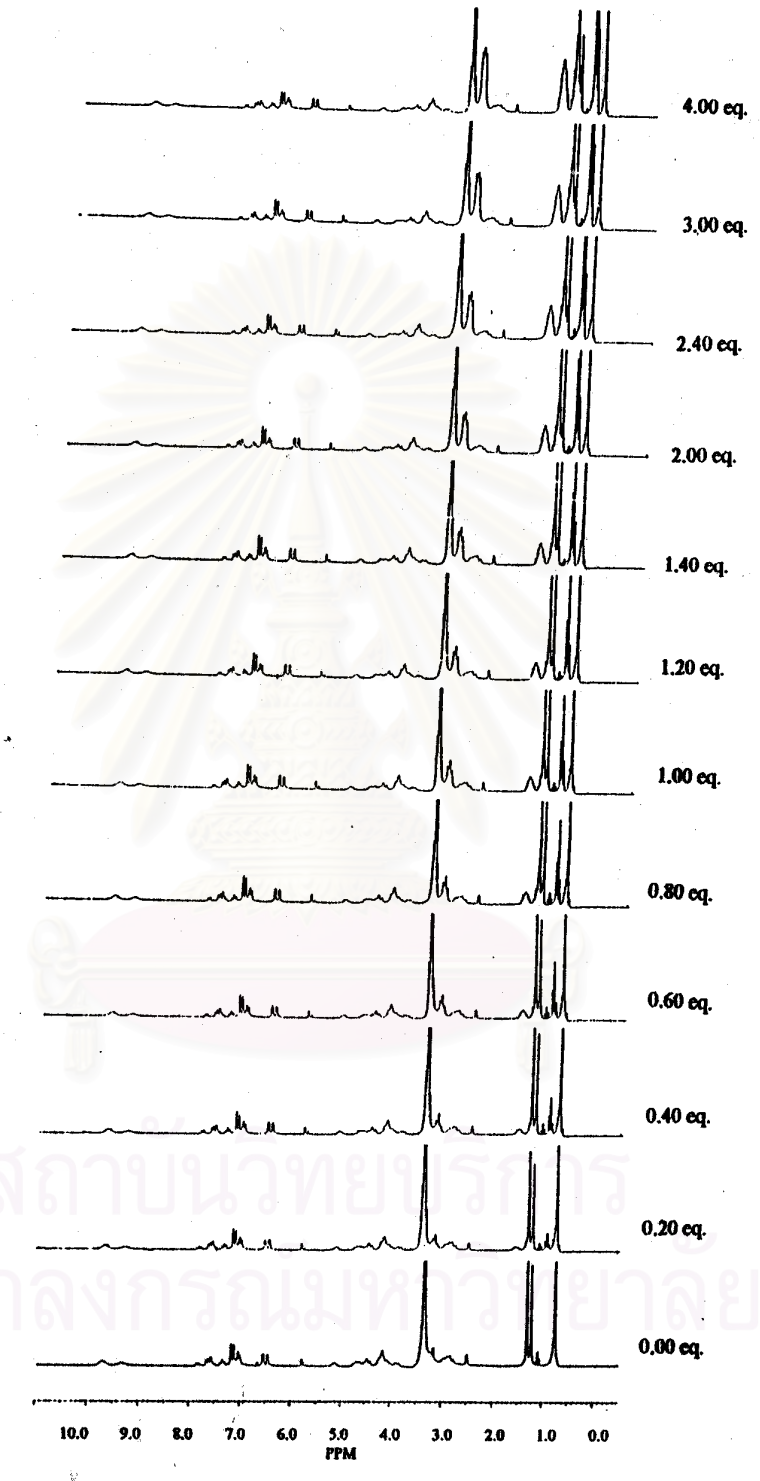

Figure C.5 ^{1}H-NMR (DMSO-d_6) spectra of complexation between **6a** and $C_{16}H_{36}BrN$ at 0.00-4.00 ratios.

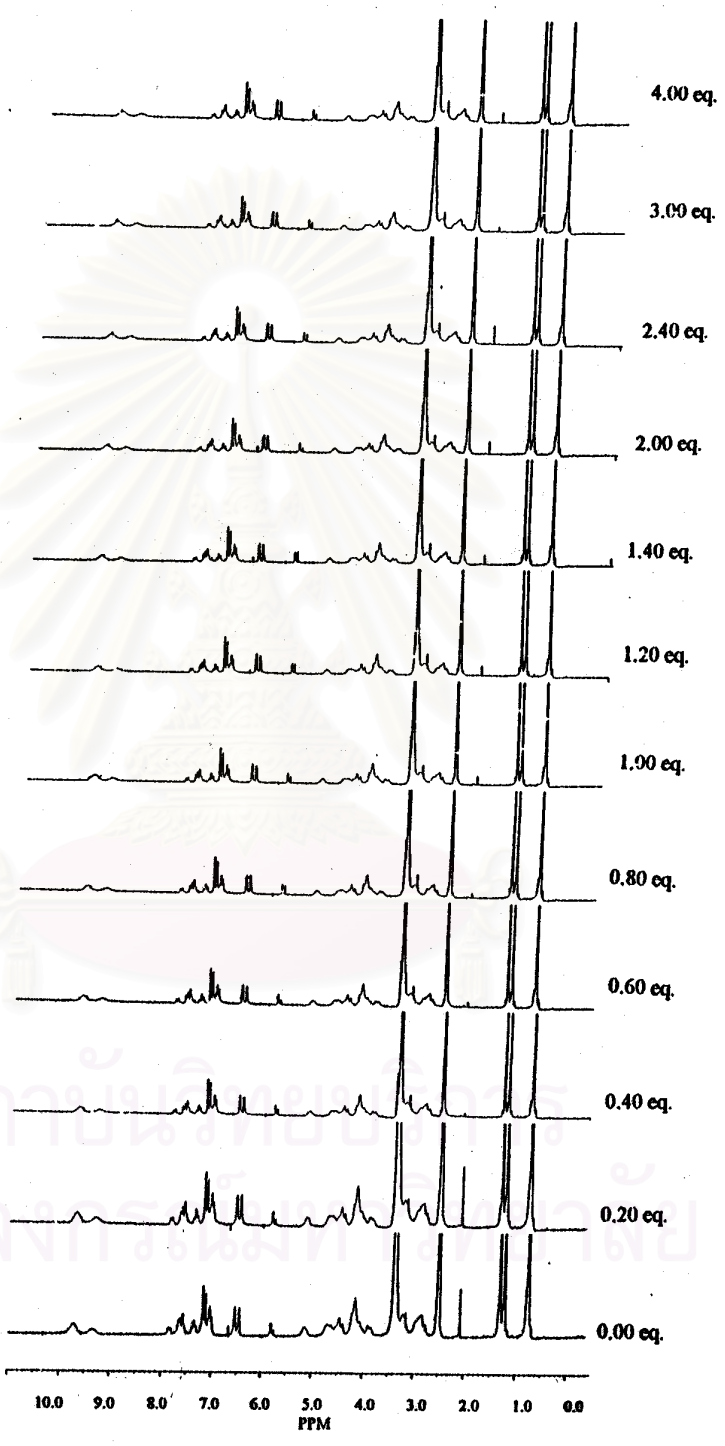

Figure C.6 ^{1}H-NMR (DMSO-d_6) spectra of complexation between **6a** and KI at 0.00-4.00 ratios.

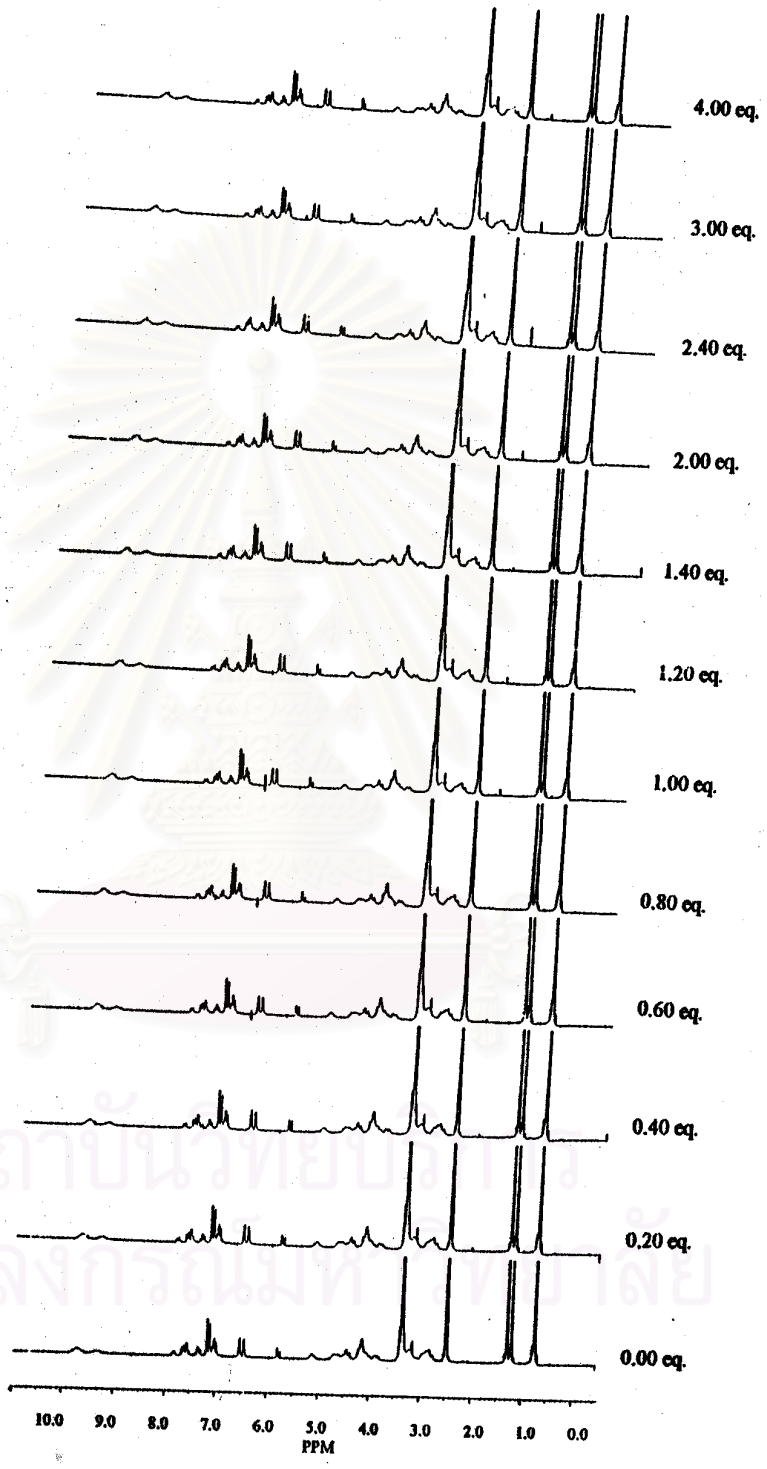

Figure C.7 ^{1}H-NMR (DMSO-d_6) spectra of complexation between **6a** and KBr at 0.00-4.00 ratios.

APPENDIX D

Figure D.1 ^{1}H-NMR ($CDCl_3$ and CD_3OD) spectra of complexation between **6b** and NaI at 0.00-4.00 ratios.

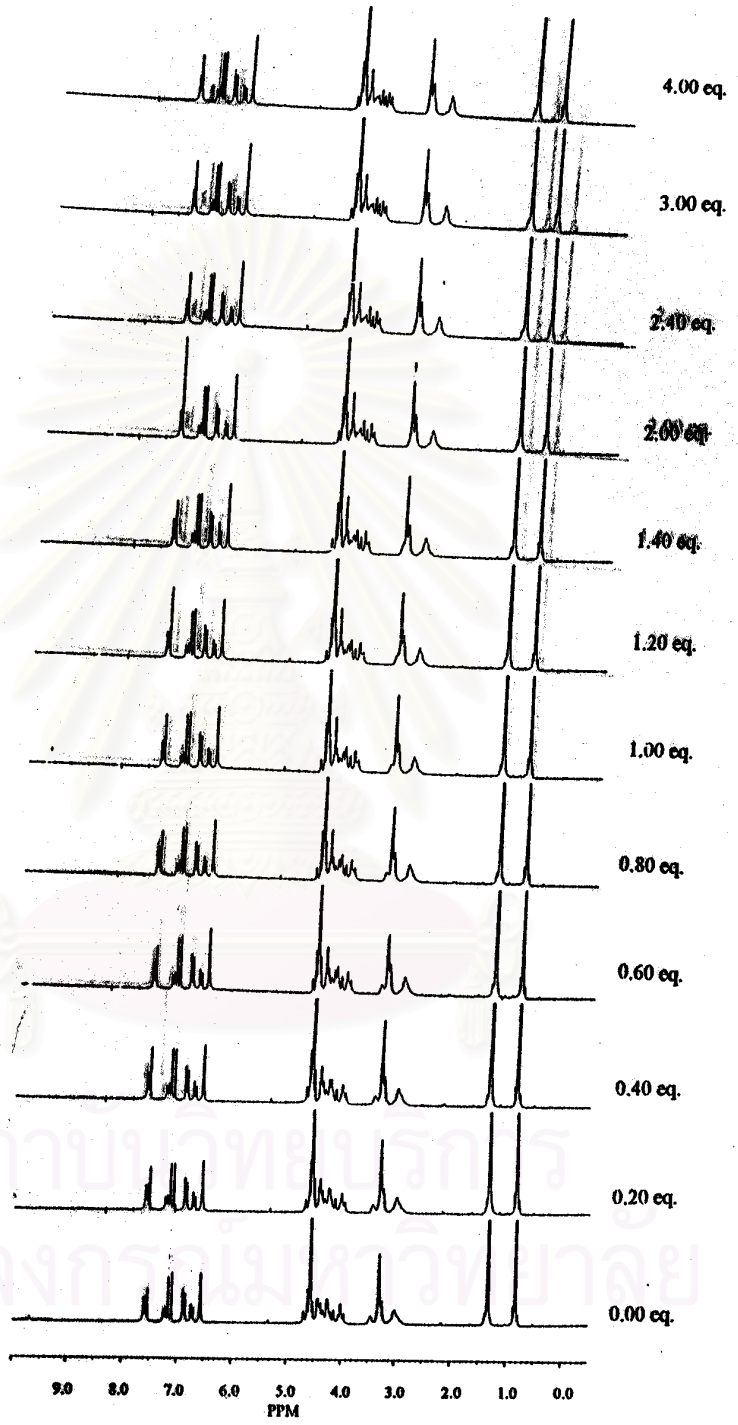

Figure D.2 ^{1}H-NMR ($CDCl_3$ and CD_3OD) spectra of complexation between **6b** and $NaNO_3$ at 0.00-4.00 ratios.

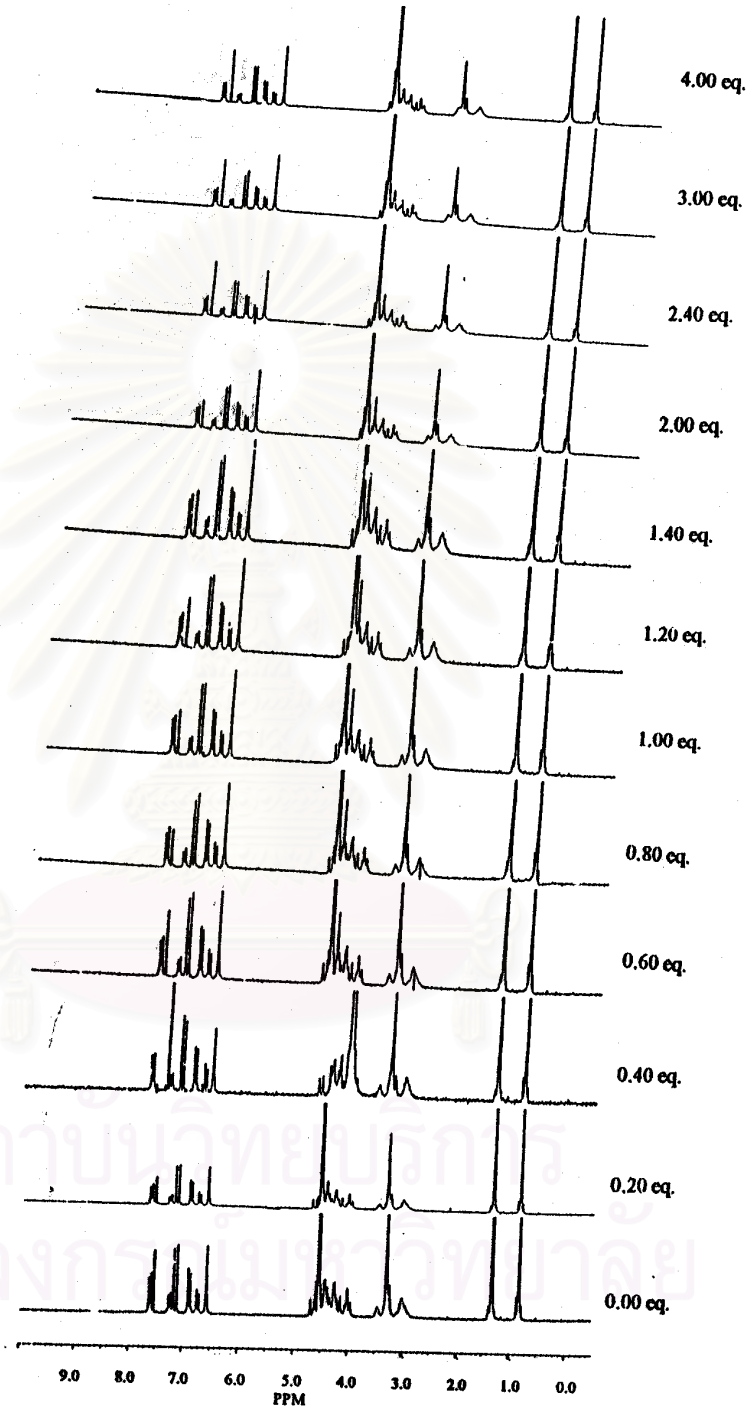

Figure D.3 ^{1}H-NMR ($CDCl_3$ and CD_3OD) spectra of complexation between **6b** and NaBr at 0.00-4.00 ratios.

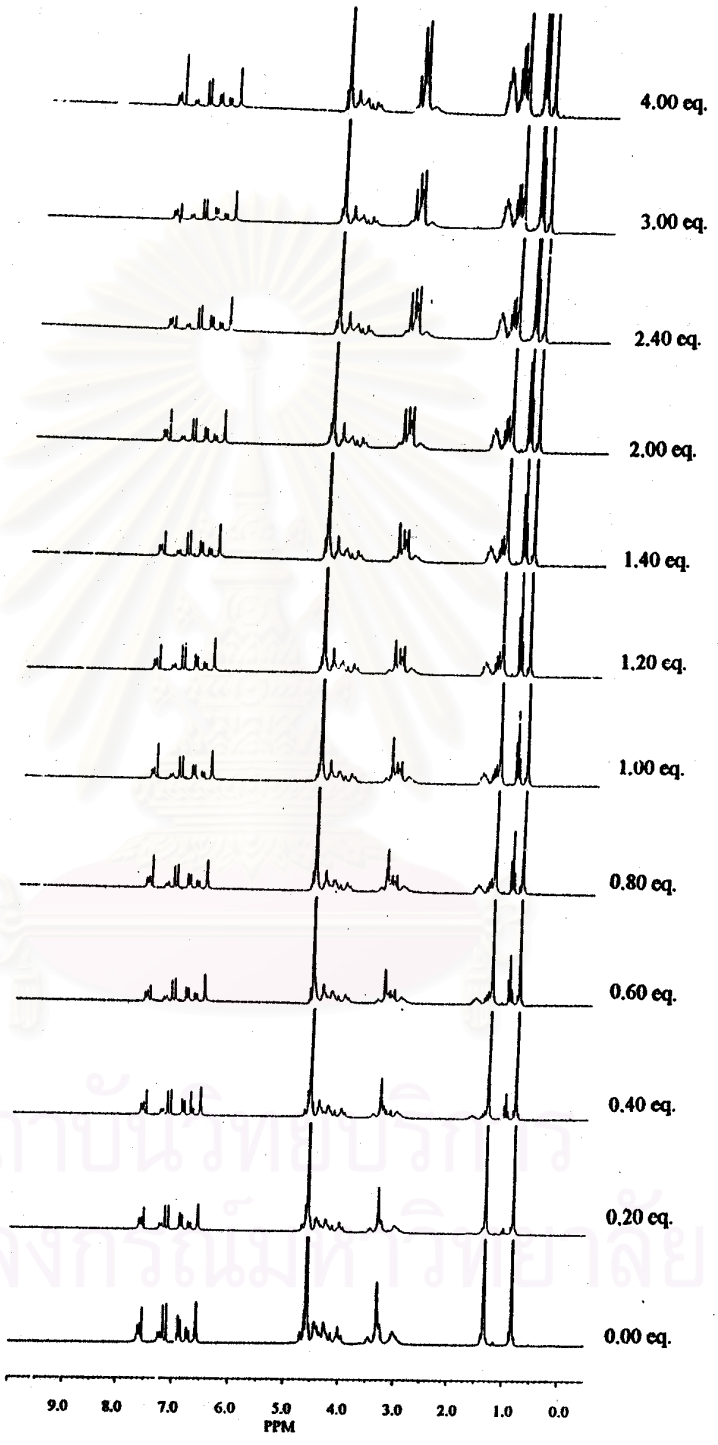

Figure D.4 ^{1}H-NMR ($CDCl_3$ and CD_3OD) spectra of complexation between **6b** and $C_{16}H_{36}IN$ at 0.00-4.00 ratios.

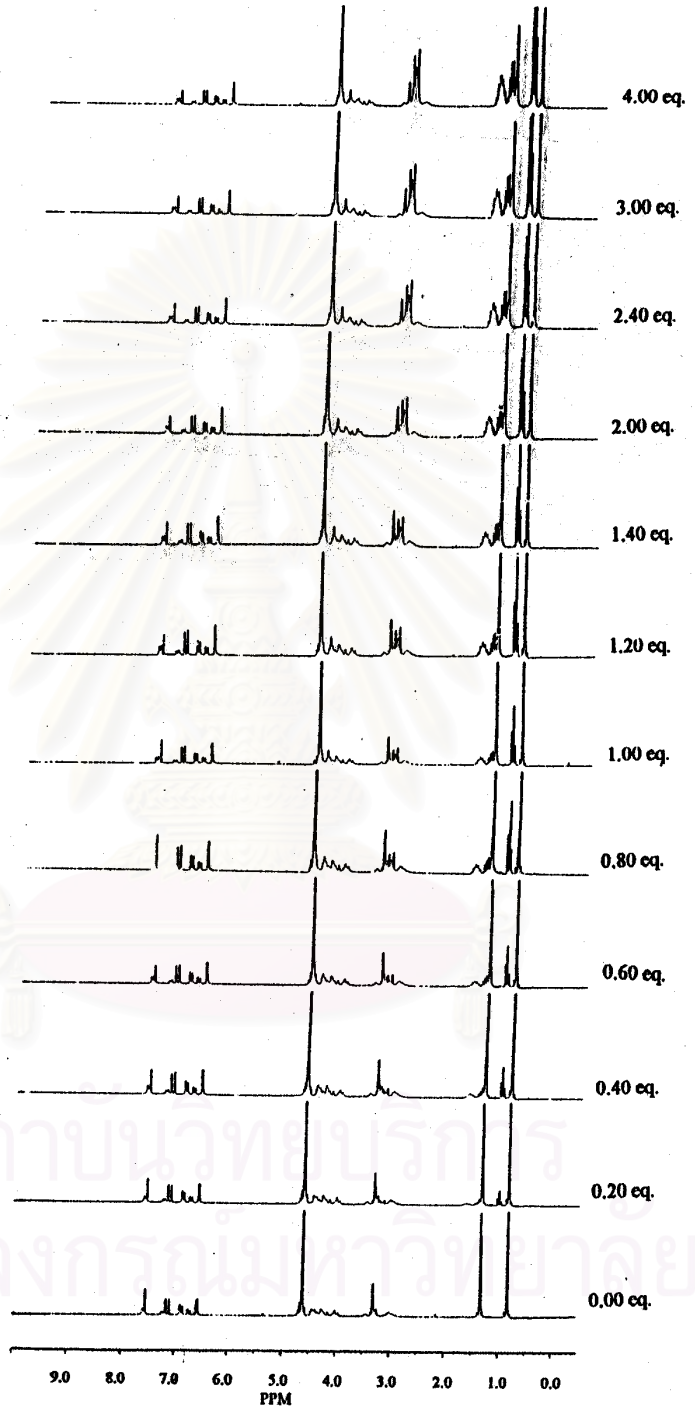

Figure D.5 ^{1}H-NMR ($CDCl_3$ and CD_3OD) spectra of complexation between **6b** and $C_{16}H_{36}BrN$ at 0.00-4.00 ratios.

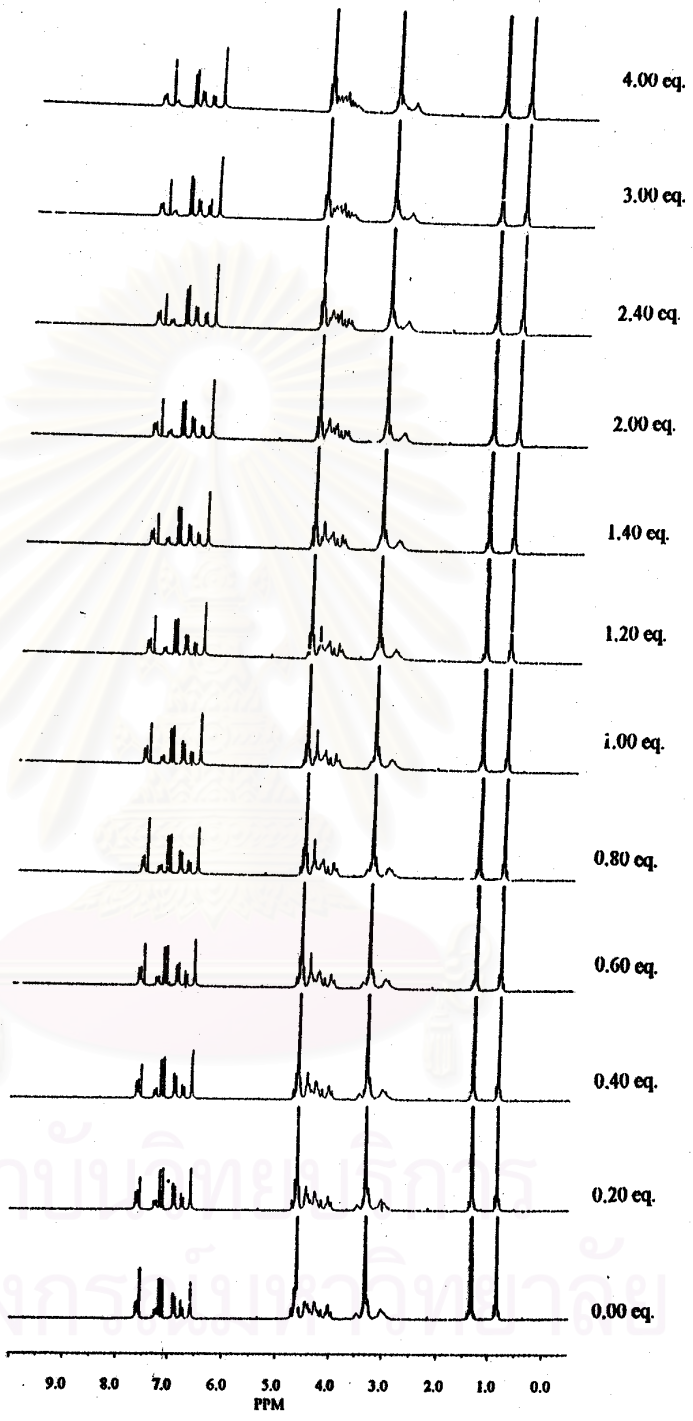

Figure D.6 ^{1}H-NMR ($CDCl_3$ and CD_3OD) spectra of complexation between **6b** and KI at 0.00-4.00 ratios.

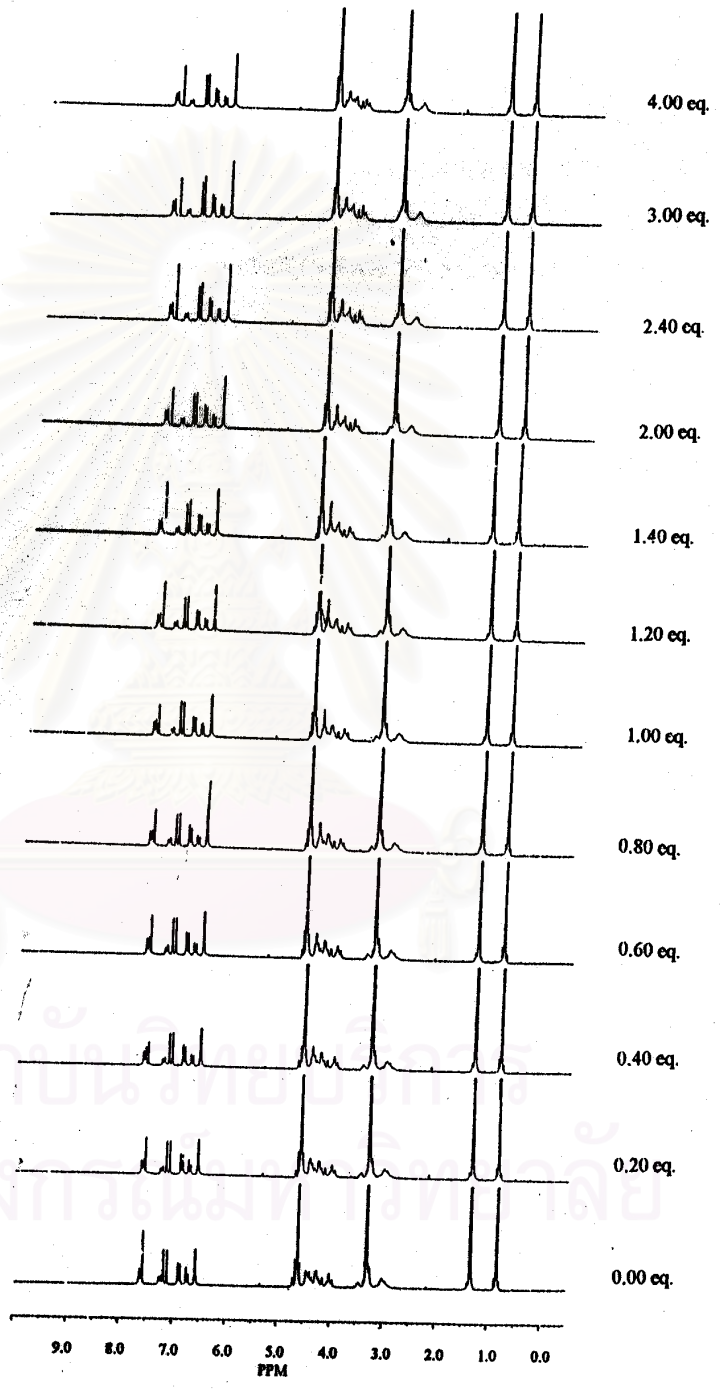

Figure D.7 ^{1}H-NMR ($CDCl_3$ and CD_3OD) spectra of complexation between **6b** and KBr at 0.00-4.00 ratios.

VITA

Miss Sirilux Poompradub was born on June 16, 1976 in Bangkok, Thailand. She graduated with Bachelor's degree of Science in Chemistry from Chulalongkorn University in 1997. She then pursued her Master's degree in Chemistry at Chulalongkorn University and finished her study in the academic year 2000.